MV009 - Convex Bowl

An Exploration of Precision
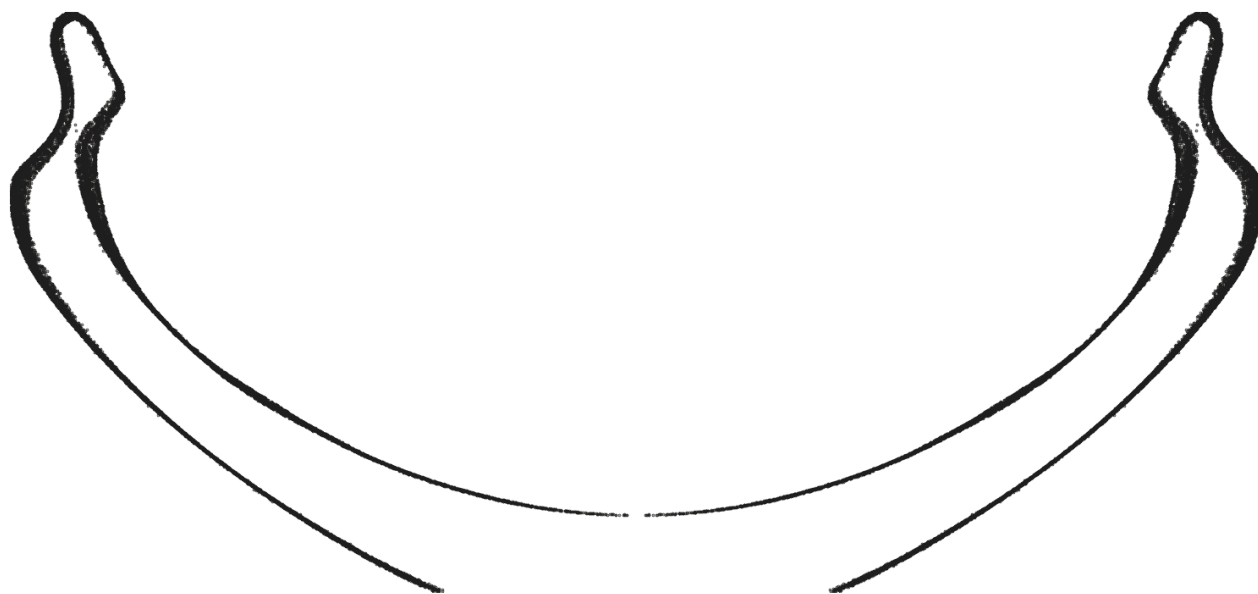
Petrie Museum, CC BY-NC-SA

Contents

Artifact Information

Artifact Data

Collection	Petrie Museum of Egyptian Archaeology
Provenance[1]	Petrie Museum of Egyptian Archaeology (London), recovered by Flinders Petrie
Provenience[2]	Unknown
Attribution	3rd Dynasty

Museum information

Ref.	LDUCE-UC17722
Description	Banded grey Diorite gneiss bowl, part of rim missing.
URL	https://collections.ucl.ac.uk/Details/collect/58807

Maijers vessel classification[3]

Short classification	Convex Bowl
Long classification	The vessel is created in an open form classified as a bowl with a convex shape, the vessels Convex curves are ending in a carinated rim.

Physical properties

Precision score[4]	15	
Height (approximate)	58 mm	2.28 in
Width (approximate)	123 mm	4.84 in
Material	Diorite	
Mohs Hardness[5]	5.5 - 7 (Diorite)	
Weight		

Scan information

Source	Scanned by Artifact Foundation
Source file name	UC17722_base_0.09.stl
Scan method	Laser
Scanner	FreeScale Combo+
Rated scan accuracy	37 μm	1.51 thou
Scan date	2024-10-14
Scanned by	Károly Póka
Mesh decimation	None, raw scan file used in the analysis
Number of vertices	8 015 998
Mesh density[6]	36 μm	1.41 thou
Max vertex distance	138 μm	5.443 thou
Min vertex distance	0 μm	0.000 thou
Vertices per cm2	21 876 (approximated)
Vertices per in2	141 135 (approximated)

---

[1] The verifiable chain of custody of an artifact

[2] The location or site where an artifact was recovered

[3] Vessel artifact classification developed by W. Arnold Maijer and described in his publication Masters of Stone, ISBN 978-90-829212-0-5

[4] The precision score metric is described in Precision Score Of The Artifact, p. 61

[5] The Mohs scale is an ordinal scale, from 1 to 10, describing the materials resistance to abrasion (the ability of harder material to scratch softer material)

[6] Median distance between vertices

Alignment In The Cartesian Coordinate System

For precise and valid measurements of the vessel's geometry to be possible, the points of the scanned dataset must first and foremost be placed optimally in a Cartesian coordinate system. Several alignment methods and algorithms have been tested on a number of different vessels to determine the best way to achieve optimal alignment.

Any misalignment of the artifact will increase the error of the precision measurements, due to the distortion/wobble effect caused by the misaligned object. To visualize this distortion, we can consider a representation of the three-dimensional point cloud data, folded to a two-dimensional plane. This folded representation is obtained by rotating all scanned points around an assumed center axis to y = 0, x > 0, thus resulting in a two-dimensional profile representation of all scanned vertices in the object.

Figure 1 illustrates this effect on a ideal ellipsoid. In the first image, the ellipsoid is perfectly aligned, resulting in a narrow and precise two-dimensional folded profile. As misalignments are introduced, the two-dimensional profile increases in width, visually showing the distortion, causing the error in the precision measurements to increase. While easy to understand visually, this distortion can also be objectively quantified, and as such used to compare the fitness of different assumed center axes against each other, and further to create an automated and solid process for optimal Cartesian alignment of the scan data.
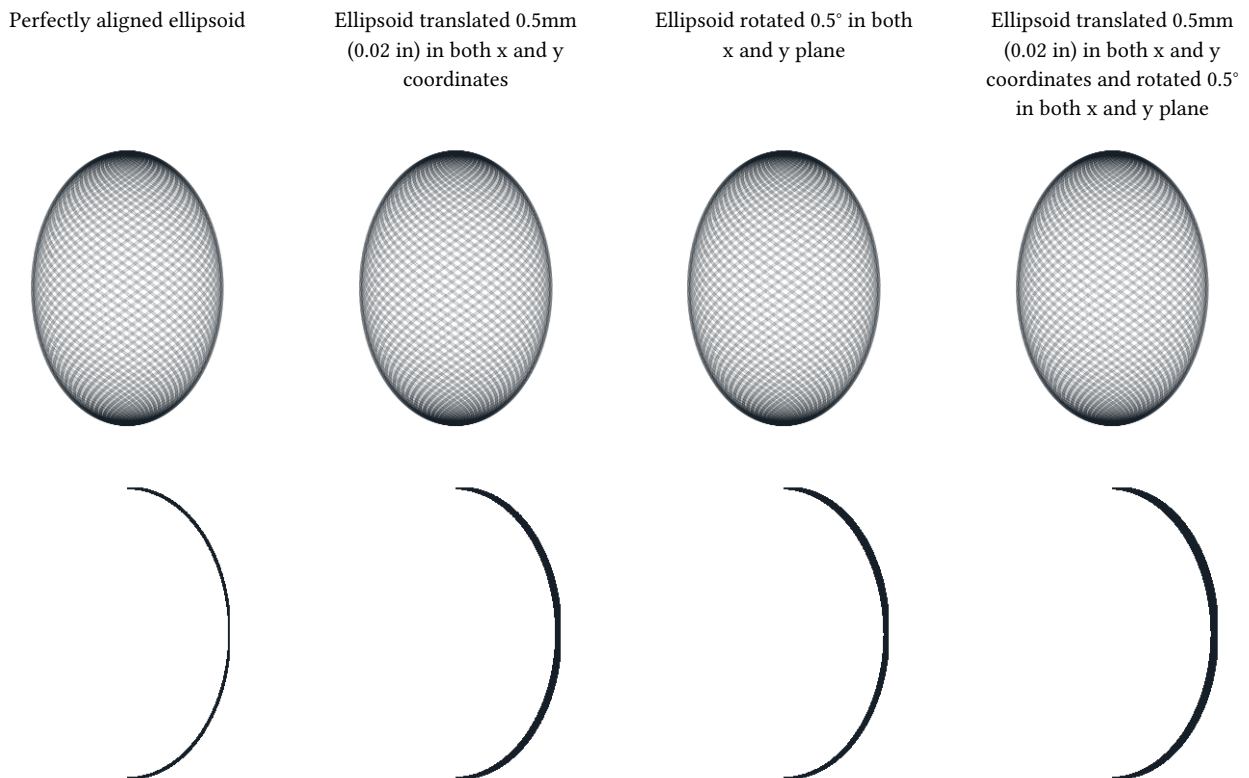

Figure 1: Distortion caused by a misalignment of the artifact

In contemporary metrology analysis of modern production objects, it is common to align the object in a Cartesian coordinate system by fitting a flat surface of the object to a reference plane in the coordinate system, cylindrical features to an ideal cylinder etc., or by using specific markers placed on the object in the design process. This methodology, however, is inadequate for the ancient objects in question. Most scanned artifacts, do not have a valid flat surface which could be aligned to a plane in the Cartesian coordinate system; most surfaces seem to be curved. Some artifacts do have a flat base, however this is often a worn area of the artifact and practical tests have shown that alignment to such surfaces will not produce optimal alignment of the scan data.

As conventional methods of alignment do not always yield good results with these types of artifacts, a more adequate method of alignment has been developed to enable precise measurements and statistical analysis of the scan data.

To find the optimal position of the vessel in the coordinate system, a range of rotation and translation tests are carried out to find the best fit of the central axis.

Based on the assumption that the analyzed object was created using a rotational process, and thus have symmetry around a central axis, the alignment of the artifact is carried out in a two-step process. An overview of this process is given below.

The artifact is placed in a Cartesian coordinate system, in an initially unaligned state. The first step in the alignment process estimates the central rotational axis of the vessel, by analyzing the coaxiality of thin cross-section slices of the vessel. The slices will be as thin as possible based on the mesh density of the scan, while still ensuring enough data points in each slice to be statistically valid.

For each slice, circular regression[7] (estimate of best fit circle) is used to estimate the center point of this slice. Combined over the total Z-axis range of the vessel, these center points provide us with an indicator of the incline and position of the vessel's central axis.

The next step will optimize the center axis alignment by progressively minimizing the deviation (perpendicular to the surface curvature) of the two-dimensional profile, see Figure 1. By ascertaining and comparing the resulting fit of many thousands of different potential rotations, the best fit alignment of the scan data can be estimated, and an optimal center axis (in relation to the data points) can be reconstructed. The actual three-dimensional point-cloud is then aligned to this axis, by rotating and translating the scanned data points to match the Z-axis of the Cartesian coordinate system.

To enable extensive analysis of the full surface of the artifact, the mesh is split into exterior and interior surfaces. The exterior surface is aligned independently of interior data points, providing a baseline for exterior quality assessment. The interior surface is represented by two alignments:
- Aligned with the exterior mesh to analyze concentricity, and
- Aligned separately to assess its precision and compare the true tilt/displacement between interior and exterior surfaces.

---

[7]Circle regression algorithm used: Kenichi Kanatani, Prasanna Rangarajan, "Hyper least squares fitting of circles and ellipses" Computational Statistics & Data Analysis, Vol. 55, pages 2197-2208, (2011)

Statistics used throughout the report

This section provides an overview of the key statistical and model-evaluation metrics employed throughout the report to analyze dataset variability, model fit, and predictive accuracy.

Each measure is introduced with its mathematical formulation, practical interpretation, and explicit reference to how it is calculated in the context of the evaluated models and residuals. Together, these metrics quantify:

- Data variability (e.g., MAD, Standard Deviation, Range).
- Model accuracy (e.g., MSD, RMSD).
- Robustness vs. sensitivity to extreme values and central tendencies.

Mean Squared Deviation (MSD), also known as Mean Squared Error (MSE).

$$\text{MSD} = \frac{\sum_{i=1}^{n} (y_i - \hat{y})^2}{n}$$

The Mean Squared Deviation (MSD) measures the average magnitude of squared differences between observed (y_i) and predicted ($\hat{y}$) values, calculated as the mean of squared residuals, and is a used as a measure of discrepancy in regression and model-fitting contexts.

This measure amplifies the influence of larger deviations through squaring, emphasizes imperfections in the observed data, but retains sensitivity to outliers.

Root Mean Squared Deviation (RMSD), also known as Root Mean Squared Error (RMSE).

$$\text{RMSD} = \sqrt{\frac{\sum_{i=1}^{n} (y_i - \hat{y})^2}{n}}$$

The Root Mean Square Deviation (RMSD) measures the magnitude of differences between observed (y_i) and predicted ($\hat{y}$) values by calculating the square root of the average of squared residuals.

RMSD is a commonly used measure of discrepancy in regression and model-fitting contexts. It quantifies the average magnitude of residuals while retaining sensitivity to larger deviations (via squaring), making it particularly useful for evaluating model accuracy.

Standard Deviation (SD)

$$s = \sqrt{\frac{\sum_{i=1}^{n} (y_i - \bar{y})^2}{n-1}}$$

The Standard Deviation measures the spread of data (y_i) around the mean ($\bar{y}$) by calculating the square root of the average of squared differences between each value and the mean.

It is sensitive to outliers as it amplifies their influence through squaring, in contrast to MAD.

Throughout this report, the Standard Deviation is calculated using the absolute residuals from regression models.

Median Absolute Deviation (MedianAD)

$$\text{MedianAD} = \text{median}(|y_i - \text{median}(y)|)$$

The Median Absolute Deviation (MAD) measures the spread of data around the median by calculating the median of absolute differences between each value and the median.

MAD is a robust measure of spread, analogous to the interquartile range (a robust measure centered on the middle 50% of data), and differs from the standard deviation in that it minimizes the impact of outliers.

Throughout this report, the MAD is calculated using the absolute values of residuals from regression models.

Range

$$\max(y_i) - \min(y_i)$$

The Range measures the spread of a dataset by calculating the difference between the maximum and minimum values.

The Range is a simple measure of spread, capturing the full extent of variability. Range is very sensitive to extreme values, as it is entirely determined by the two most extreme data points.

Throughout this report, the Range is calculated using the full range of residuals from regression models.

Precision

To explore the manufacturing precision of the artifact in depth, the following analysis have been carried out:

- Circularity around the axis of symmetry is examined in detail at selected cross-sections.
- Overall circularity around the axis of symmetry is measured for the full height of the vessel (areas of the vessel with extensive damage are not taken into account for this metric).
- Concentricity of the vessel between selected cross-sections are examined in detail to determine if the existence of an axis of rotation in the manufacture of the object can be established.
- The coaxiality of the vessel is analyzed to explore the precision of the central axis of the object.
- The surface variability is analyzed and visualized on through a heatmap.

Circularity

Circularity is the measurement of how round the surface of an object is, optionally in reference to a datum axis. The *circularity tolerance* is the radial distance of two circles, each with their centers in the datum axis, and each of them conforming, respectively, to the minimum and maximum deviations of the data-set to a true circle, see Figure 2.
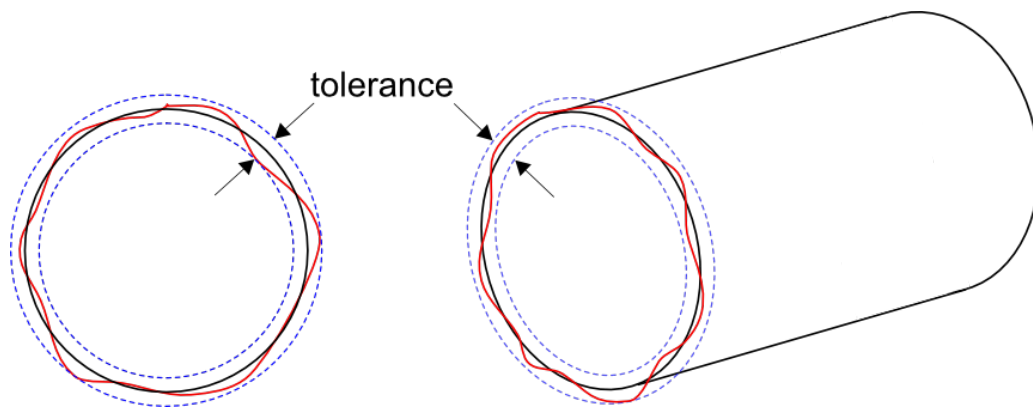

Figure 2: Circularity tolerance.

Circularity is examined at different cross-sections of the vessel, using the established Z-axis as the datum axis (axis of symmetry). The distance between the scanned points in the local datum plane is measured to determine the range between the two concentric circles encompassing the measured points, see Figure 3.

Referencing all of the individual circularity measurements to the global (reconstructed) axis of symmetry of the object, allows us to ascertain not only circularity of local features of the object, but how well circularity was *maintained* over the entire manufacturing process. This is an important distinction, which may be able to provide valuable insights into requirements of the construction methods. For reference, and seeing that the variance in local circularity also holds interest, measurements of circularity of the vessel without reference to the axis of symmetry can additionally be found in the Concentricity, p. 33.
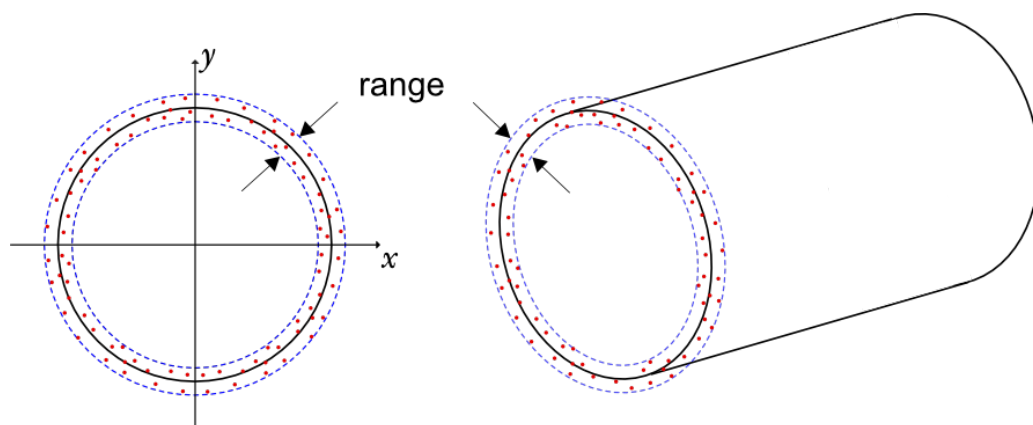

Figure 3: Circularity measurements.

If the circularity is determined from slices of the vessel exclusively in the *Z-plane* (actually measuring the cylindricity of a very thin slices of the vessel, in an attempt to approximate circularity), this would - in some areas - introduce significant distortion (increasing measurement errors) in the samples, due to the curvature of the vessel's surface.

Each sample slice of the vessel is therefore obtained perpendicular to the surface curvature, see Figure 6 to Figure 18. The measurements are taken conservatively without filtration of potential outliers.

To explore the potential distortion caused by obtaining samples in the Z-plane only, please refer to Appendix A, where measurements in the Z-plane and measurements perpendicular to surface curvature are compared side by side.

Detailed circularity measurements of selected points
Circularity measurements across a range of selected slices of the vessel (see Table 1) have been analyzed in-depth, and detailed plots of each measurement is provided. Furthermore, full circularity measurements are shown for each available scanned surface including a detailed plot to visualize the circularity of all areas of the vessel.
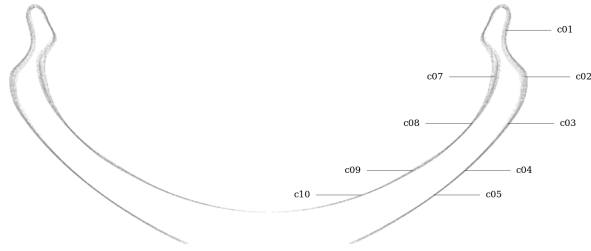
<div style="display:flex">

Figure 4: Circularity measurement sample locations,
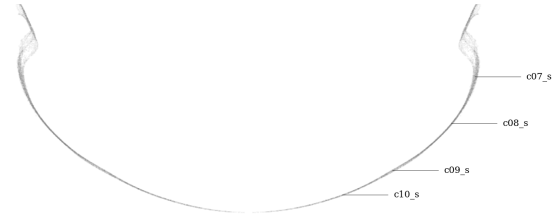full mesh aligned with exterior surface

Figure 5: Circularity measurement sample location,
separately aligned interior mesh

</div>

Metric

Tag	Area	Measured deviation[8]	Residuals				Sample size	Slice		
			Range	RMSD[9]	MAD[10]	SD		Height	Z coord.	Radius[11]
		mm	mm	mm	mm	mm		mm	mm	mm
c01	exterior	Ø113.245±0.700	1.175	0.310	0.110	0.158	2721	0.050	51.298	56.623
c02	exterior	Ø122.219±1.187	1.980	0.493	0.190	0.256	3572	0.050	40.124	61.110
c03	exterior	Ø114.580±0.622	0.924	0.174	0.060	0.123	2724	0.050	28.951	57.290
c04	exterior	Ø93.798±0.362	0.539	0.058	0.026	0.034	1899	0.050	17.777	46.899
c05	exterior	Ø79.189±0.246	0.384	0.038	0.013	0.025	1441	0.050	11.921	39.595
c07	interior	Ø108.298±0.990	1.909	0.477	0.204	0.289	4299	0.050	40.124	54.149
c07_s	interior sep.	Ø108.483±0.661	1.320	0.302	0.110	0.156	4069	0.050	40.124	54.242
c08	interior	Ø96.988±0.205	0.384	0.094	0.038	0.046	2221	0.050	28.951	48.494
c08_s	interior sep.	Ø97.142±0.160	0.310	0.064	0.028	0.035	2196	0.050	28.951	48.571
c09	interior	Ø69.021±0.269	0.499	0.124	0.049	0.066	969	0.050	17.777	34.510
c09_s	interior sep.	Ø69.145±0.272	0.467	0.133	0.041	0.057	1007	0.050	17.777	34.573
c10	interior	Ø44.703±0.154	0.242	0.045	0.016	0.023	391	0.050	11.921	22.352
c10_s	interior sep.	Ø45.002±0.150	0.242	0.046	0.017	0.026	425	0.050	11.921	22.501

Imperial

Tag	Area	Measured deviation[8]	Residuals				Sample size	Slice		
			Range	RMSD[9]	MAD[10]	SD		Height	Z coord.	Radius[11]
		in	in	in	in	in		in	in	in
c01	exterior	Ø4.4585±0.0276	0.0463	0.0122	0.0043	0.0062	2721	0.0020	2.0196	2.2292
c02	exterior	Ø4.8118±0.0467	0.0780	0.0194	0.0075	0.0101	3572	0.0020	1.5797	2.4059
c03	exterior	Ø4.5110±0.0245	0.0364	0.0068	0.0024	0.0048	2724	0.0020	1.1398	2.2555
c04	exterior	Ø3.6928±0.0143	0.0212	0.0023	0.0010	0.0013	1899	0.0020	0.6999	1.8464
c05	exterior	Ø3.1177±0.0097	0.0151	0.0015	0.0005	0.0010	1441	0.0020	0.4693	1.5588
c07	interior	Ø4.2637±0.0390	0.0752	0.0188	0.0080	0.0114	4299	0.0020	1.5797	2.1319
c07_s	interior sep.	Ø4.2710±0.0260	0.0520	0.0119	0.0043	0.0061	4069	0.0020	1.5797	2.1355
c08	interior	Ø3.8184±0.0081	0.0151	0.0037	0.0015	0.0018	2221	0.0020	1.1398	1.9092
c08_s	interior sep.	Ø3.8245±0.0063	0.0122	0.0025	0.0011	0.0014	2196	0.0020	1.1398	1.9123
c09	interior	Ø2.7174±0.0106	0.0196	0.0049	0.0019	0.0026	969	0.0020	0.6999	1.3587
c09_s	interior sep.	Ø2.7223±0.0107	0.0184	0.0052	0.0016	0.0022	1007	0.0020	0.6999	1.3611
c10	interior	Ø1.7600±0.0061	0.0095	0.0018	0.0006	0.0009	391	0.0020	0.4693	0.8800
c10_s	interior sep.	Ø1.7717±0.0059	0.0095	0.0018	0.0007	0.0010	425	0.0020	0.4693	0.8859

Table 1: Detailed circularity measurements at selected samples of MV009.

Figure 6 to Figure 18 shows a detailed plots of each circularity measurement.

---

[8] Sample diameter Ø± maximum measured deviation from measured radius
[9] Root mean square deviation (RMSD) also called Root mean square error (RMSE)
[10] Median absolute deviation
[11] Median sample radius from z-axis

Graphical overview of circularity measurement c01

Top view of sample slice

Sample location

Ø113.2±0.7 mm
Ø4.5±0.026 inch

- Sample in z-plane (n = 2721)
- circle

Side view of sample slice

- Z-plane sample (n=2827)
- Sample perpendicular to surface profile (n=2721)
- Artifact datapoints

Residuals Plot - Circle circumference unwrapped to a line

- Residuals z-plane sample (n=2827)
- Radius

Histogram, PDF and Box-plot of Residuals perpendicular to surface tangent

- Histogram
- KDE
- Theoretical PDF

Median: 0.06 mm | 0.003 in

62.0%

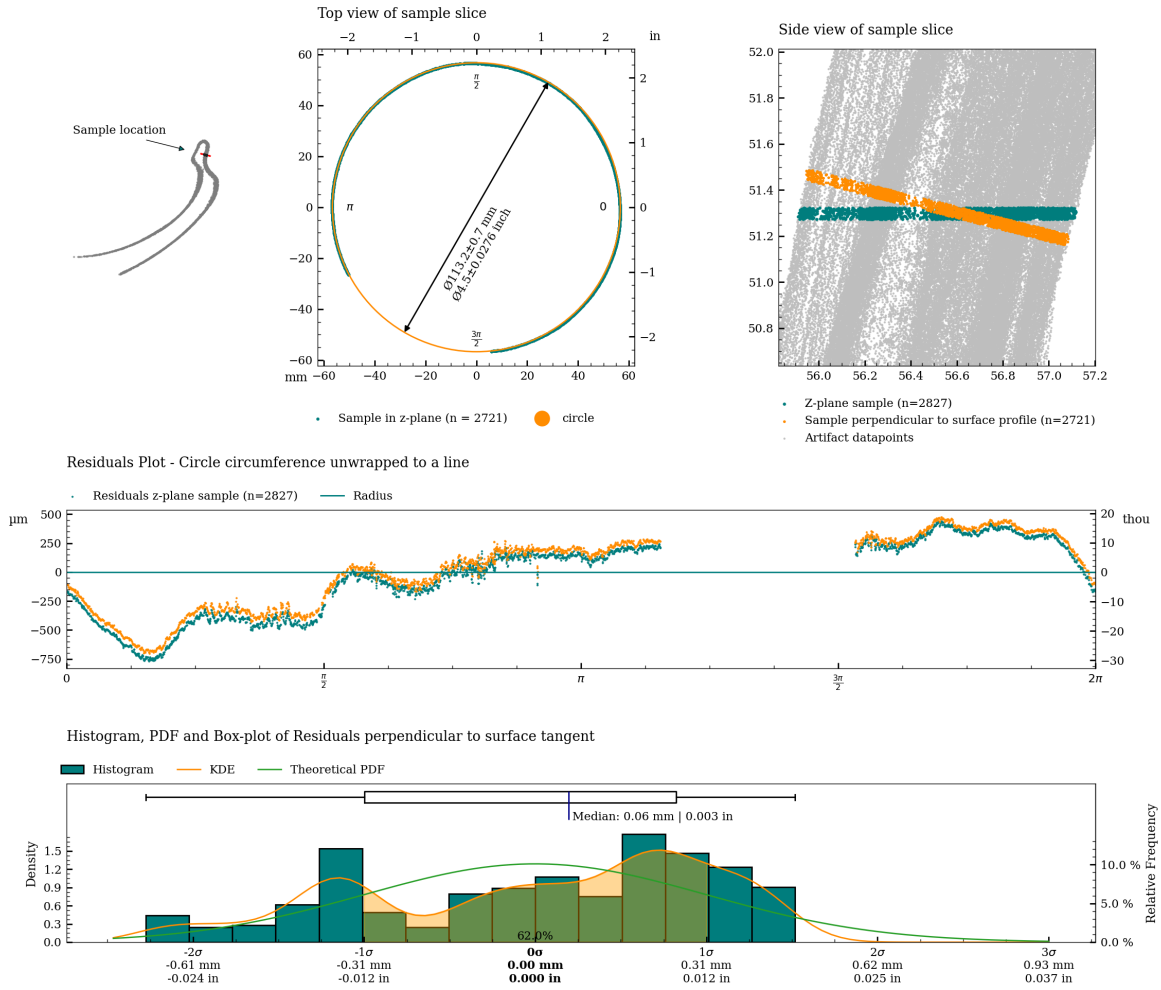|	-2σ	-1σ	0σ	1σ	2σ	3σ
	-0.61 mm	-0.31 mm	**0.00 mm**	0.31 mm	0.62 mm	0.93 mm
	-0.024 in	-0.012 in	**0.000 in**	0.012 in	0.025 in	0.037 in

Figure 6: Charts with statistics for the measurement of c01.

Graphical overview of circularity measurement c02

Figure 7: Charts with statistics for the measurement of c02.
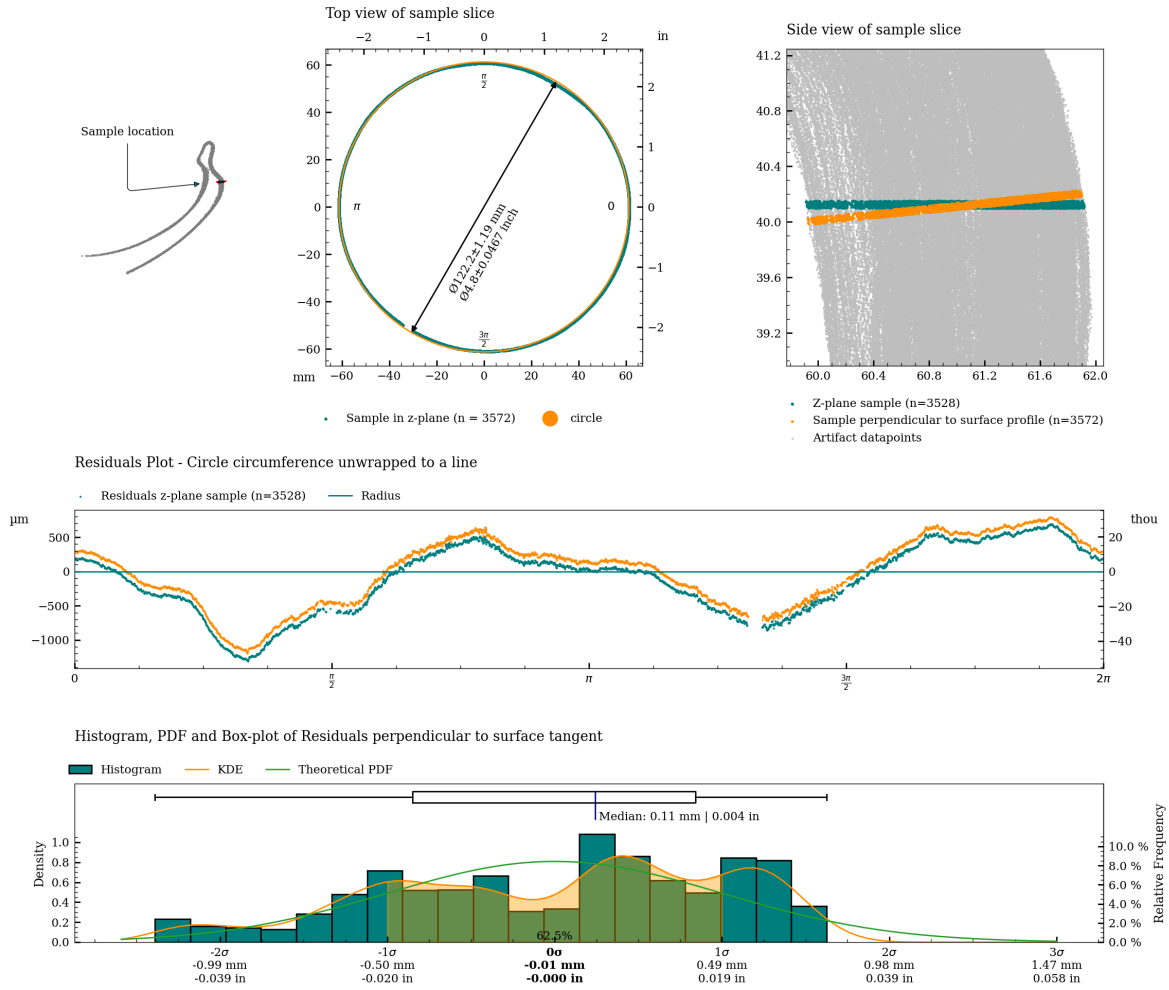
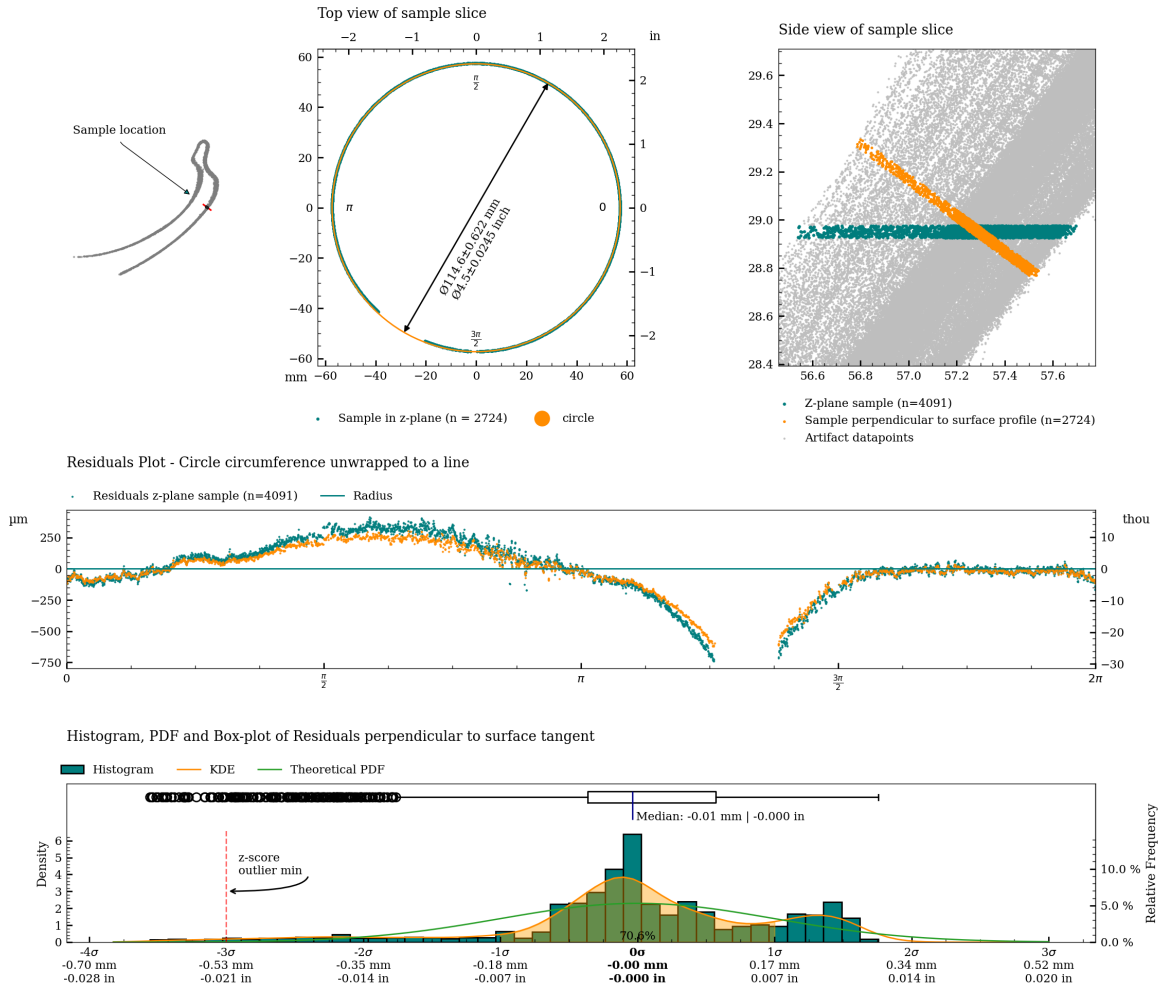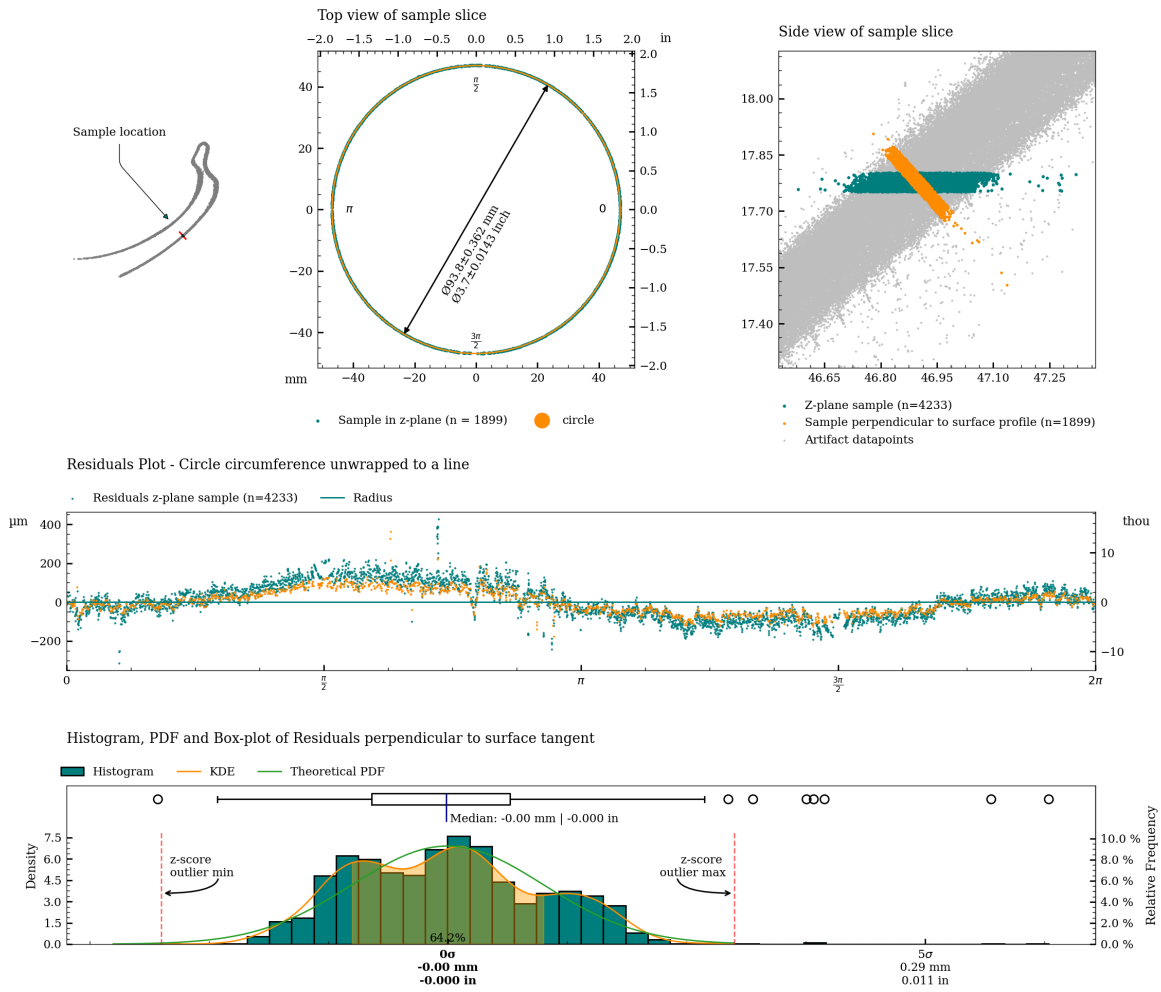# Graphical overview of circularity measurement c03

Top view of sample slice

Sample location

Ø114.6±0.622 mm
Ø4.5±0.025 inch

Sample in z-plane (n = 2724)   circle

Side view of sample slice

• Z-plane sample (n=4091)
• Sample perpendicular to surface profile (n=2724)
Artifact datapoints

Residuals Plot - Circle circumference unwrapped to a line

• Residuals z-plane sample (n=4091)   — Radius

Histogram, PDF and Box-plot of Residuals perpendicular to surface tangent

Histogram   KDE   Theoretical PDF

Median: -0.01 mm | -0.000 in

z-score outlier min

70.6%

Figure 8: Charts with statistics for the measurement of c03.

Graphical overview of circularity measurement c04

Figure 9: Charts with statistics for the measurement of c04.

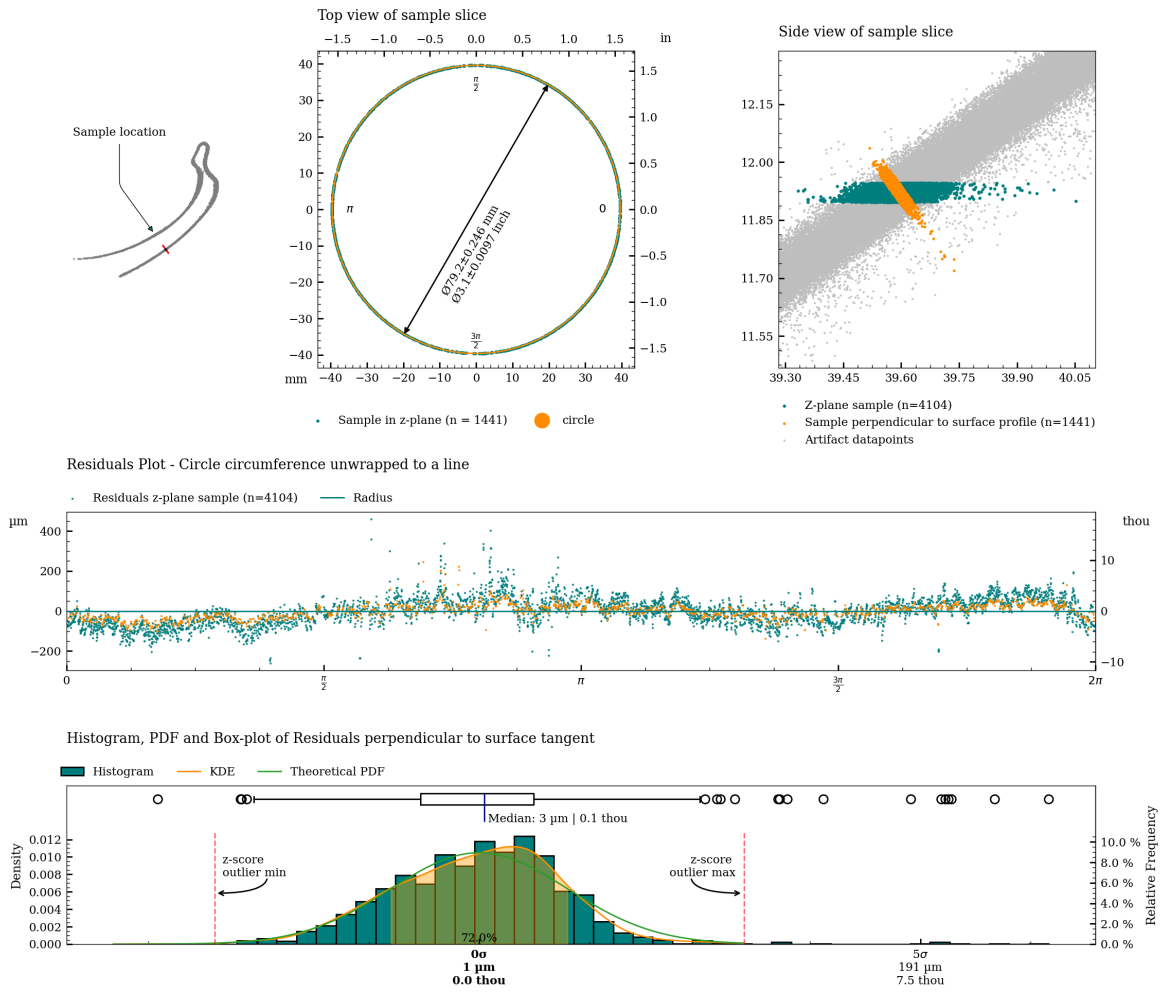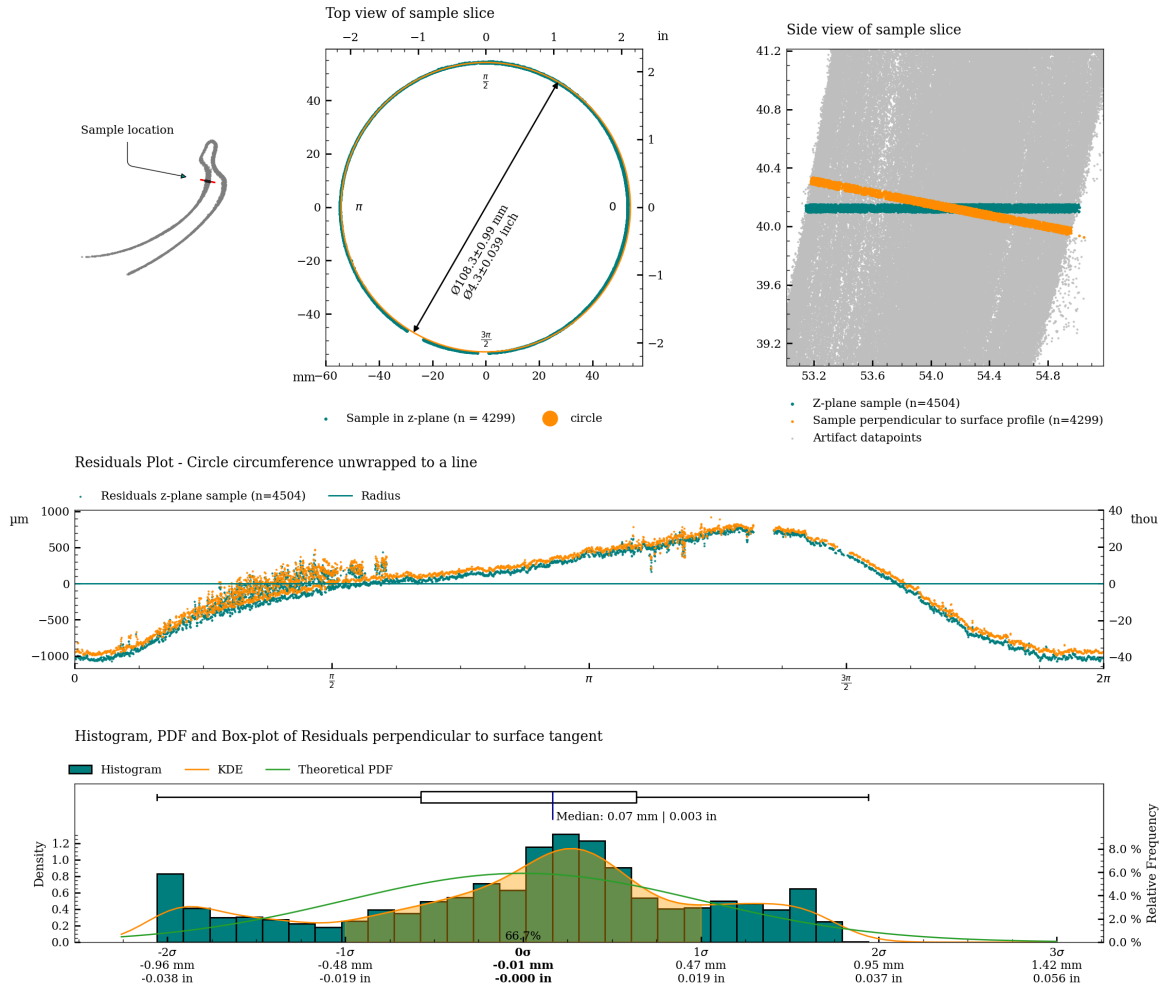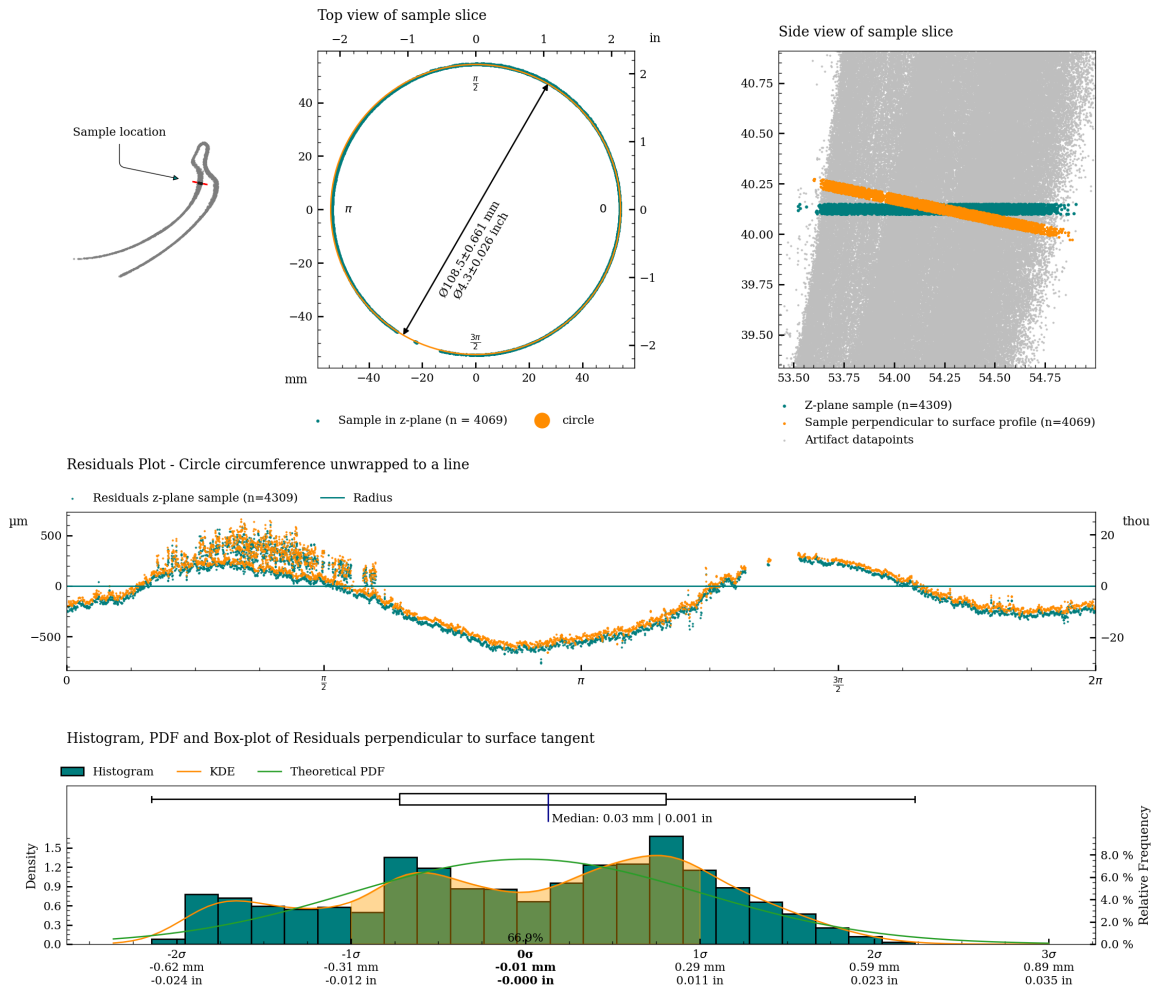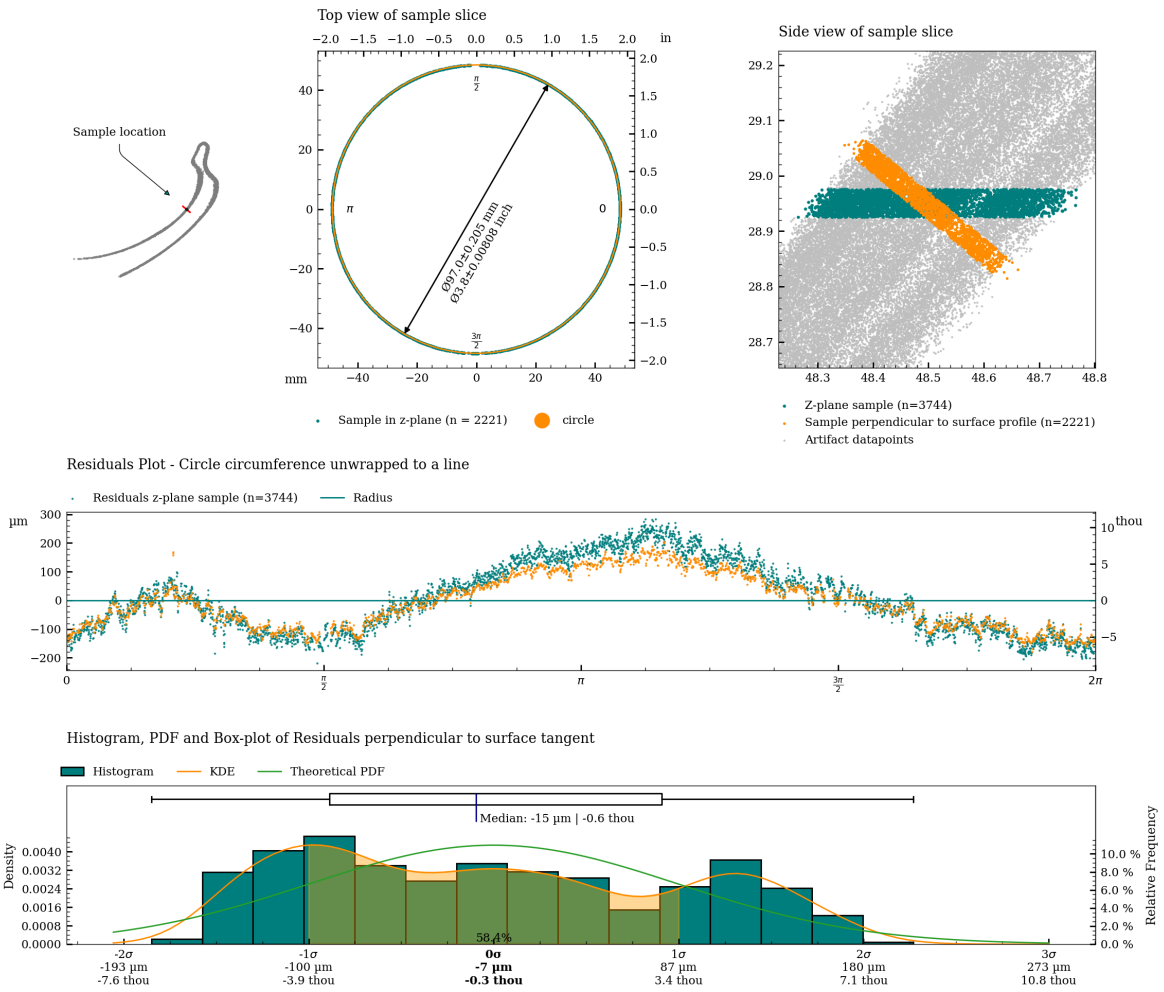# Graphical overview of circularity measurement c05

Top view of sample slice

Side view of sample slice

Sample location

Ø79.2±0.246 mm
Ø3.1±0.0097 inch

- Sample in z-plane (n = 1441)
- circle

- Z-plane sample (n=4104)
- Sample perpendicular to surface profile (n=1441)
- Artifact datapoints

Residuals Plot - Circle circumference unwrapped to a line

- Residuals z-plane sample (n=4104) — Radius

Histogram, PDF and Box-plot of Residuals perpendicular to surface tangent

- Histogram — KDE — Theoretical PDF

Median: 3 µm | 0.1 thou

z-score outlier min

z-score outlier max

72.0%

0σ
1 µm
0.0 thou

5σ
191 µm
7.5 thou

Figure 10: Charts with statistics for the measurement of c05.

Graphical overview of circularity measurement c07

Top view of sample slice

Side view of sample slice

Sample location

Ø108.3±0.99 mm
Ø4.3±0.039 inch

- Sample in z-plane (n = 4299)
- circle

- Z-plane sample (n=4504)
- Sample perpendicular to surface profile (n=4299)
- Artifact datapoints

Residuals Plot - Circle circumference unwrapped to a line

- Residuals z-plane sample (n=4504)
- Radius

Histogram, PDF and Box-plot of Residuals perpendicular to surface tangent

- Histogram
- KDE
- Theoretical PDF

Median: 0.07 mm | 0.003 in

66.7%

	-2σ	-1σ	0σ	1σ	2σ	3σ
	-0.96 mm	-0.48 mm	**-0.01 mm**	0.47 mm	0.95 mm	1.42 mm
	-0.038 in	-0.019 in	**-0.000 in**	0.019 in	0.037 in	0.056 in

Figure 11: Charts with statistics for the measurement of c07.

Graphical overview of circularity measurement c07_s

Figure 12: Charts with statistics for the measurement of c07_s.

Graphical overview of circularity measurement c08

Figure 13: Charts with statistics for the measurement of c08.
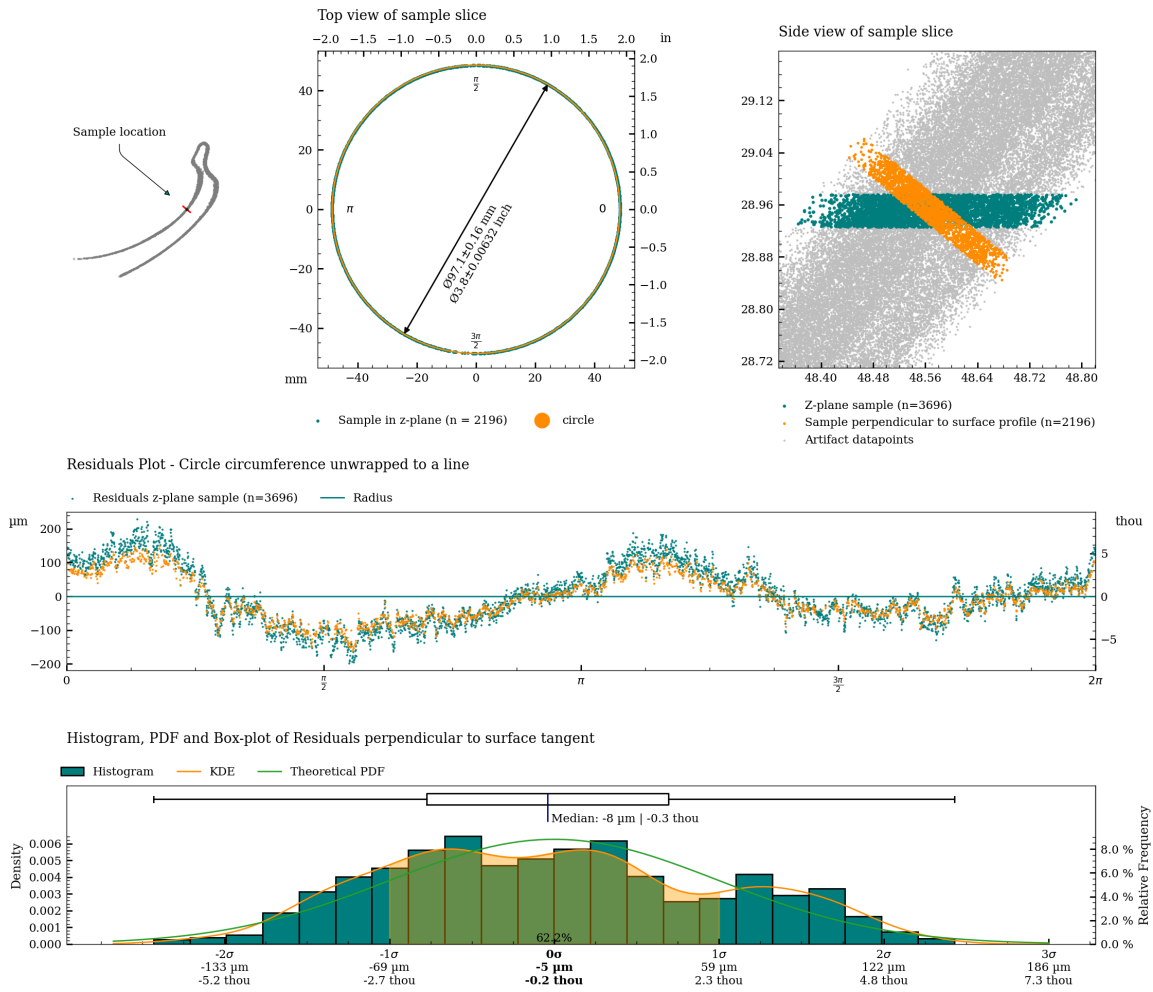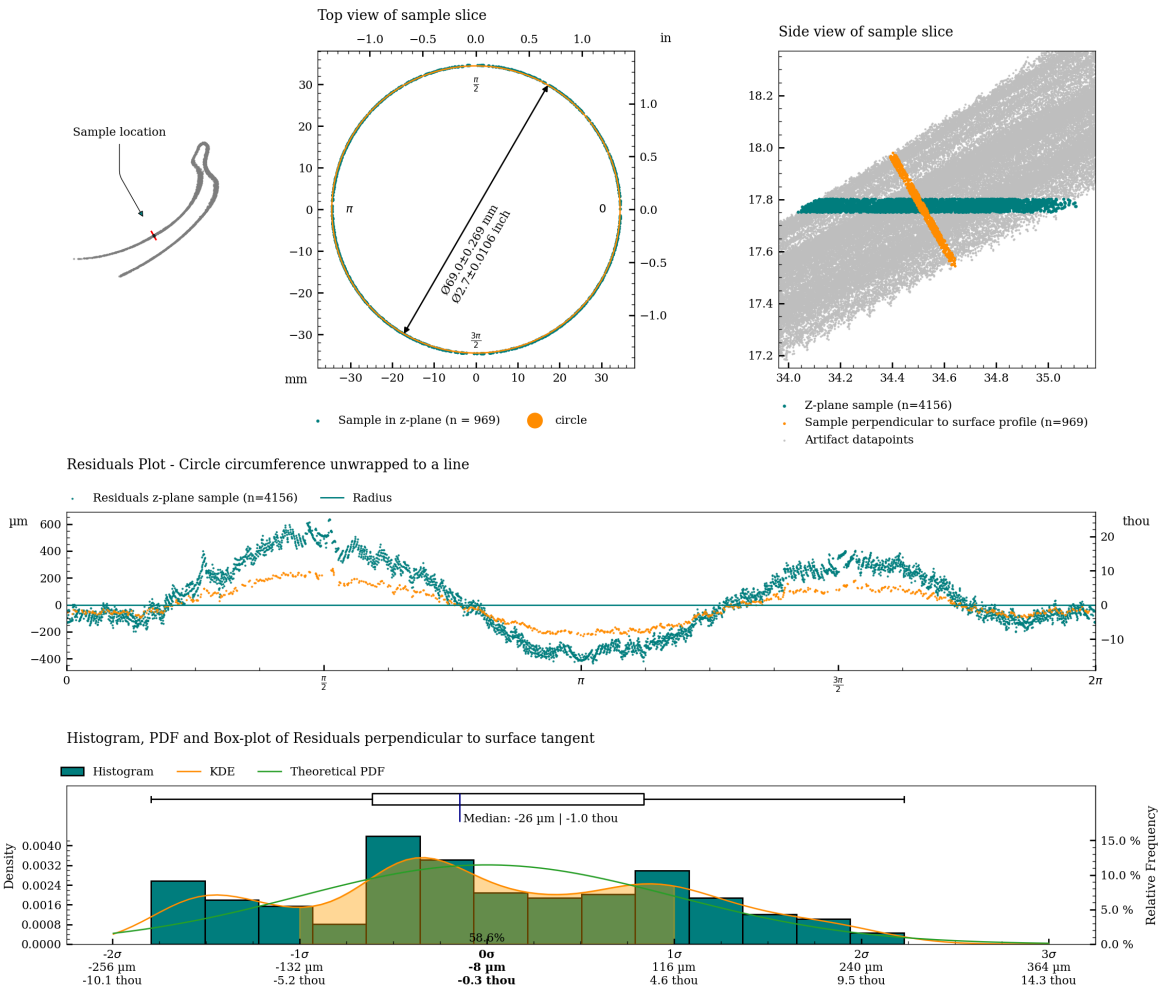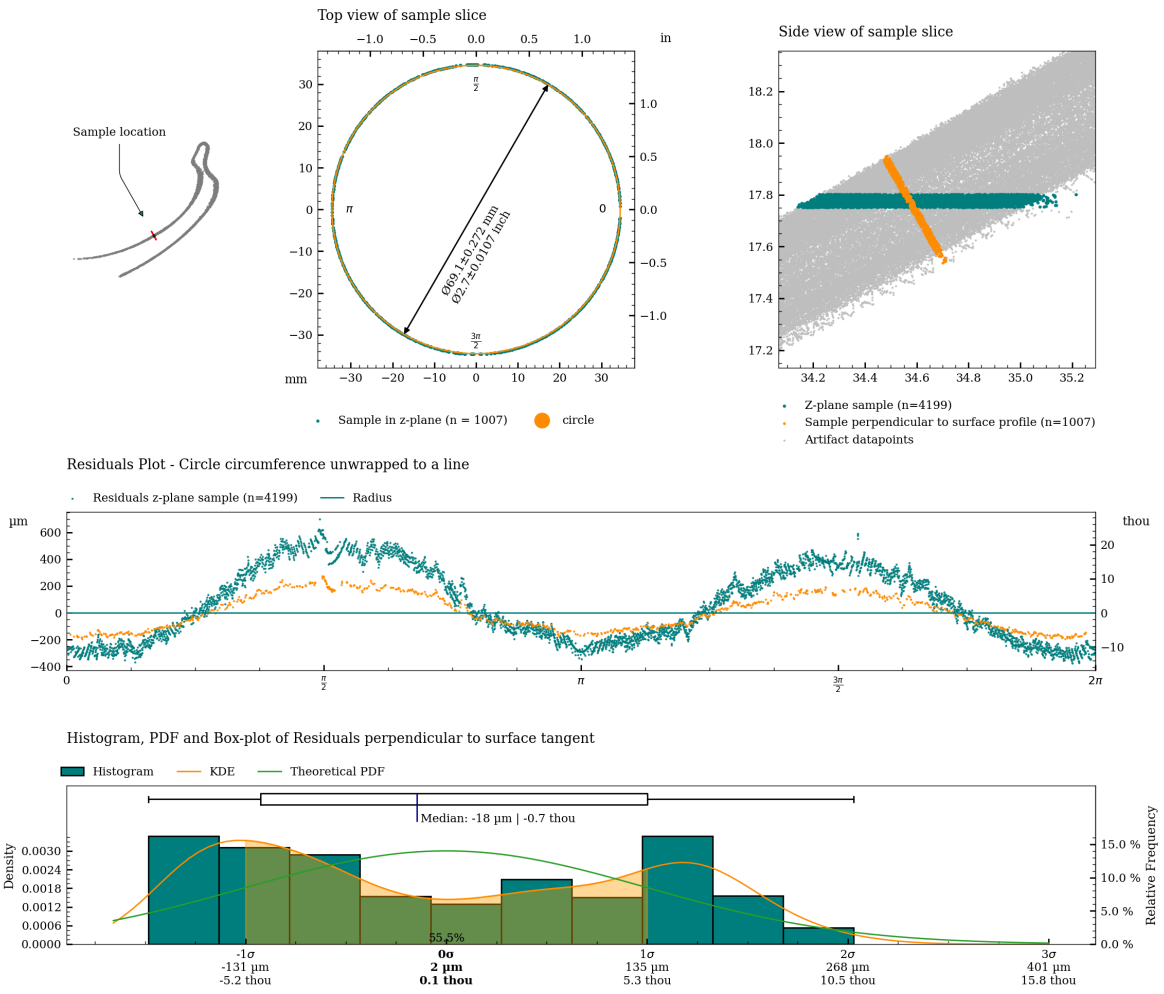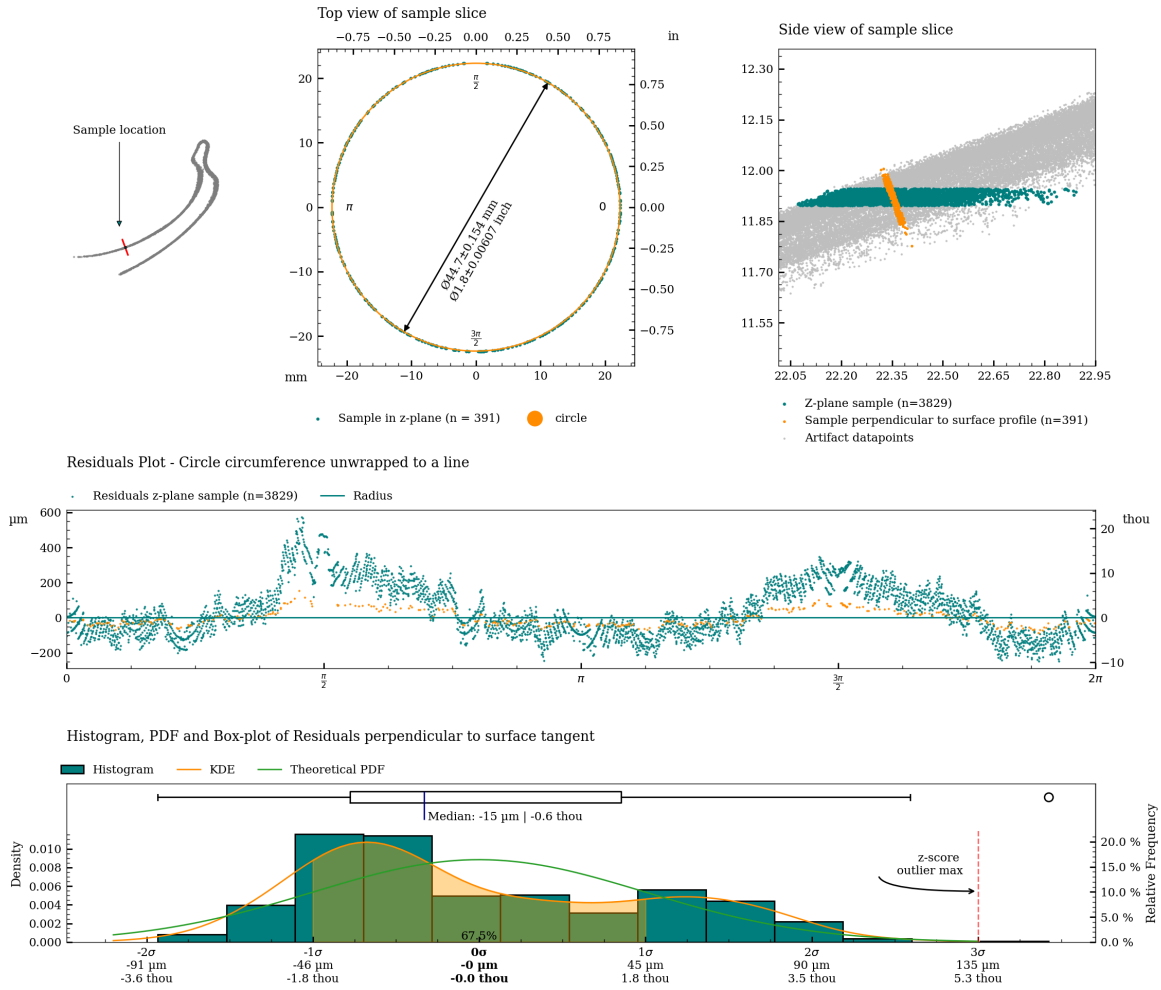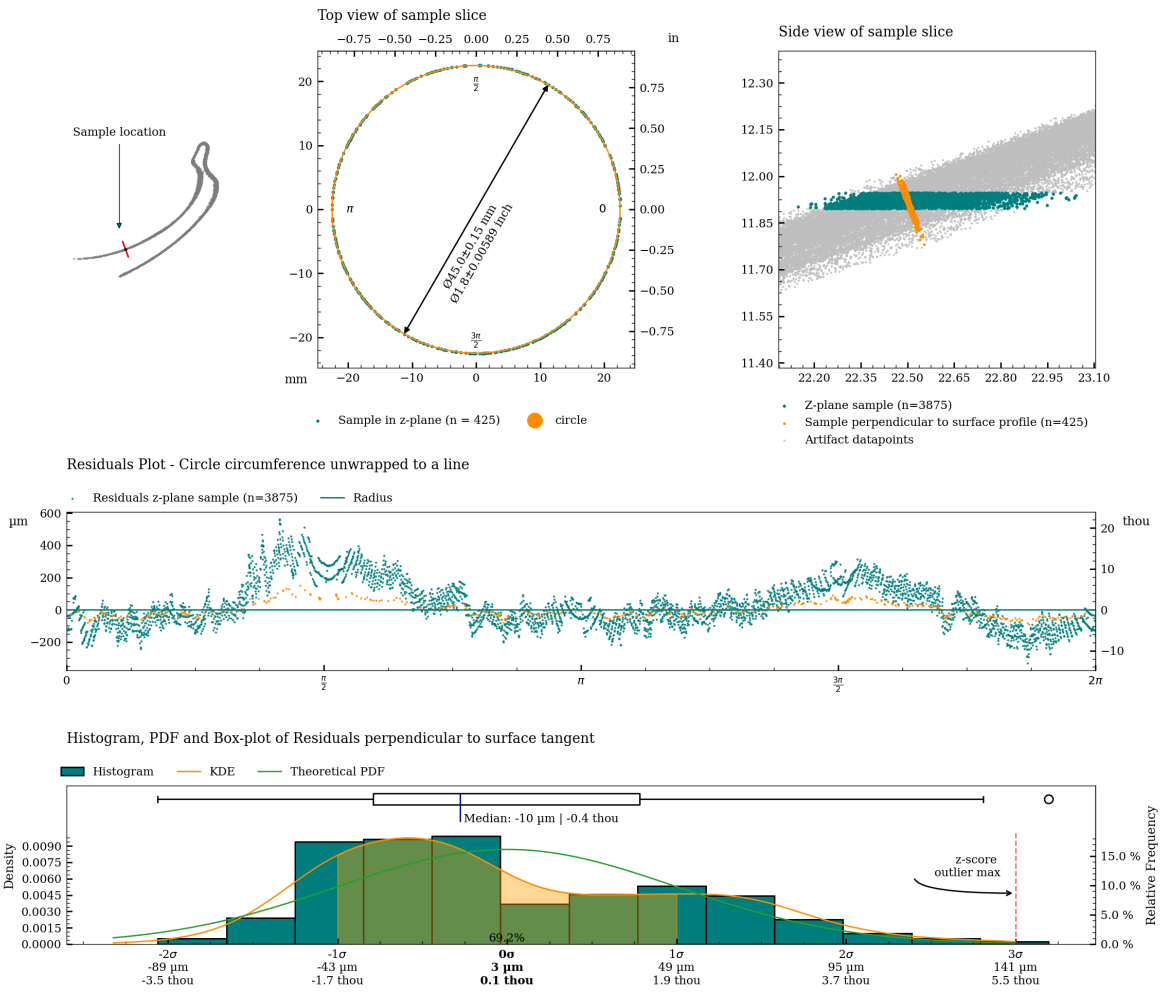
Graphical overview of circularity measurement c08_s

Top view of sample slice

Side view of sample slice

Sample location

Ø971±0.16 mm
Ø3.8±0.00632 inch

- Sample in z-plane (n = 2196)
- circle

- Z-plane sample (n=3696)
- Sample perpendicular to surface profile (n=2196)
- Artifact datapoints

Residuals Plot - Circle circumference unwrapped to a line

- Residuals z-plane sample (n=3696) — Radius

Histogram, PDF and Box-plot of Residuals perpendicular to surface tangent

- Histogram — KDE — Theoretical PDF

Median: -8 µm | -0.3 thou

62.2%

	-2σ	-1σ	0σ	1σ	2σ	3σ
	-133 µm	-69 µm	**-5 µm**	59 µm	122 µm	186 µm
	-5.2 thou	-2.7 thou	**-0.2 thou**	2.3 thou	4.8 thou	7.3 thou

Figure 14: Charts with statistics for the measurement of c08_s.

Graphical overview of circularity measurement c09

Top view of sample slice

Side view of sample slice

Sample location

Ø69.0±0.269 mm
Ø2.7±0.0106 inch

- Sample in z-plane (n = 969)
- circle

- Z-plane sample (n=4156)
- Sample perpendicular to surface profile (n=969)
- Artifact datapoints

Residuals Plot - Circle circumference unwrapped to a line

- Residuals z-plane sample (n=4156)
- Radius

Histogram, PDF and Box-plot of Residuals perpendicular to surface tangent

- Histogram
- KDE
- Theoretical PDF

Median: -26 µm | -1.0 thou

	-2σ	-1σ	0σ	1σ	2σ	3σ
	-256 µm	-132 µm	-8 µm	116 µm	240 µm	364 µm
	-10.1 thou	-5.2 thou	-0.3 thou	4.6 thou	9.5 thou	14.3 thou

58.6%

Figure 15: Charts with statistics for the measurement of c09.

Graphical overview of circularity measurement c09_s

Top view of sample slice

Side view of sample slice

Sample location

Ø69.1±0.272 mm
Ø2.7±0.0107 inch

- Sample in z-plane (n = 1007)
- circle

- Z-plane sample (n=4199)
- Sample perpendicular to surface profile (n=1007)
- Artifact datapoints

Residuals Plot - Circle circumference unwrapped to a line

- Residuals z-plane sample (n=4199) — Radius

Histogram, PDF and Box-plot of Residuals perpendicular to surface tangent

- Histogram — KDE — Theoretical PDF

Median: -18 μm | -0.7 thou

55.5%

	-1σ	0σ	1σ	2σ	3σ
	-131 μm	2 μm	135 μm	268 μm	401 μm
	-5.2 thou	0.1 thou	5.3 thou	10.5 thou	15.8 thou

Figure 16: Charts with statistics for the measurement of c09_s.

Graphical overview of circularity measurement c10

Top view of sample slice

Side view of sample slice

Sample location

Ø44.7±0.154 mm
Ø1.8±0.00607 inch

- Sample in z-plane (n = 391)
- circle

- Z-plane sample (n=3829)
- Sample perpendicular to surface profile (n=391)
- Artifact datapoints

Residuals Plot - Circle circumference unwrapped to a line

- Residuals z-plane sample (n=3829) — Radius

Histogram, PDF and Box-plot of Residuals perpendicular to surface tangent

- Histogram — KDE — Theoretical PDF

Median: -15 µm | -0.6 thou

67.5%

z-score outlier max

	-2σ	-1σ	0σ	1σ	2σ	3σ
-91 µm	-46 µm	-0 µm	45 µm	90 µm	135 µm
-3.6 thou	-1.8 thou	-0.0 thou	1.8 thou	3.5 thou	5.3 thou

Figure 17: Charts with statistics for the measurement of c10.

Graphical overview of circularity measurement c10_s

Figure 18: Charts with statistics for the measurement of c10_s.

Table 2 shows statistical measures of the circularity of the vessel, measured along the full height (areas on the artifact scan containing damaged parts have been removed to the best extent possible to reduce the influence of the measurement).

Metric

Area	Range			Standard Deviation			RMSD			Slices	Slice height
	Median	Min.	Max.	Median	Min.	Max.	Median	Min.	Max.		
	mm	mm	mm	mm	mm	mm	mm	mm	mm		mm
Exterior	1.055	0.241	1.989	0.131	0.021	0.259	0.184	0.034	0.498	1042	0.050
Interior	0.454	0.146	1.999	0.057	0.018	0.296	0.108	0.034	0.497	637	0.050
Interior separate	0.424	0.107	1.403	0.040	0.014	0.158	0.077	0.027	0.310	637	0.050

Imperial

Area	Range			Standard Deviation			RMSD			Slices	Slice height
	Median	Min.	Max.	Median	Min.	Max.	Median	Min.	Max.		
	in	in	in	in	in	in	in	in	in		in
Exterior	1.055	0.241	1.989	0.131	0.021	0.259	0.184	0.034	0.498	1042	0.050
Interior	0.454	0.146	1.999	0.057	0.018	0.296	0.108	0.034	0.497	637	0.050
Interior separate	0.424	0.107	1.403	0.040	0.014	0.158	0.077	0.027	0.310	637	0.050

Table 2: Perpendicular Circularity analysis of MV009.

Circularity analysis of exterior surface
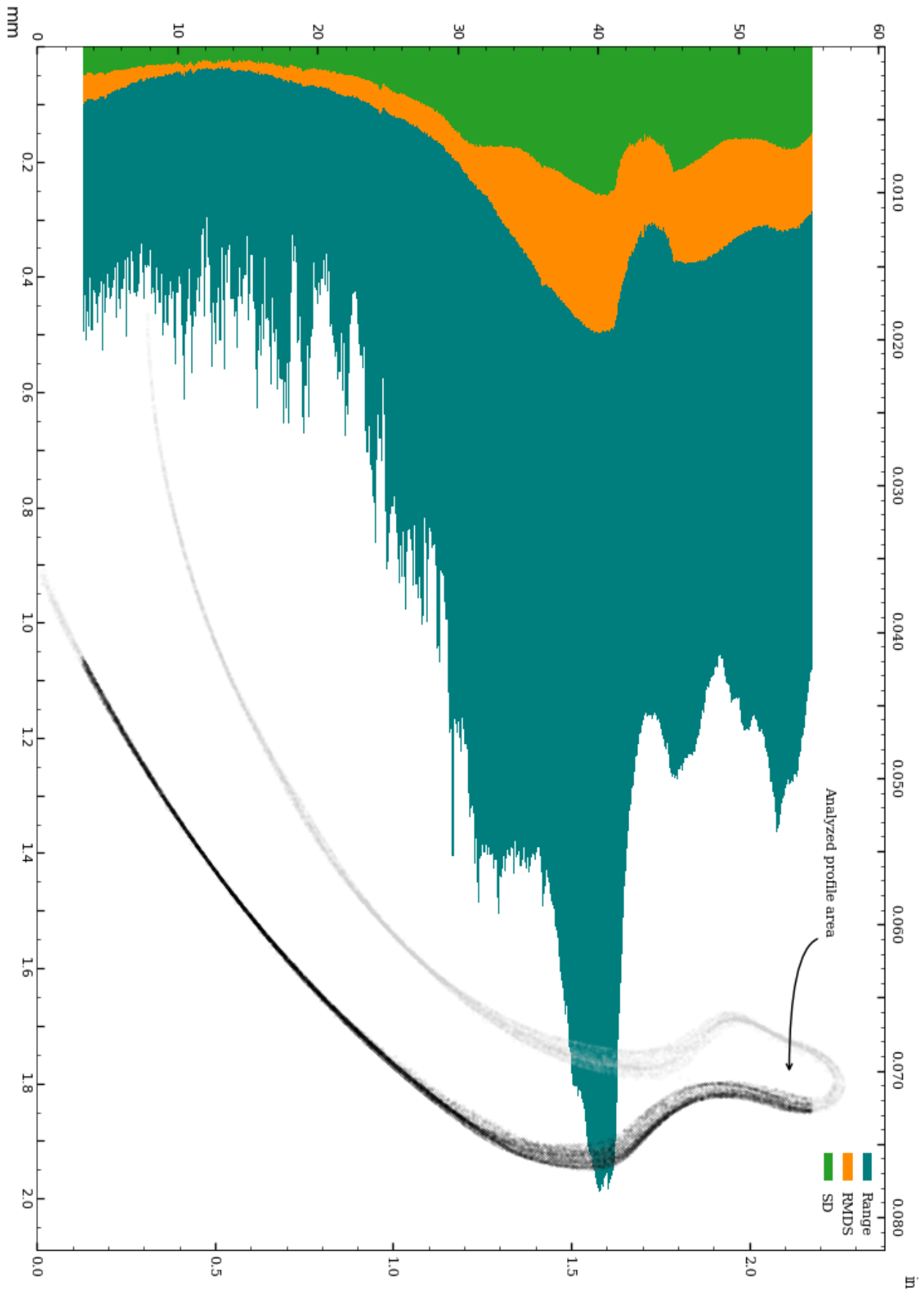
Figure 19: Circularity of exterior surface.

Circularity analysis of exterior surface, Standard Deviation and Root Mean Squared Deviation
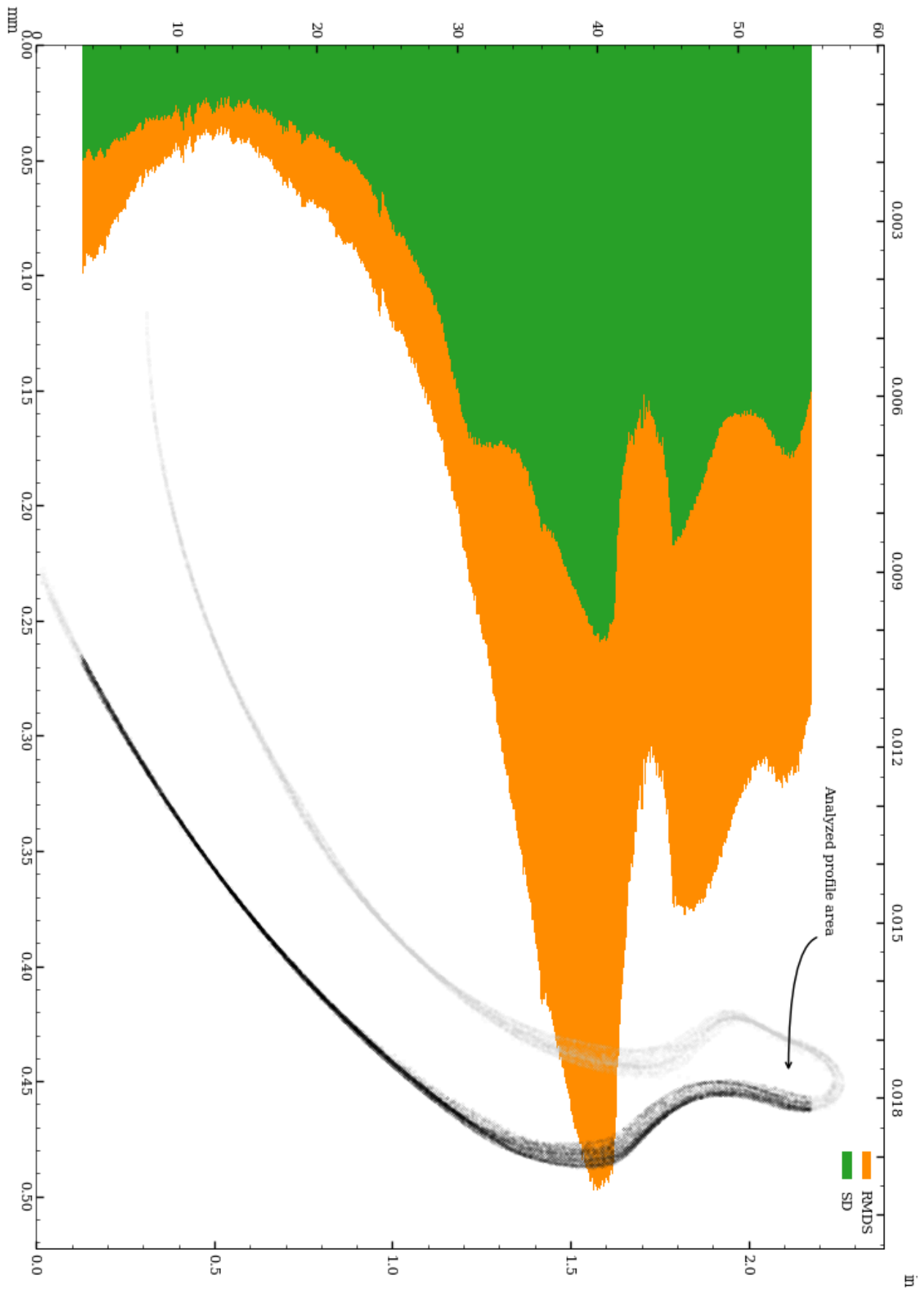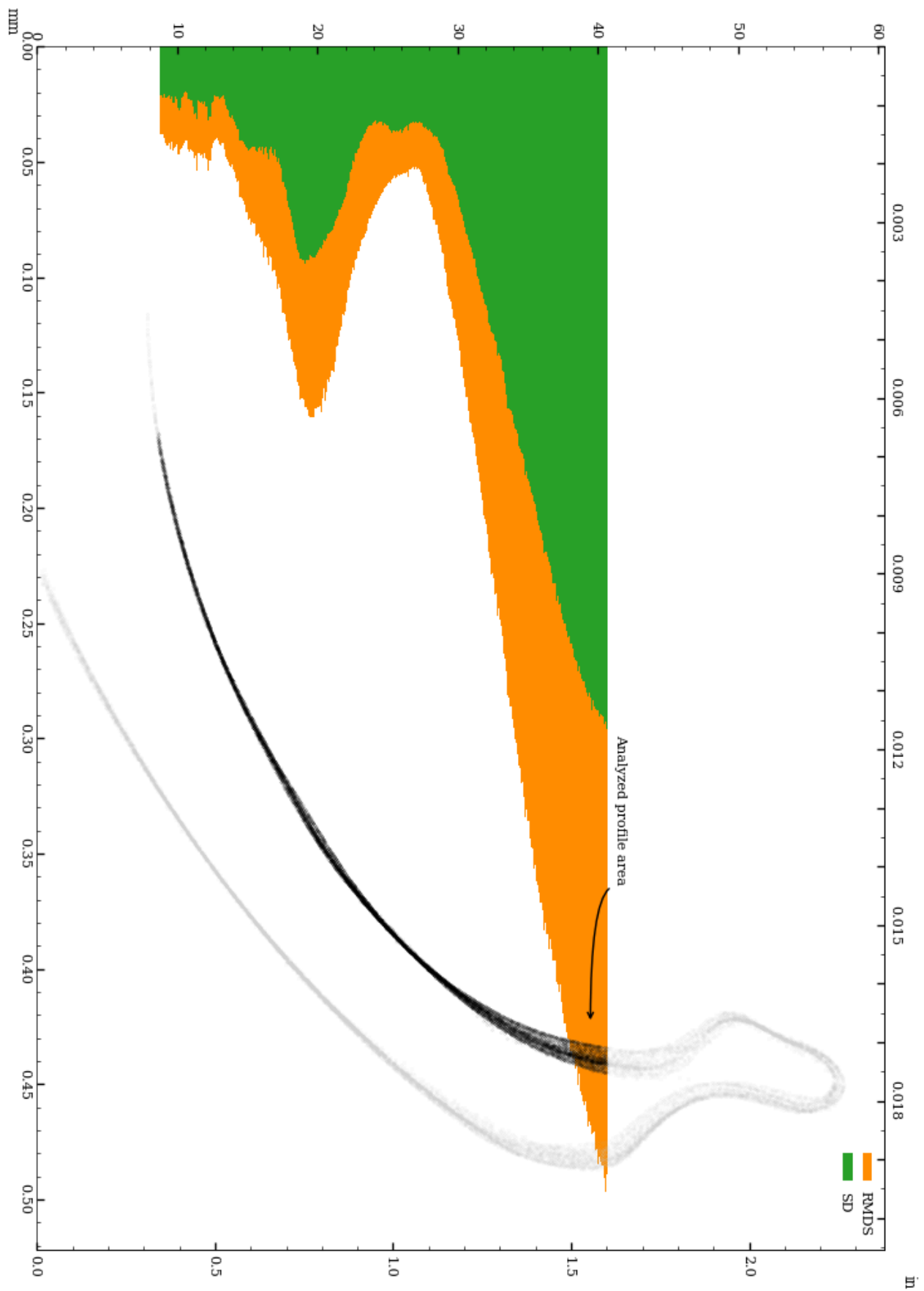

Figure 20: Vessel circularity of exterior surface, standard deviation and median absolute deviation.

The distributions of the circularity measurements across 1042 slices of the exterior surface are shown below.

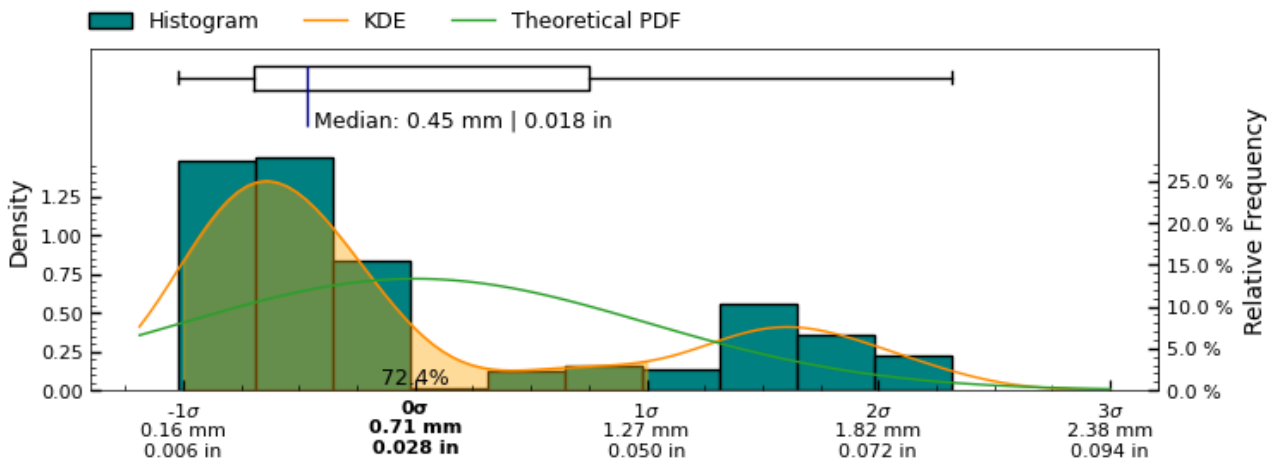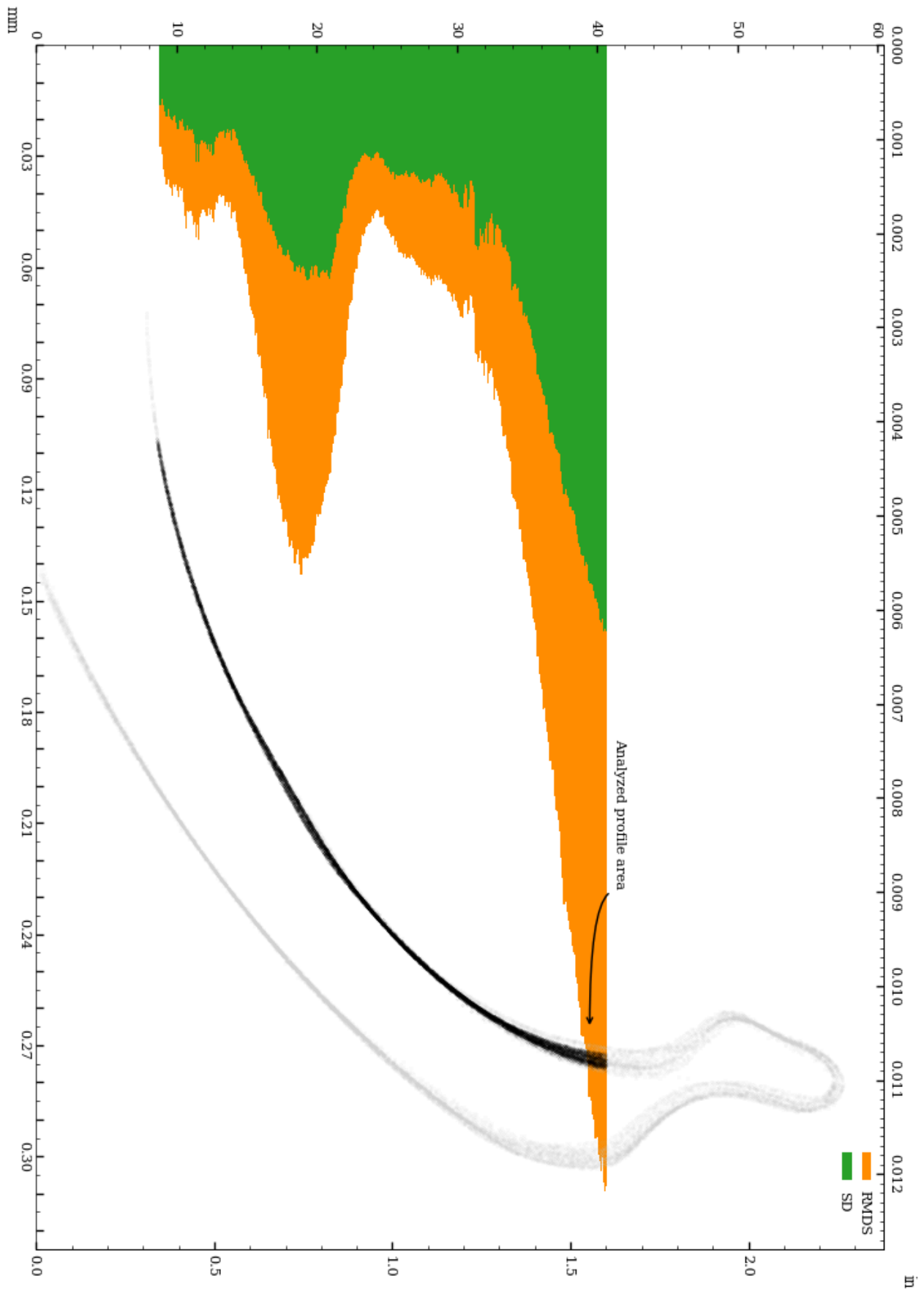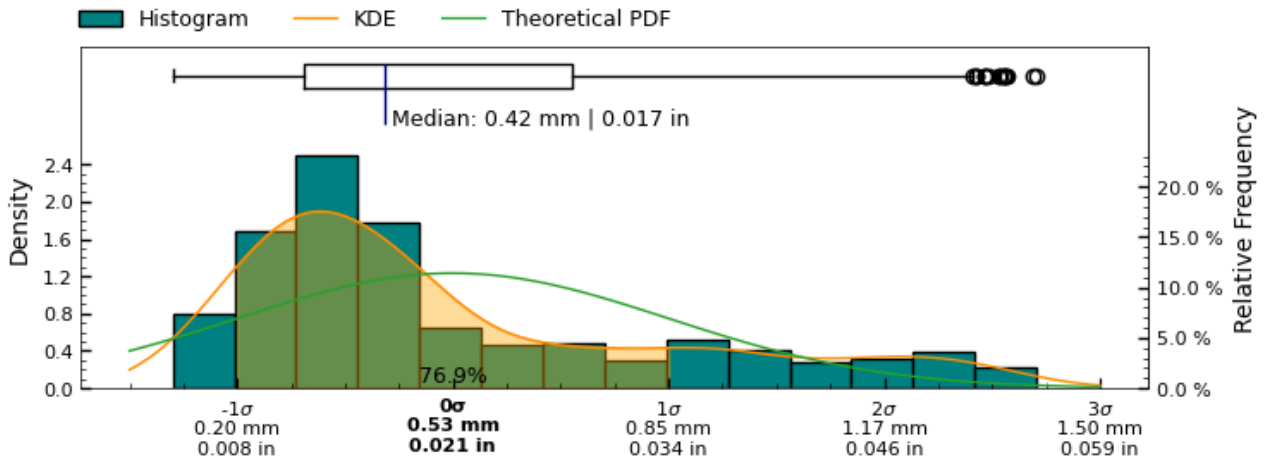**Range measurement distribution across 1042 slices of exterior surface**
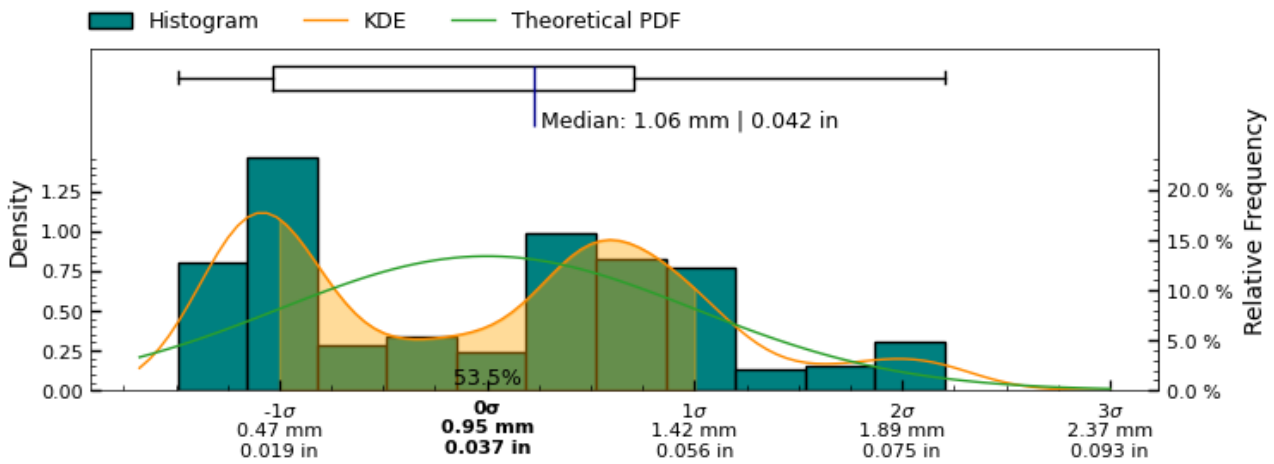
Figure 21: Range measurement distribution across measured slices of exterior surface

Standard Deviation measurement distribution across 1042 slices of exterior surface
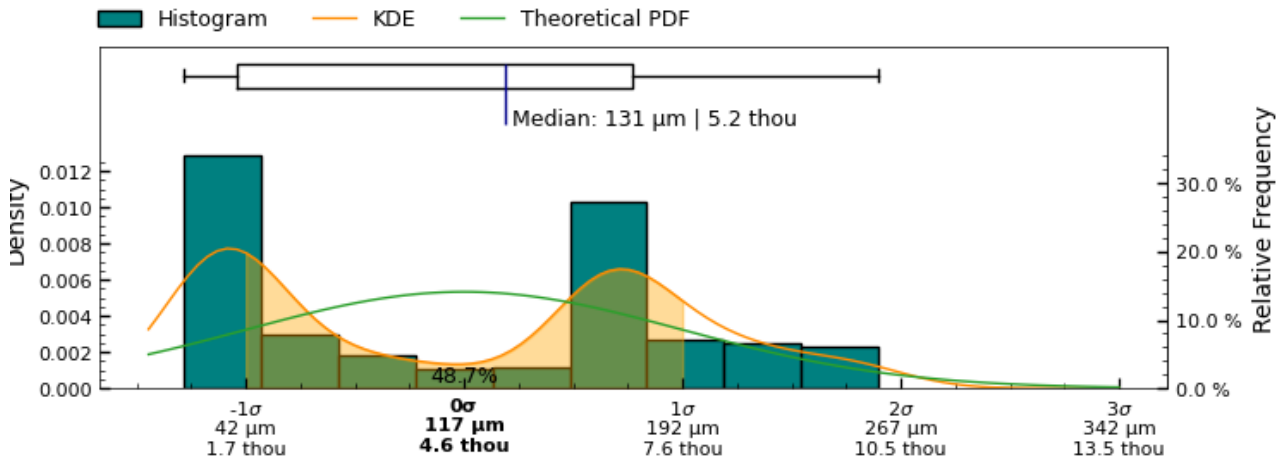
Figure 22: Standard Deviation measurement distribution across measured slices of " + exterior + " surface

Root Mean Squared Deviation measurement distribution across 1042 slices of exterior surface
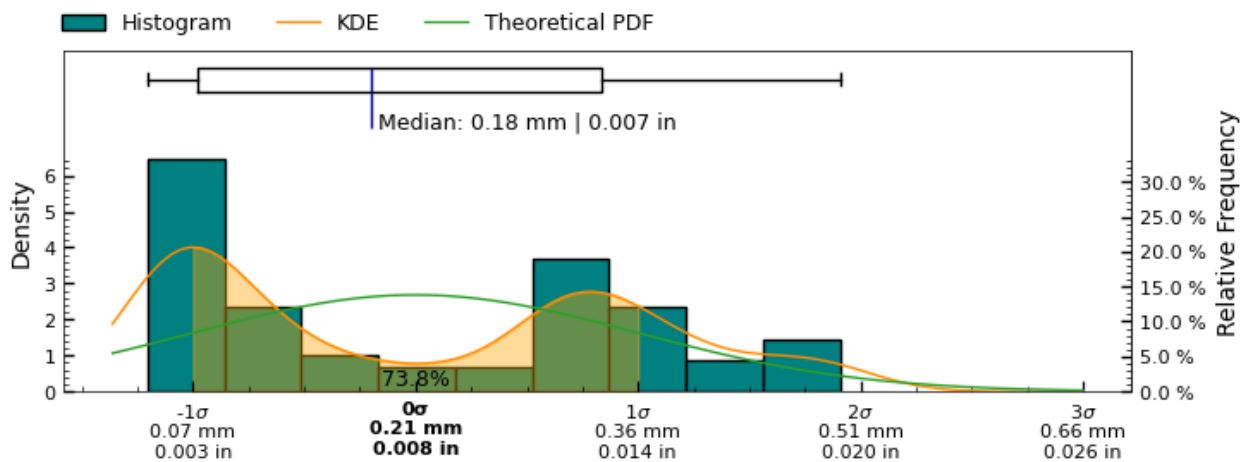
Figure 23: Root Mean Squared Deviation measurement distribution across measured slices of exterior surface

Circularity analysis of interior surface
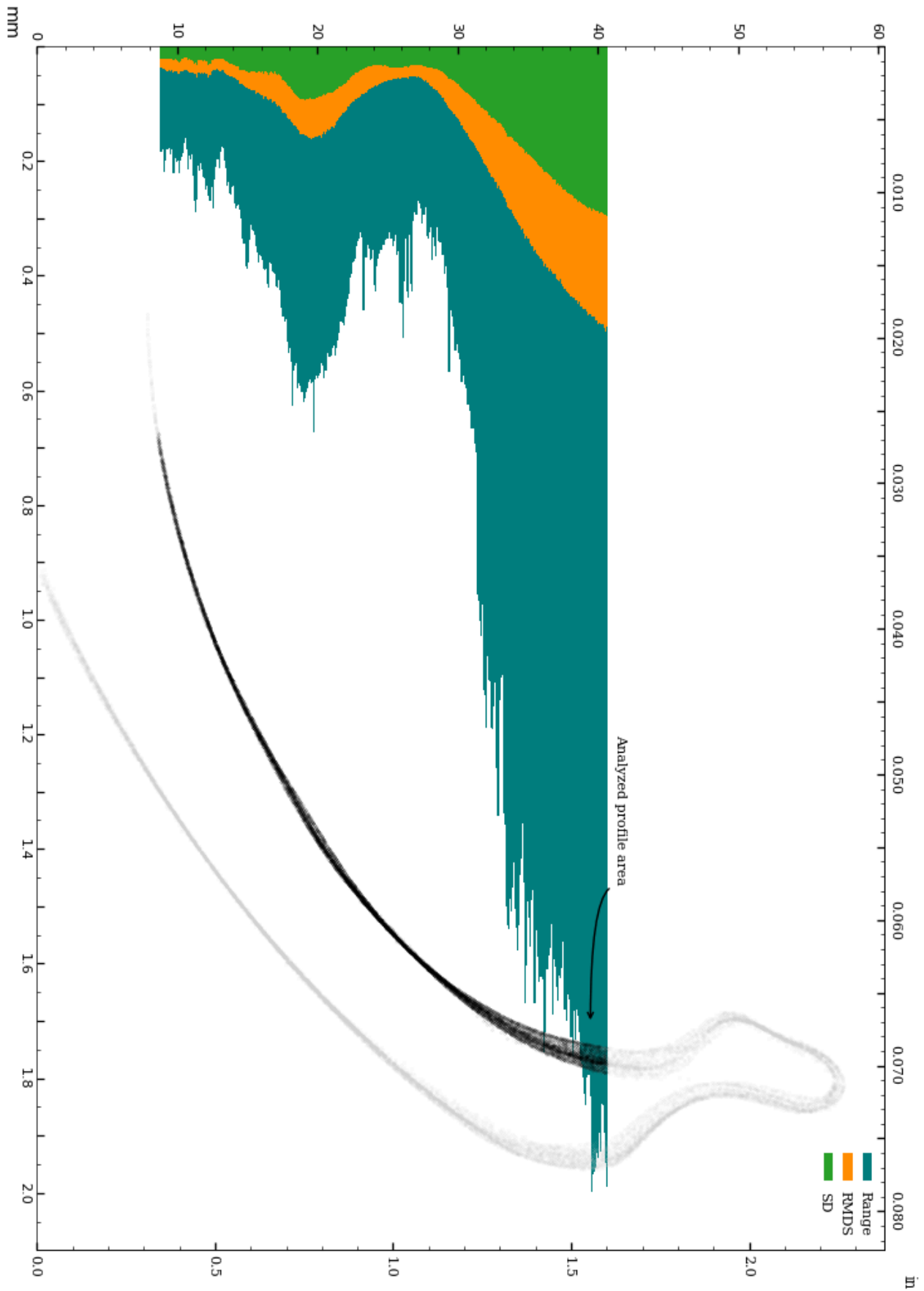
Figure 24: Circularity of interior surface.

Circularity analysis of interior surface, Standard Deviation and Root Mean Squared Deviation

Figure 25: Vessel circularity of interior surface, standard deviation and median absolute deviation.

The distributions of the circularity measurements across 637 slices of the interior surface are shown below.

Range measurement distribution across 637 slices of interior surface

Figure 26: Range measurement distribution across measured slices of interior surface

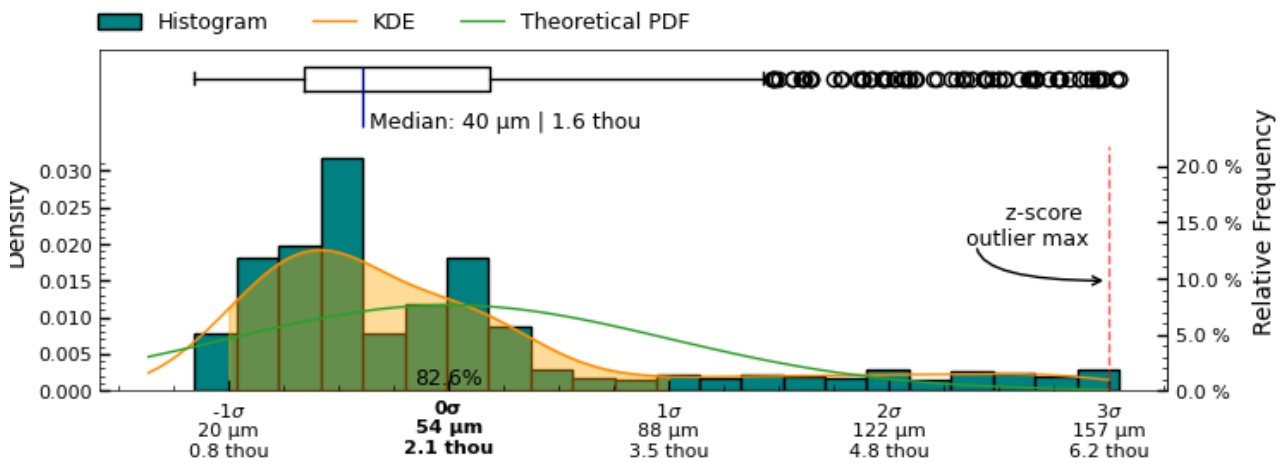**Standard Deviation measurement distribution across 637 slices of interior surface**
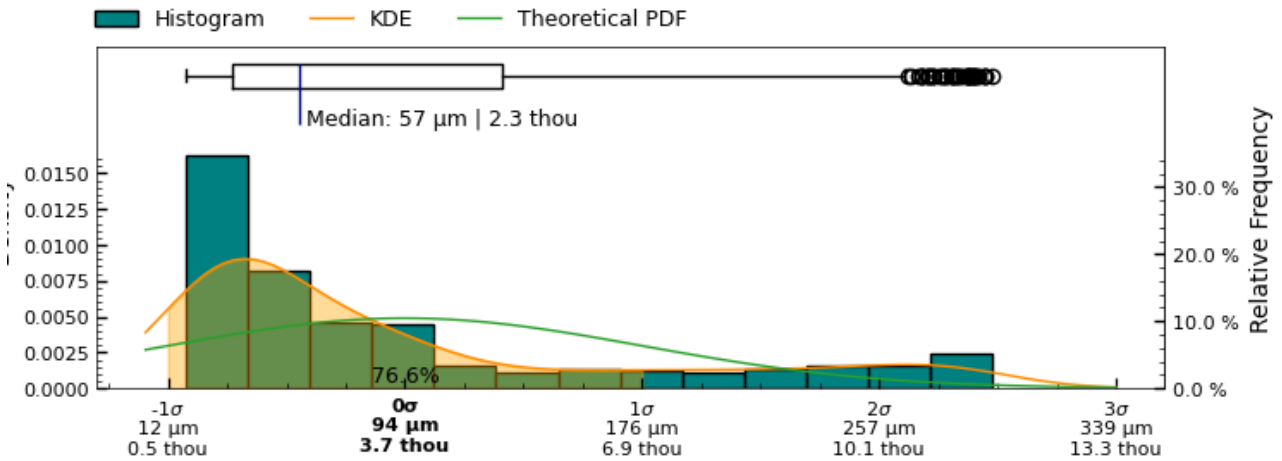
Figure 27: Standard Deviation measurement distribution across measured slices of " + interior + " surface

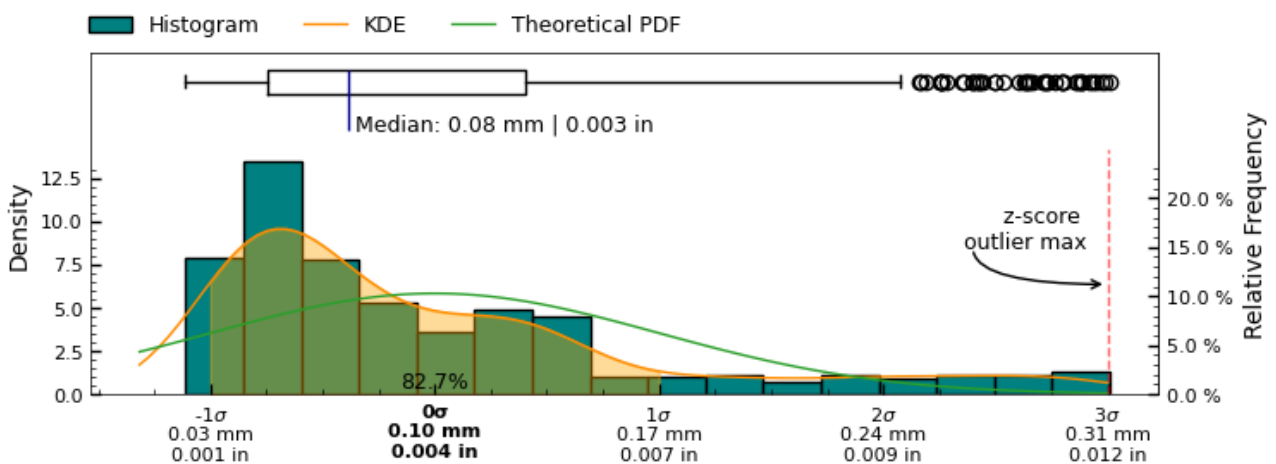**Root Mean Squared Deviation measurement distribution across 637 slices of interior surface**
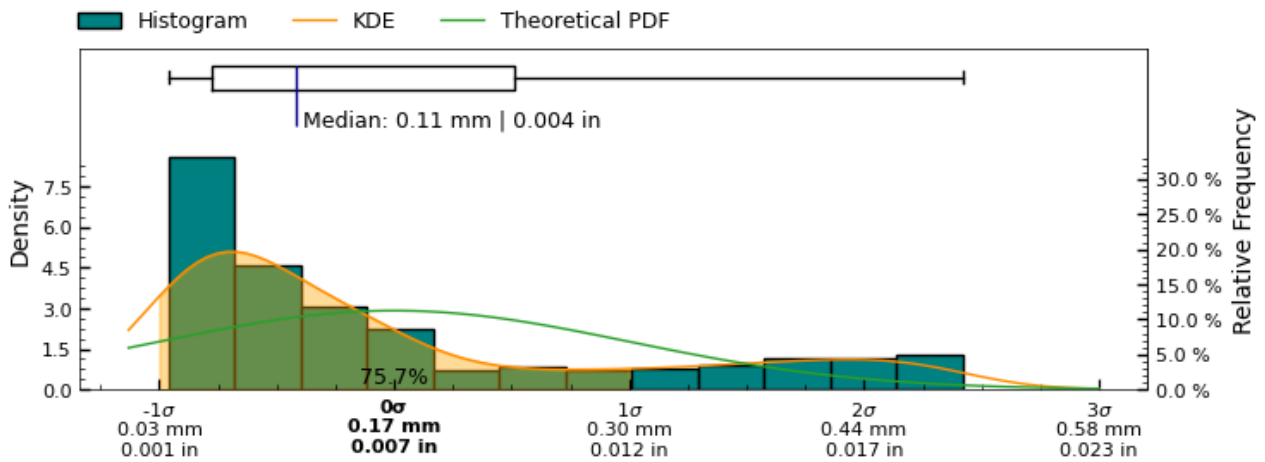
Figure 28: Root Mean Squared Deviation measurement distribution across measured slices of interior surface

Circularity analysis of interior separately aligned surface
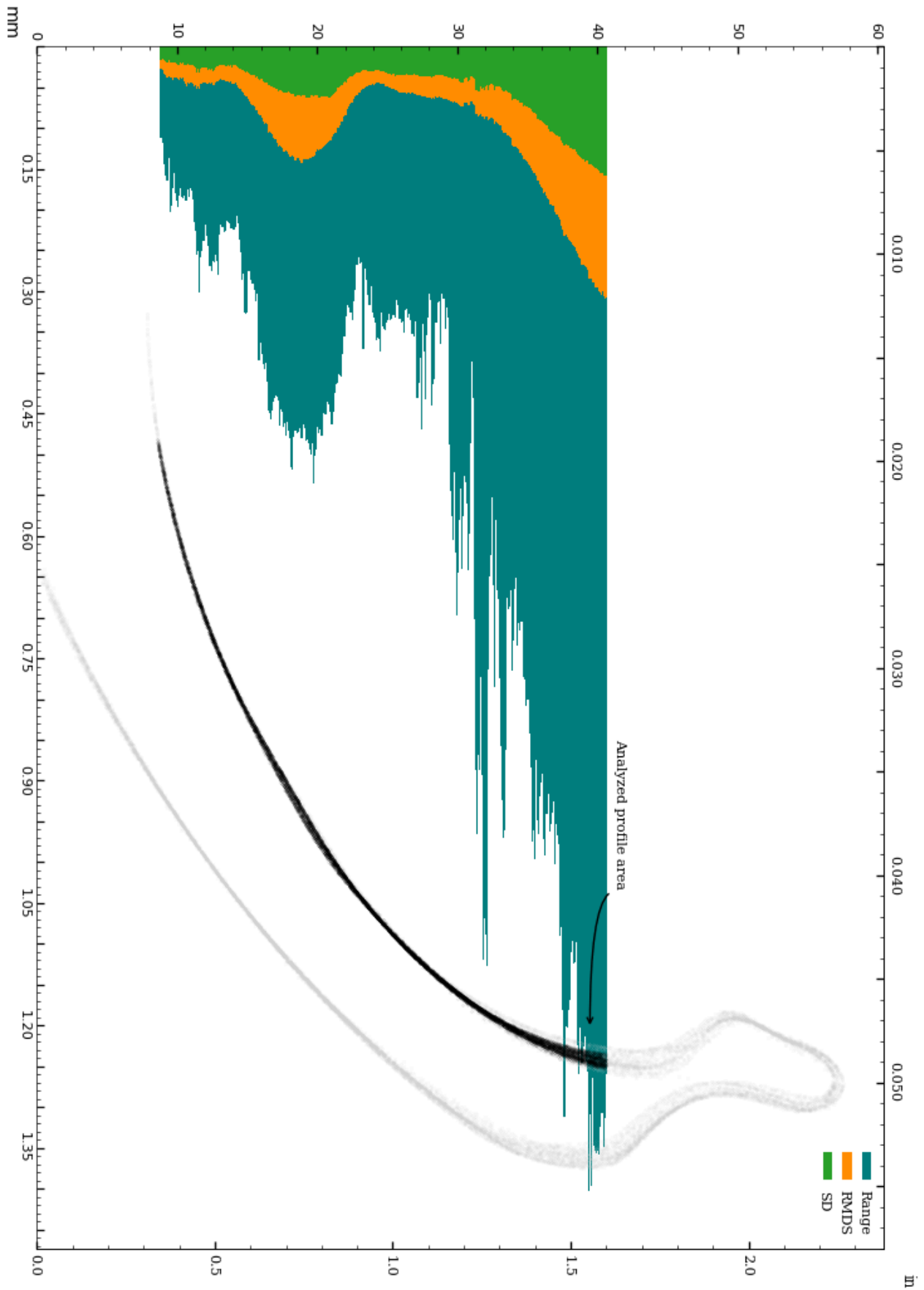
Figure 29: Circularity of interior_separate surface.

Circularity analysis of interior separately aligned surface, Standard Deviation and Root Mean Squared Deviation

Figure 30: Vessel circularity of interior_separate surface, standard deviation and median absolute deviation.

The distributions of the circularity measurements across 637 slices of the interior_separate surface are shown below.

Range measurement distribution across 637 slices of interior separately aligned surface

Figure 31: Range measurement distribution across measured slices of interior_separate surface

Standard Deviation measurement distribution across 637 slices of interior separately aligned surface

Figure 32: Standard Deviation measurement distribution across measured slices of " + interior_separate + " surface

Root Mean Squared Deviation measurement distribution across 637 slices of interior separately aligned surface

Figure 33: Root Mean Squared Deviation measurement distribution across measured slices of interior separately aligned surface

Concentricity

The concentricity metric describes the deviation in the center-point of the referenced features. As such, it is a measure to determine if several features of the object share the same center point/axis, and how closely. See Figure 34 for a visual representation of this metric.
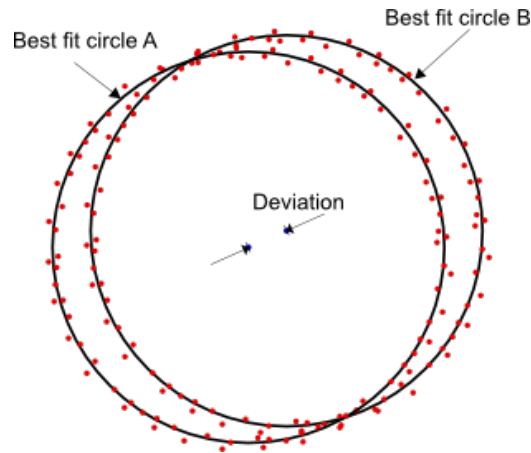
Figure 34: Concentricity measures the deviation (distance) between the center of two circles.

Determination of concentricity has been carried out by establishing the best fit circles of sample slices, using RANSAC (Random sample consensus) algorithm for outlier detection of a least squares circle regression on the scanned data-points at each cross-section, to estimate centers of each cross-section.

The concentricity between both the interior and exterior circular cross-sections is explored for cross-section measurements with the same Z-coordinates.

Additionally, the concentricity between each cross-section measurement defined in Figure 4 and the datum axis $(x, y) = (0, 0)$ has been calculated to establish the deviation of the feature center from the datum axis.
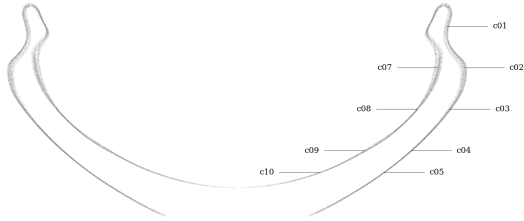
Figure 35: Circularity measurement sample locations, full mesh aligned to exterior surface
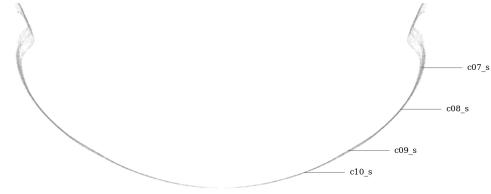

Figure 36: Circularity measurement sample location, separately aligned interior mesh

Metric

Tag	Reference	Deviation	Sample size	Circle fit residuals analysis for sample listed in Tag column						
				Range full	Range inliers	RMSD full	RMDS inliers	SD full	SD inliers	Center (x,y)
		mm		mm	mm	mm	mm	mm	mm	μm
c01	z-axis	0.411	2721	1.942	1.942	0.612	0.612	0.335	0.335	−180, −369
c02	z-axis	0.189	3572	2.179	2.179	0.551	0.551	0.302	0.302	44, −184
c03	z-axis	0.146	2724	1.174	1.073	0.255	0.241	0.159	0.146	11, 146
c04	z-axis	0.042	1899	0.575	0.311	0.077	0.075	0.041	0.038	6, 41
c05	z-axis	0.009	1441	0.380	0.212	0.039	0.035	0.025	0.020	−8, −4
c07	z-axis	0.621	4299	2.004	2.004	0.506	0.506	0.312	0.312	−619, −39
c07_s	z-axis	0.256	4069	1.540	1.540	0.376	0.376	0.202	0.202	233, 106
c08	z-axis	0.085	2221	0.425	0.425	0.110	0.110	0.053	0.053	−81, −27
c08_s	z-axis	0.023	2196	0.335	0.335	0.068	0.068	0.038	0.038	8, −22
c09	z-axis	0.035	969	0.516	0.516	0.128	0.128	0.071	0.071	30, 18
c09_s	z-axis	0.021	1007	0.467	0.467	0.133	0.133	0.057	0.057	−17, 13
c10	z-axis	0.001	391	0.242	0.242	0.045	0.045	0.023	0.023	−1, −0
c10_s	z-axis	0.003	425	0.242	0.242	0.046	0.046	0.026	0.026	−3, 2
c02	c07_s	0.346								−189, −290
c03	c08_s	0.168								3, 168
c04	c09_s	0.036								22, 28
c05	c10_s	0.008								−5, −6

Imperial

Tag	Reference	Deviation	Sample size	Circle fit residuals analysis for sample listed in Tag column						
				Range full	Range inliers	RMSD full	RMDS inliers	SD full	SD inliers	Center (x,y)
		in		in	in	in	in	in	in	thou
c01	z-axis	0.0162	2721	0.0765	0.0765	0.0241	0.0241	0.0132	0.0132	−7.1, −14.5
c02	z-axis	0.0075	3572	0.0858	0.0858	0.0217	0.0217	0.0119	0.0119	1.7, −7.2
c03	z-axis	0.0058	2724	0.0462	0.0422	0.0100	0.0095	0.0062	0.0058	0.4, 5.7
c04	z-axis	0.0016	1899	0.0226	0.0122	0.0030	0.0029	0.0016	0.0015	0.2, 1.6
c05	z-axis	0.0004	1441	0.0150	0.0084	0.0015	0.0014	0.0010	0.0008	−0.3, −0.2
c07	z-axis	0.0244	4299	0.0789	0.0789	0.0199	0.0199	0.0123	0.0123	−24.4, −1.5
c07_s	z-axis	0.0101	4069	0.0606	0.0606	0.0148	0.0148	0.0080	0.0080	9.2, 4.2
c08	z-axis	0.0034	2221	0.0167	0.0167	0.0043	0.0043	0.0021	0.0021	−3.2, −1.1
c08_s	z-axis	0.0009	2196	0.0132	0.0132	0.0027	0.0027	0.0015	0.0015	0.3, −0.9
c09	z-axis	0.0014	969	0.0203	0.0203	0.0050	0.0050	0.0028	0.0028	1.2, 0.7
c09_s	z-axis	0.0008	1007	0.0184	0.0184	0.0052	0.0052	0.0023	0.0023	−0.7, 0.5
c10	z-axis	0.0001	391	0.0095	0.0095	0.0018	0.0018	0.0009	0.0009	−0.1, −0.0
c10_s	z-axis	0.0001	425	0.0095	0.0095	0.0018	0.0018	0.0010	0.0010	−0.1, 0.1
c02	c07_s	0.0136								−7.4, −11.4
c03	c08_s	0.0066								0.1, 6.6
c04	c09_s	0.0014								0.9, 1.1
c05	c10_s	0.0003								−0.2, −0.2

Table 3: Concentricity analysis of MV009.
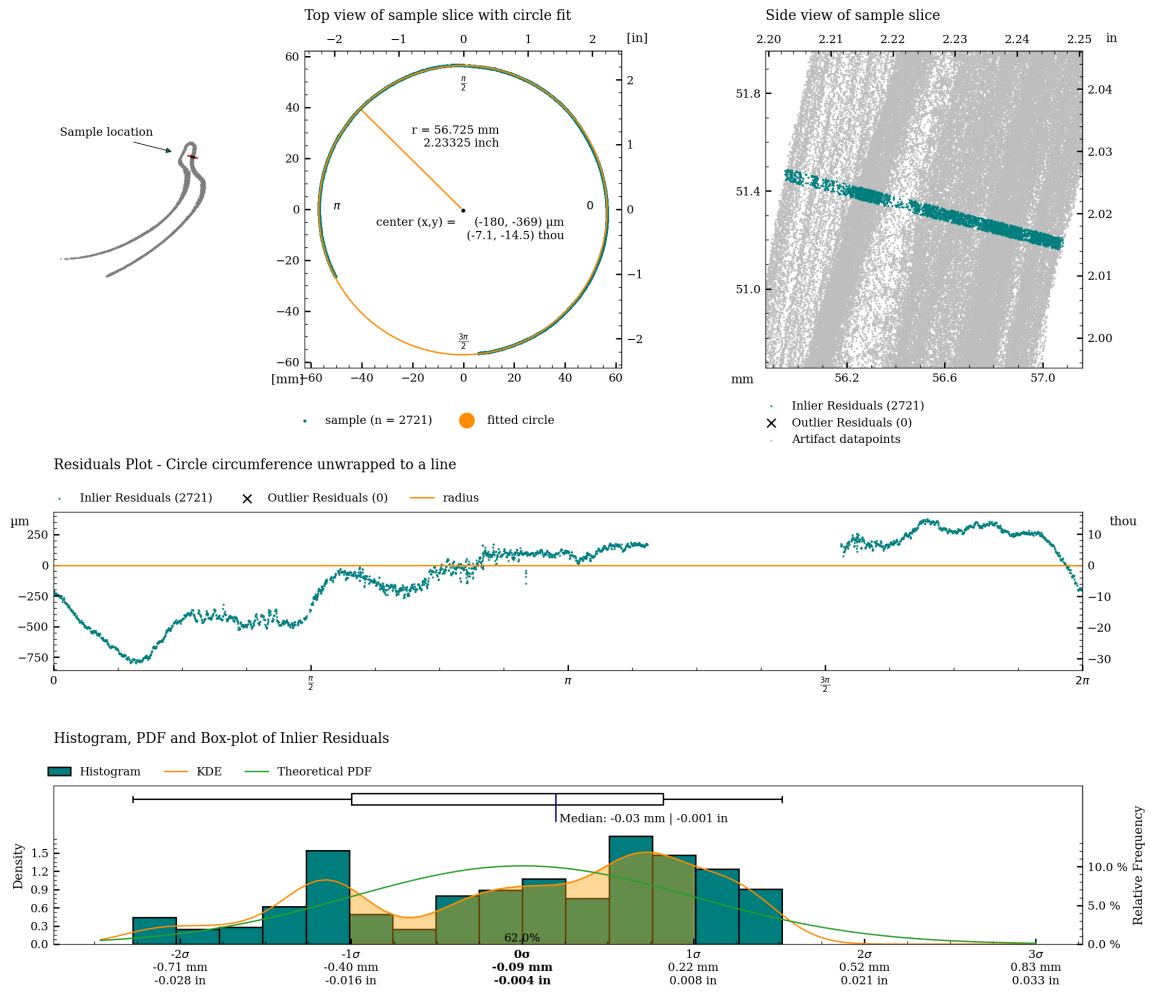
Concentricity analysis of c01

Figure 37: Detailed plot of concentricity measurement for c01.
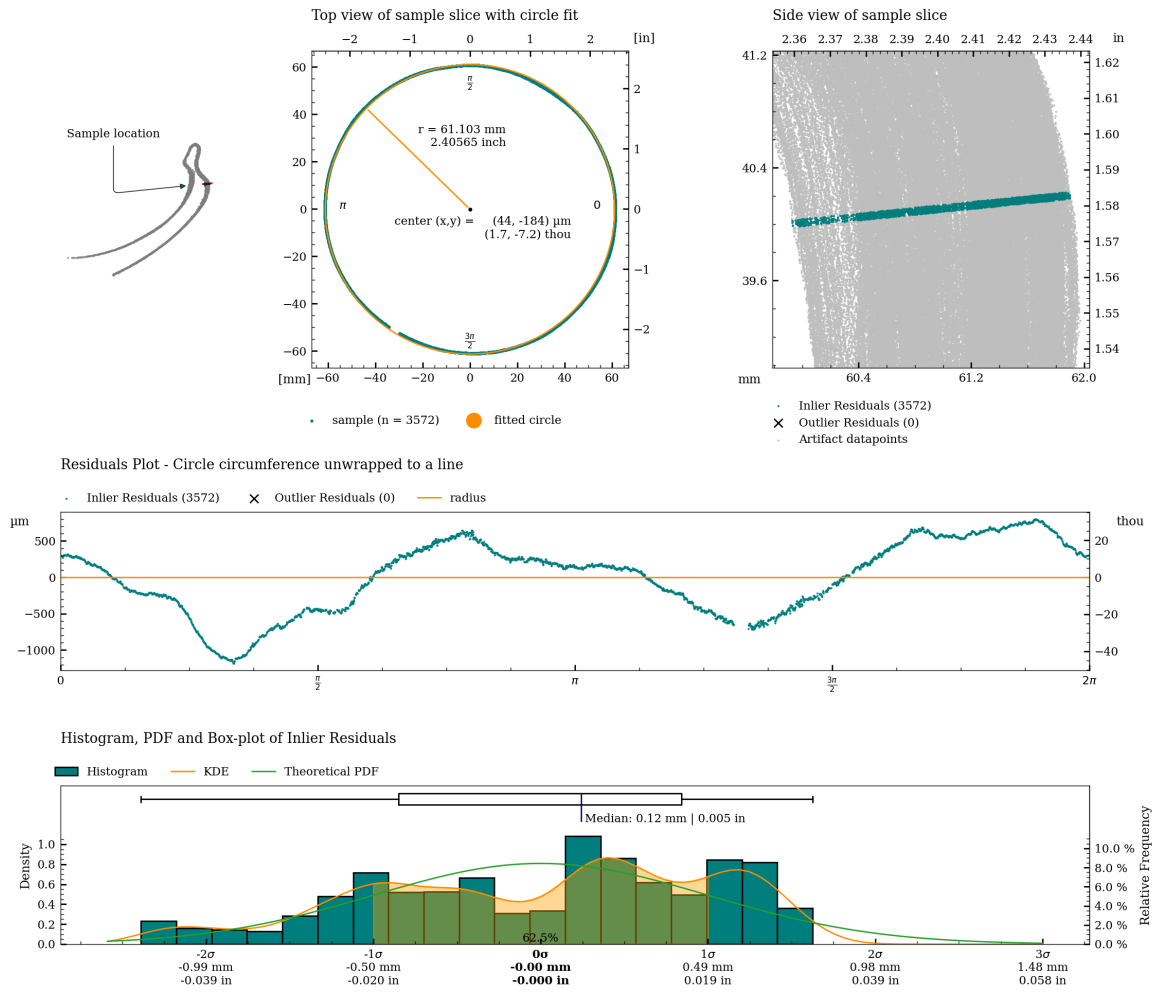
Concentricity analysis of c02

Figure 38: Detailed plot of concentricity measurement for c02.
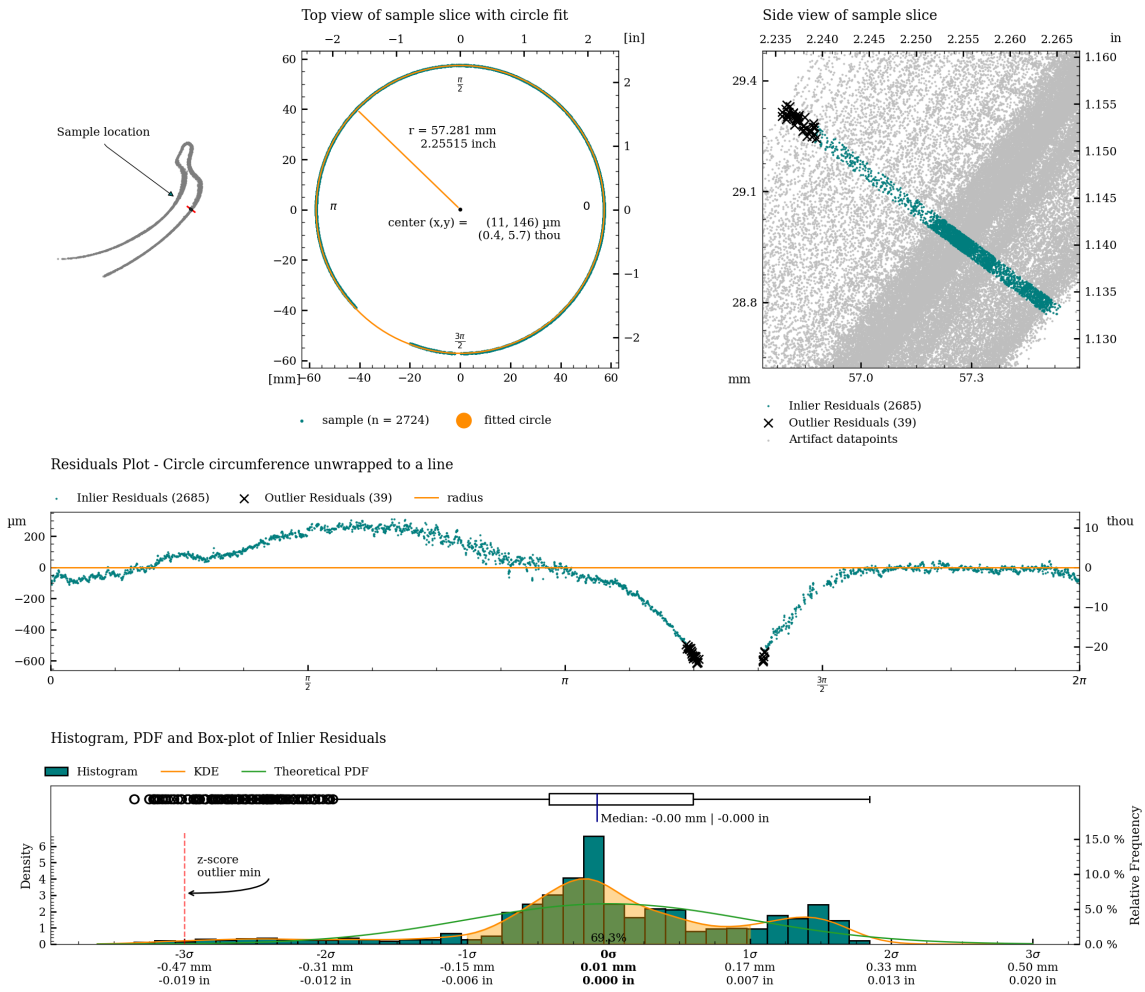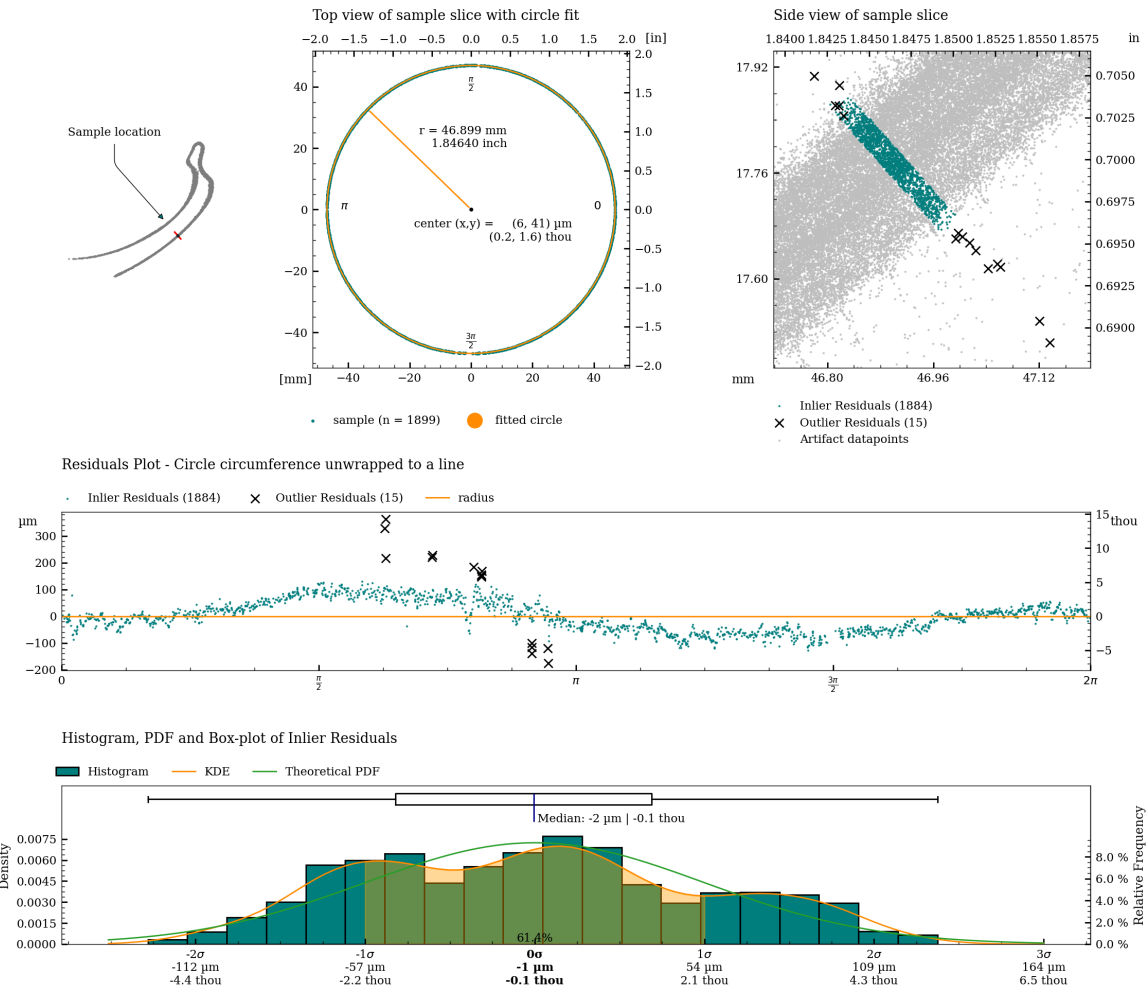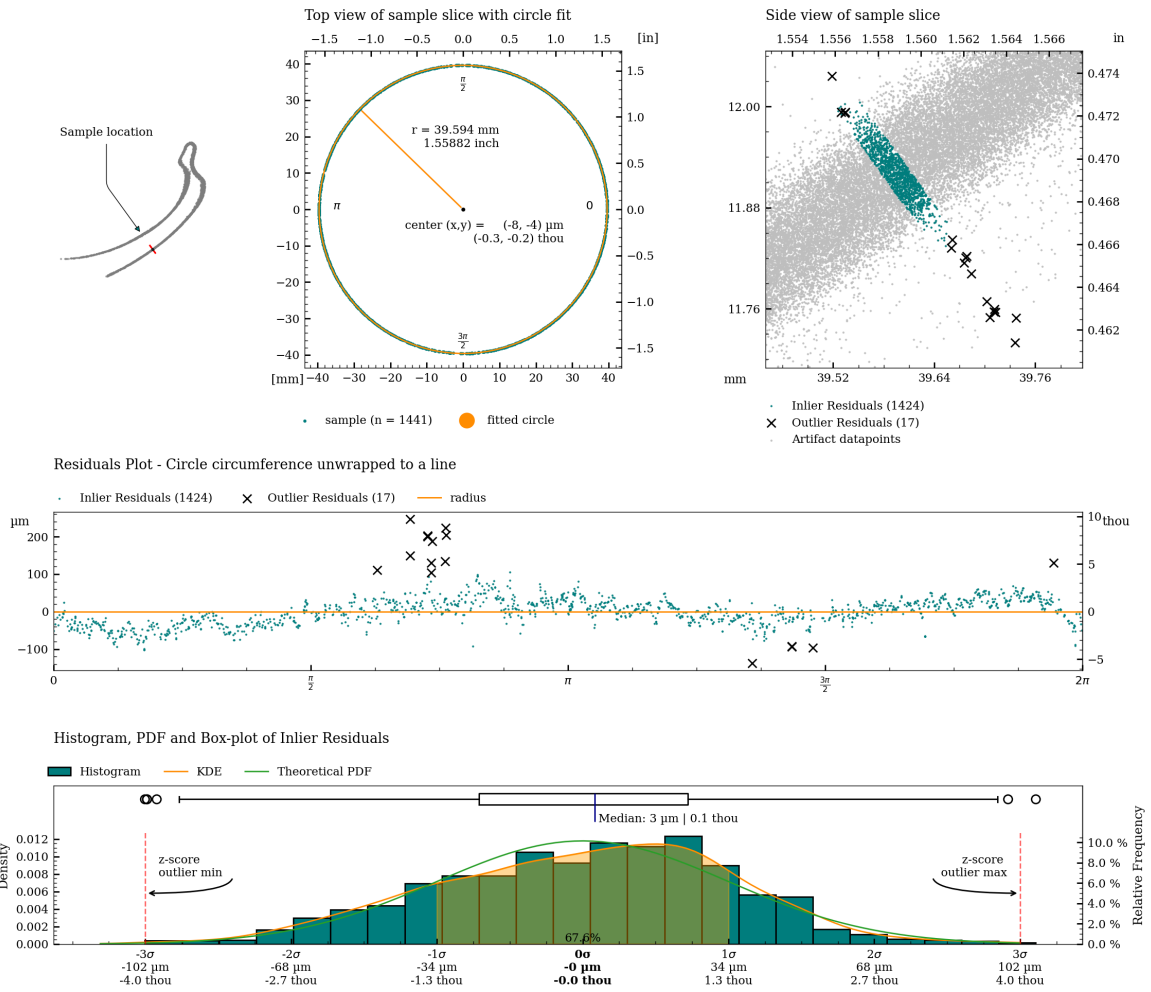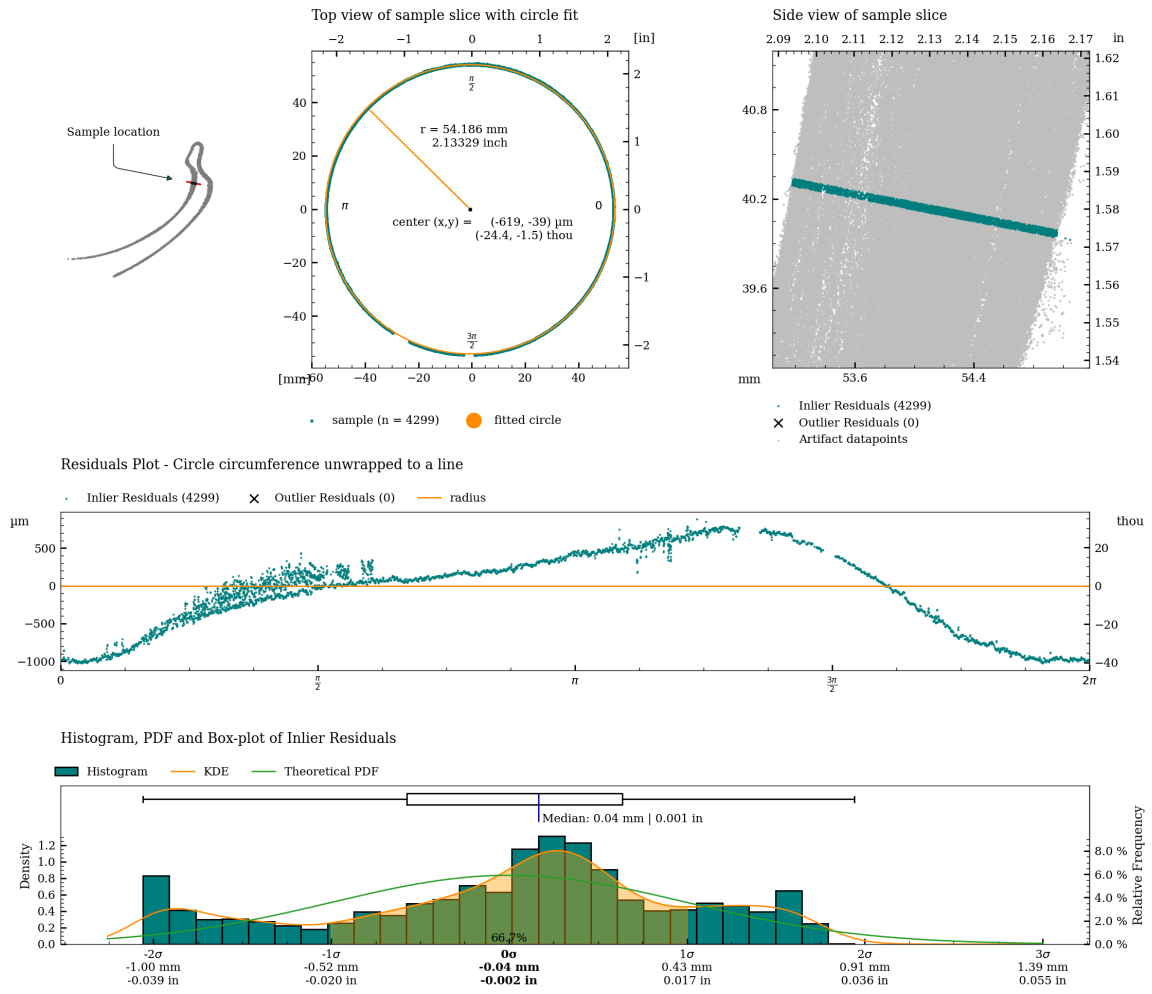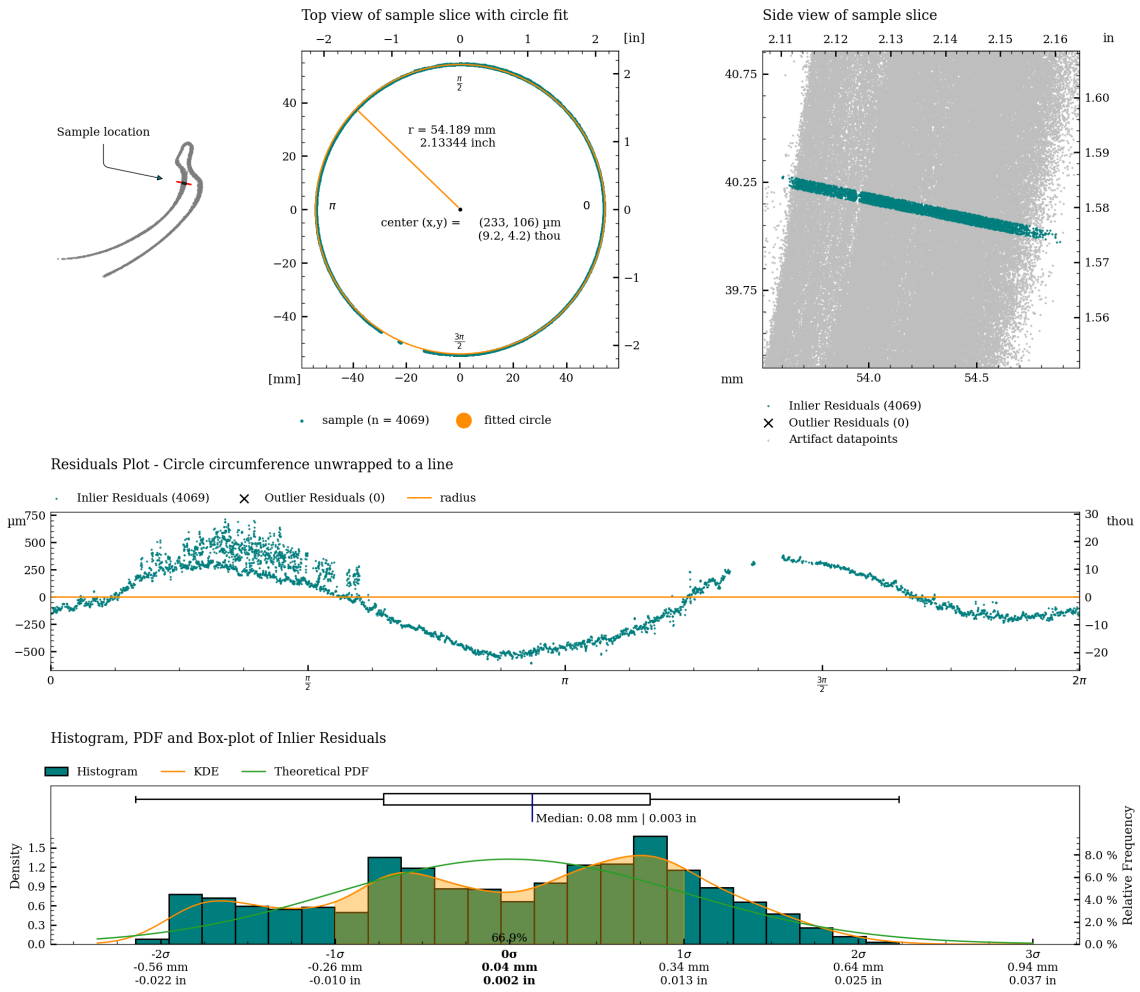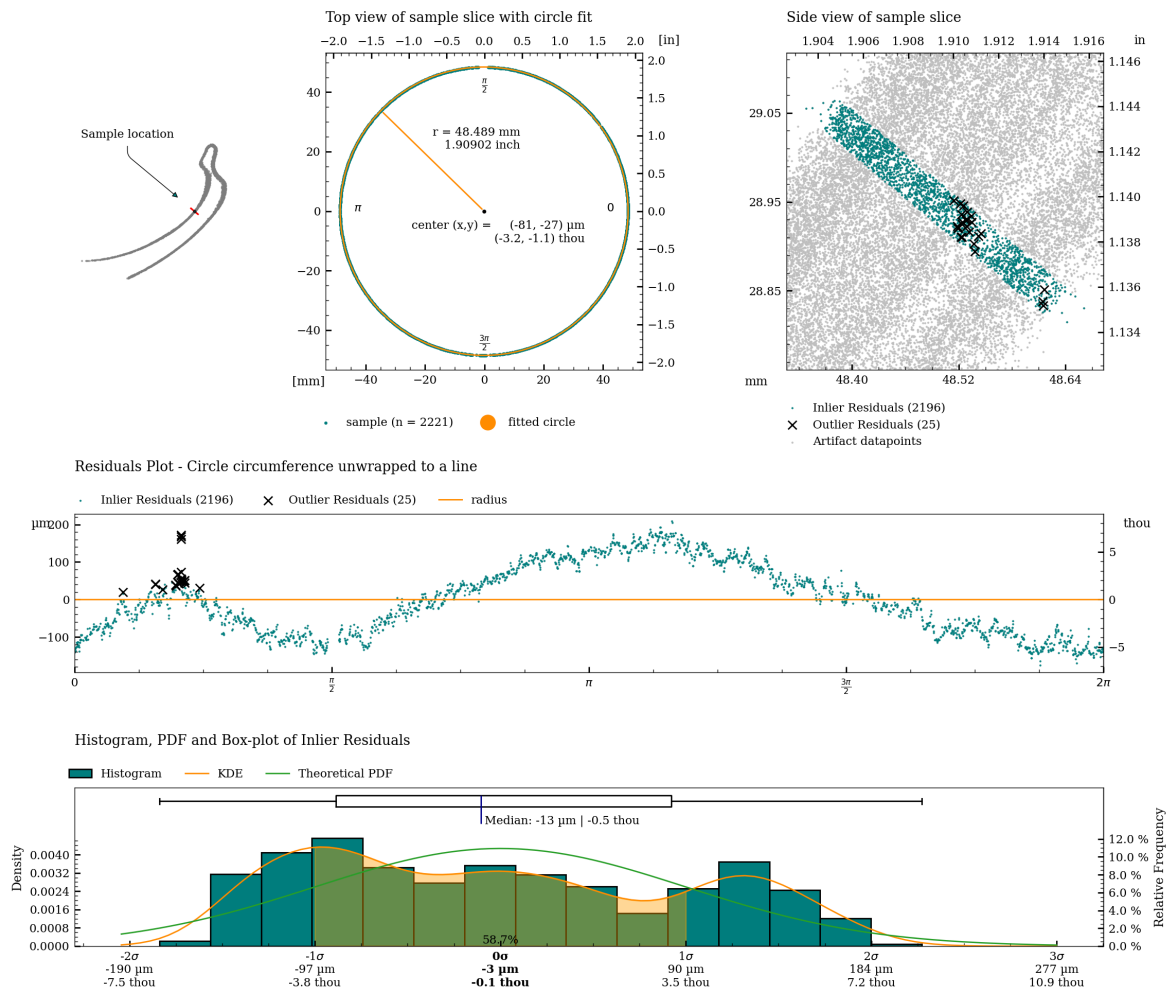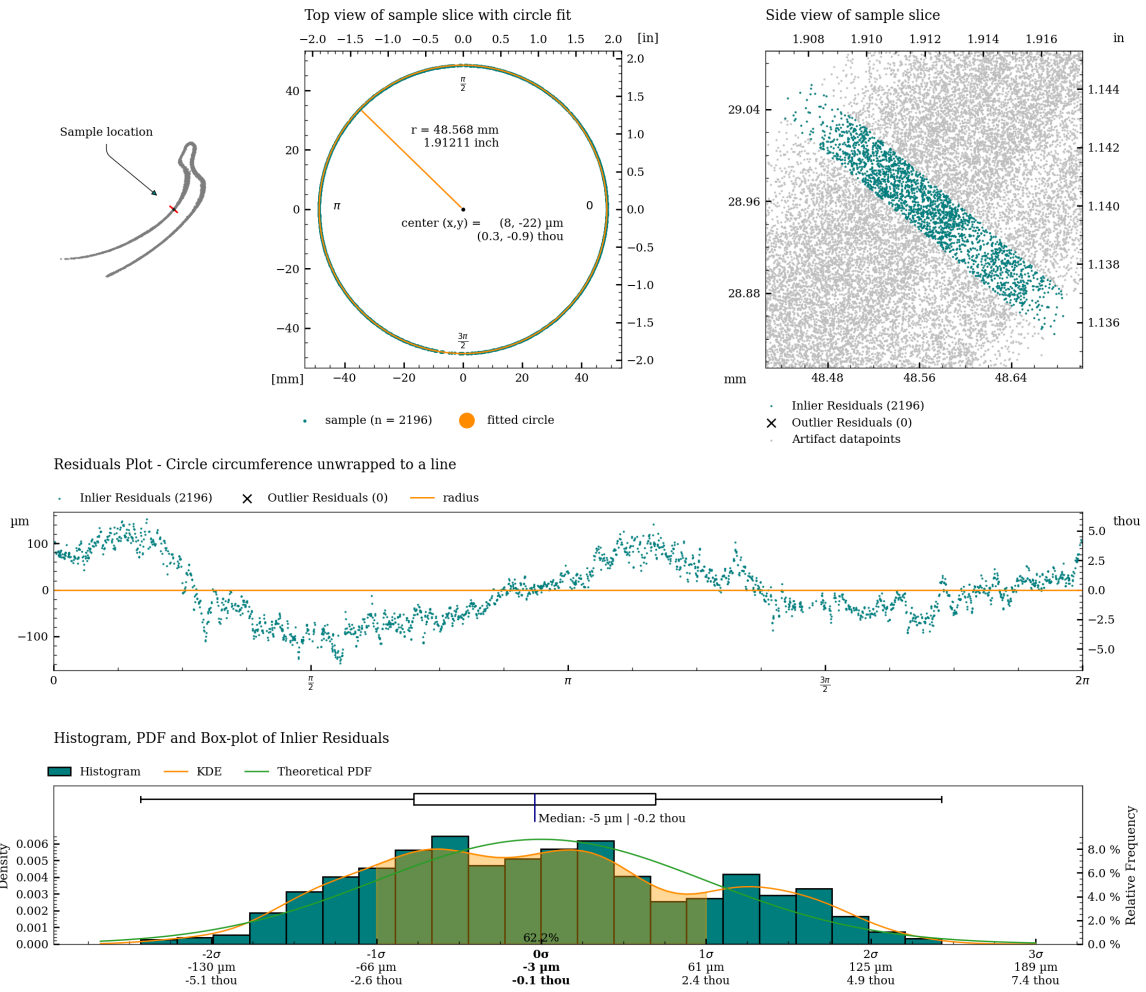
Concentricity analysis of c03

Sample location

Top view of sample slice with circle fit

r = 57.281 mm
2.25515 inch

center (x,y) = (11, 146) µm
(0.4, 5.7) thou

- sample (n = 2724)   ● fitted circle

Side view of sample slice

- Inlier Residuals (2685)
- ✕ Outlier Residuals (39)
- Artifact datapoints

Residuals Plot - Circle circumference unwrapped to a line

- Inlier Residuals (2685)   ✕ Outlier Residuals (39)   — radius

Histogram, PDF and Box-plot of Inlier Residuals

- ▮ Histogram   — KDE   — Theoretical PDF

Median: -0.00 mm | -0.000 in

z-score
outlier min

69.3%

	-3σ	-2σ	-1σ	0σ	1σ	2σ	3σ
mm	-0.47 mm	-0.31 mm	-0.15 mm	0.01 mm	0.17 mm	0.33 mm	0.50 mm
in	-0.019 in	-0.012 in	-0.006 in	0.000 in	0.007 in	0.013 in	0.020 in

Figure 39: Detailed plot of concentricity measurement for c03.

Concentricity analysis of c04

Figure 40: Detailed plot of concentricity measurement for c04.

Concentricity analysis of c05

Figure 41: Detailed plot of concentricity measurement for c05.
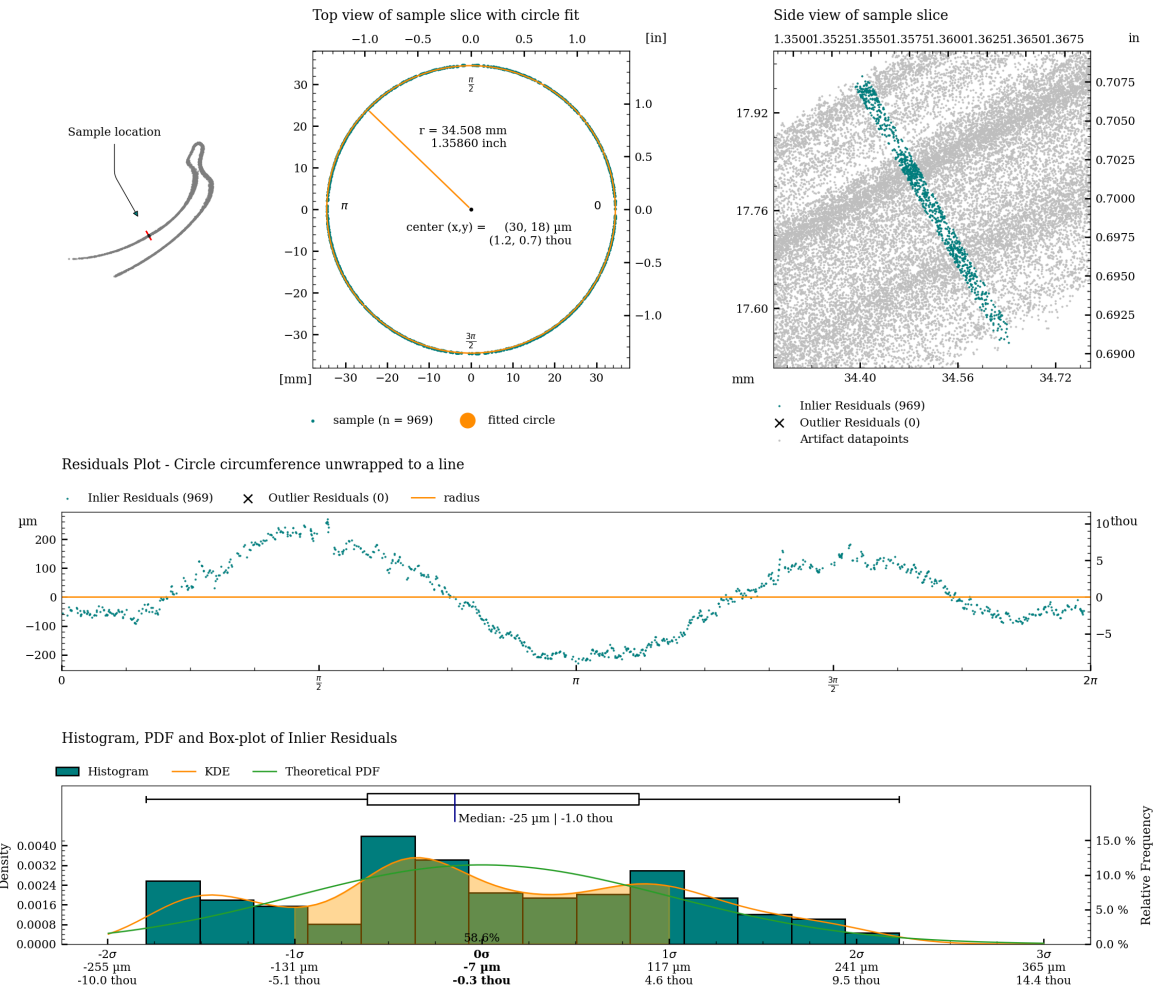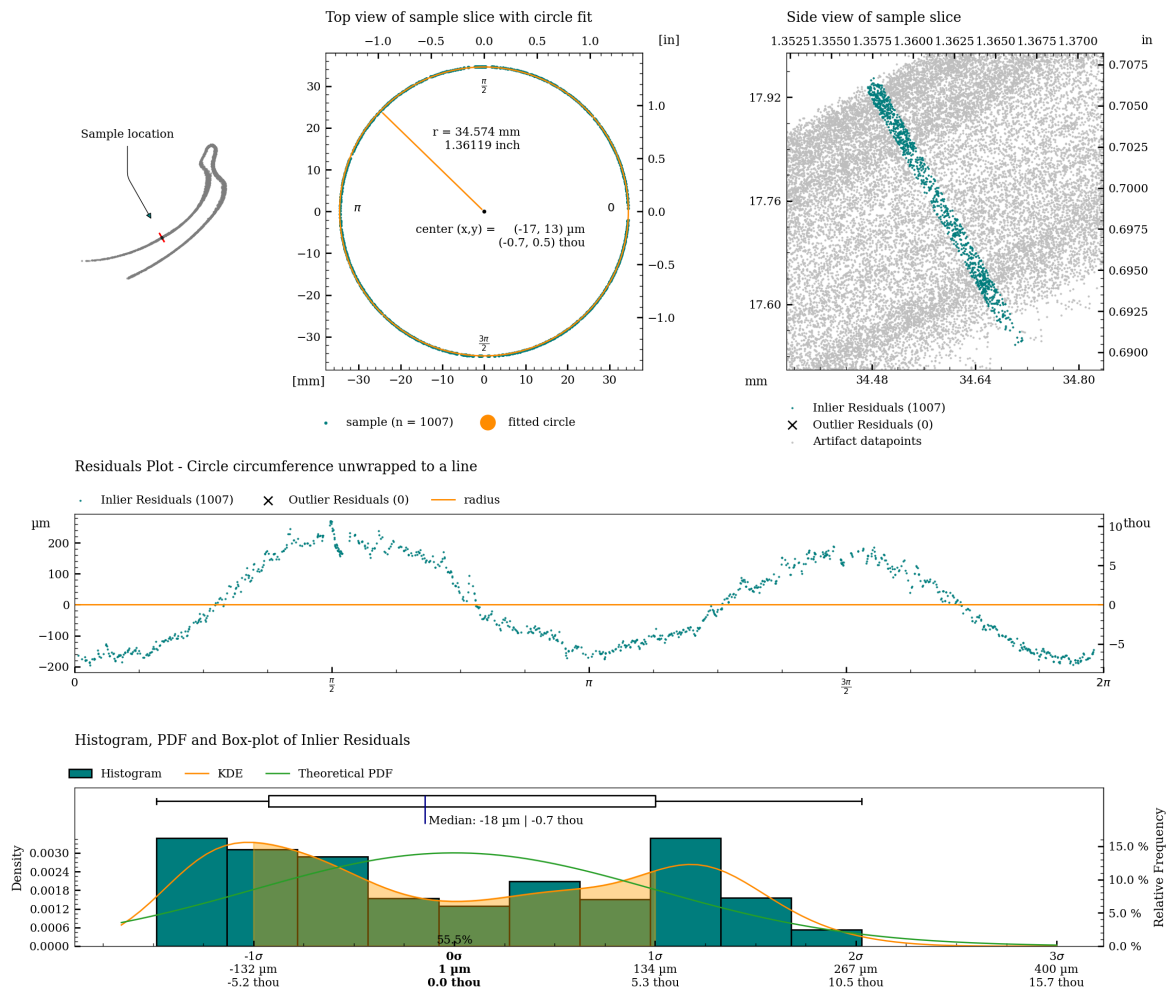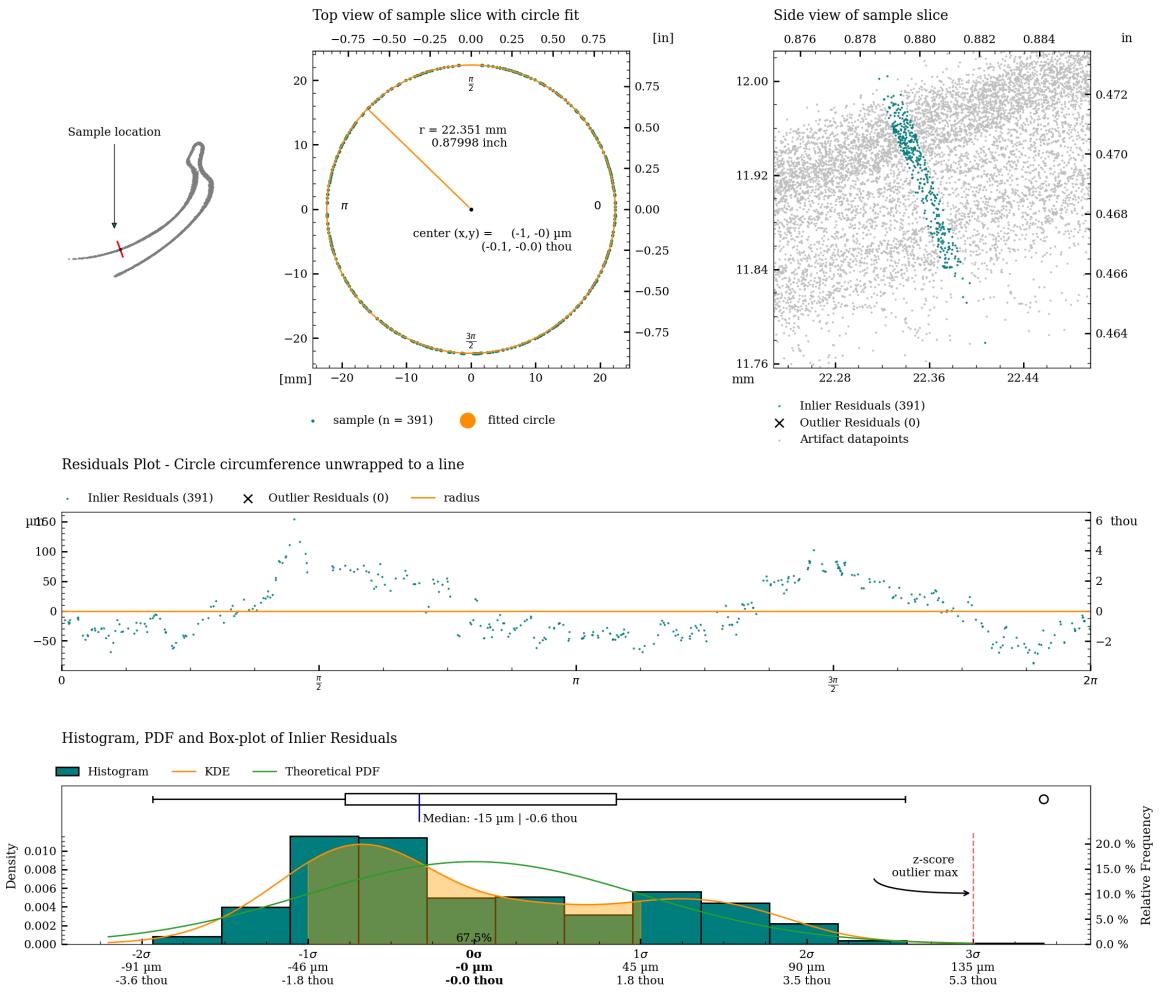
Concentricity analysis of c07

Figure 42: Detailed plot of concentricity measurement for c07.

Concentricity analysis of c07_s

Figure 43: Detailed plot of concentricity measurement for c07_s.

Concentricity analysis of c08

Figure 44: Detailed plot of concentricity measurement for c08.

Concentricity analysis of c08_s

Top view of sample slice with circle fit

Sample location

r = 48.568 mm
1.91211 inch

center (x,y) = (8, -22) μm
(0.3, -0.9) thou

sample (n = 2196)   fitted circle

Side view of sample slice

Inlier Residuals (2196)
Outlier Residuals (0)
Artifact datapoints

Residuals Plot - Circle circumference unwrapped to a line

Inlier Residuals (2196)   Outlier Residuals (0)   radius

Histogram, PDF and Box-plot of Inlier Residuals

Histogram   KDE   Theoretical PDF

Median: -5 μm | -0.2 thou

62.2%

	-2σ	-1σ	0σ	1σ	2σ	3σ
	-130 μm	-66 μm	-3 μm	61 μm	125 μm	189 μm
	-5.1 thou	-2.6 thou	-0.1 thou	2.4 thou	4.9 thou	7.4 thou

Figure 45: Detailed plot of concentricity measurement for c08_s.

Concentricity analysis of c09

Figure 46: Detailed plot of concentricity measurement for c09.

Concentricity analysis of c09_s

Sample location

Top view of sample slice with circle fit

r = 34.574 mm
1.36119 inch

center (x,y) =   (-17, 13) μm
(-0.7, 0.5) thou

- sample (n = 1007)   ● fitted circle

Side view of sample slice

- Inlier Residuals (1007)
× Outlier Residuals (0)
  Artifact datapoints

Residuals Plot - Circle circumference unwrapped to a line

- Inlier Residuals (1007)   × Outlier Residuals (0)   — radius

Histogram, PDF and Box-plot of Inlier Residuals

■ Histogram   — KDE   — Theoretical PDF

Median: -18 μm | -0.7 thou

55.5%

-1σ	0σ	1σ	2σ	3σ
-132 μm	1 μm	134 μm	267 μm	400 μm
-5.2 thou	0.0 thou	5.3 thou	10.5 thou	15.7 thou

Figure 47: Detailed plot of concentricity measurement for c09_s.

Concentricity analysis of c10

Figure 48: Detailed plot of concentricity measurement for c10.

Concentricity analysis of c10_s
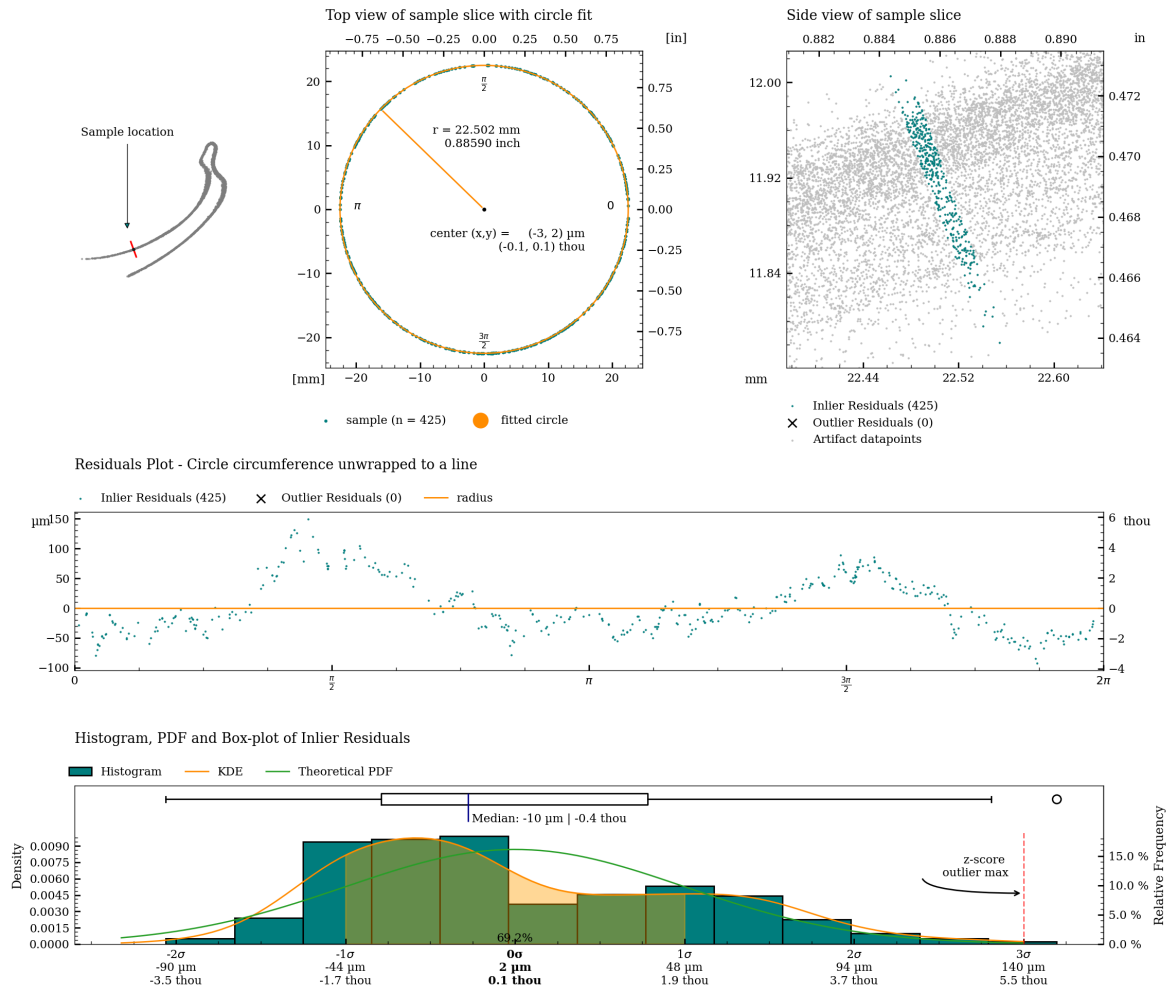
Figure 49: Detailed plot of concentricity measurement for c10_s.

Coaxiality

Coaxiality refers to the straightness and consistency of a central line running through the center of the vase. It measures how aligned the core of the vase remains along its vertical axis.

The coaxiality measurements are calculated using RANSAC (Random sample consensus) algorithm for outlier detection on least squares circle regression on cross-sections of the vessel (excluding potential handles), to estimate the best fit circle centers for each slice of the vessel. A best-fit line connects these centers, showing whether the vessels's shape twists or remains straight. This concept helps describe the symmetry and structural uniformity in a visual and analytical way.

Coaxiality is measured for:
- The exterior surface (excluding handles)
- The interior surface

	Exterior		Interior		Interior separate	
Analyzed Slices	1042		637		637	
Median sample size	2422		1788		1776	
Slice Height	50 µm	2.0 thou	50 µm	2.0 thou	50 µm	2.0 thou
Statistics with Z-axis as Reference						
Median Absolute Deviation (MAD)	85 µm	3.4 thou	53 µm	2.1 thou	20 µm	0.8 thou
Standard Deviation (SD)	143 µm	5.6 thou	193 µm	7.6 thou	59 µm	2.3 thou
Root Mean Square Deviation (RMSD)	202 µm	7.9 thou	247 µm	9.7 thou	71 µm	2.8 thou
Statistics with Best Fit Central Axis as Reference						
Best fit Central Axis Equation (in metric coordinate system with unit [mm])	x = 0.065 + t-0.00331 y = 0.157 + t-0.00738 z = 0.000 + t0.99997		x = 0.336 + t-0.01876 y = 0.038 + t-0.00225 z = 0.000 + t0.99982		x = -0.072 + t0.00377 y = -0.000 + t-0.00003 z = 0.000 + t0.99999	
Axis tilt	−0.191°		−1.077°		0.216°	
Median Absolute Deviation (MAD)	124 µm	4.9 thou	116 µm	4.6 thou	26 µm	1.0 thou
Standard Deviation (SD)	68 µm	2.7 thou	49 µm	1.9 thou	34 µm	1.4 thou
Root Mean Square Deviation (RMSD)	146 µm	5.8 thou	121 µm	4.8 thou	50 µm	2.0 thou

Table 4: Coaxiality analysis of vessel MV009.

Coaxiality plots, exterior surface
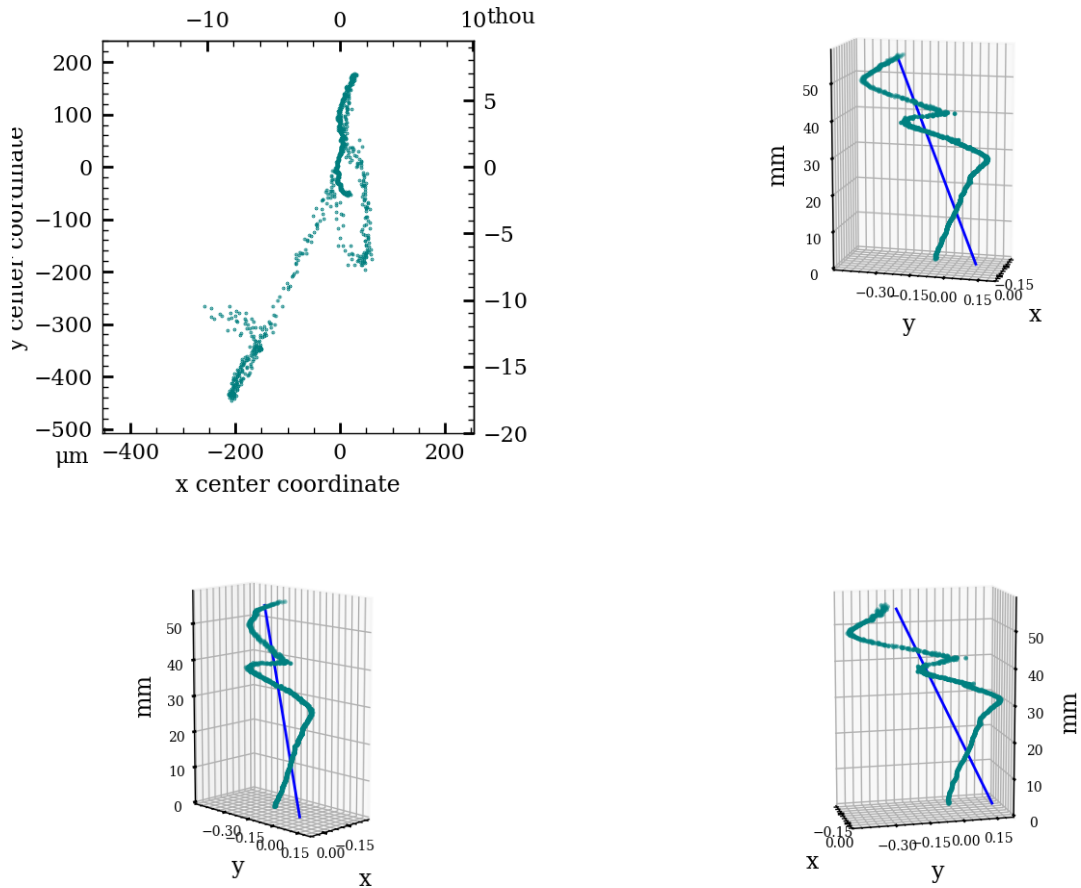
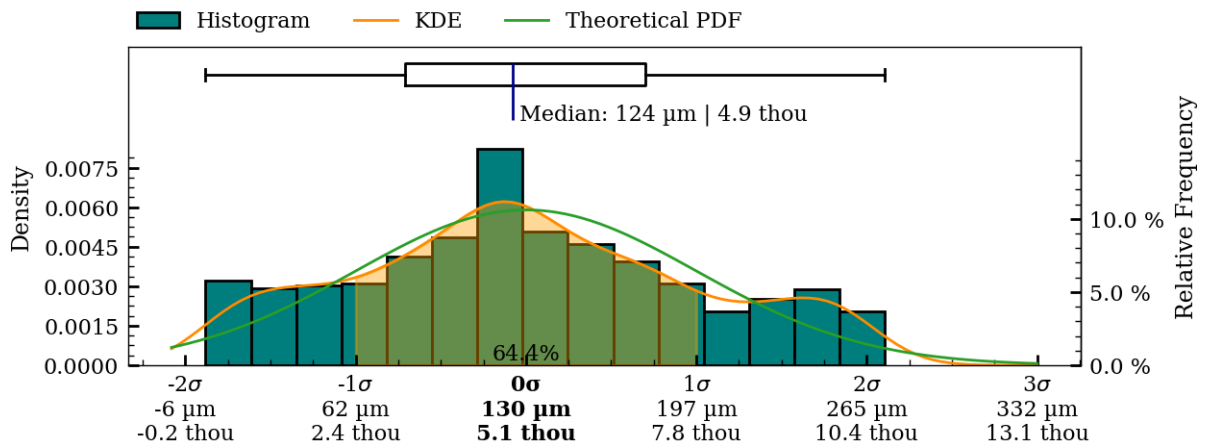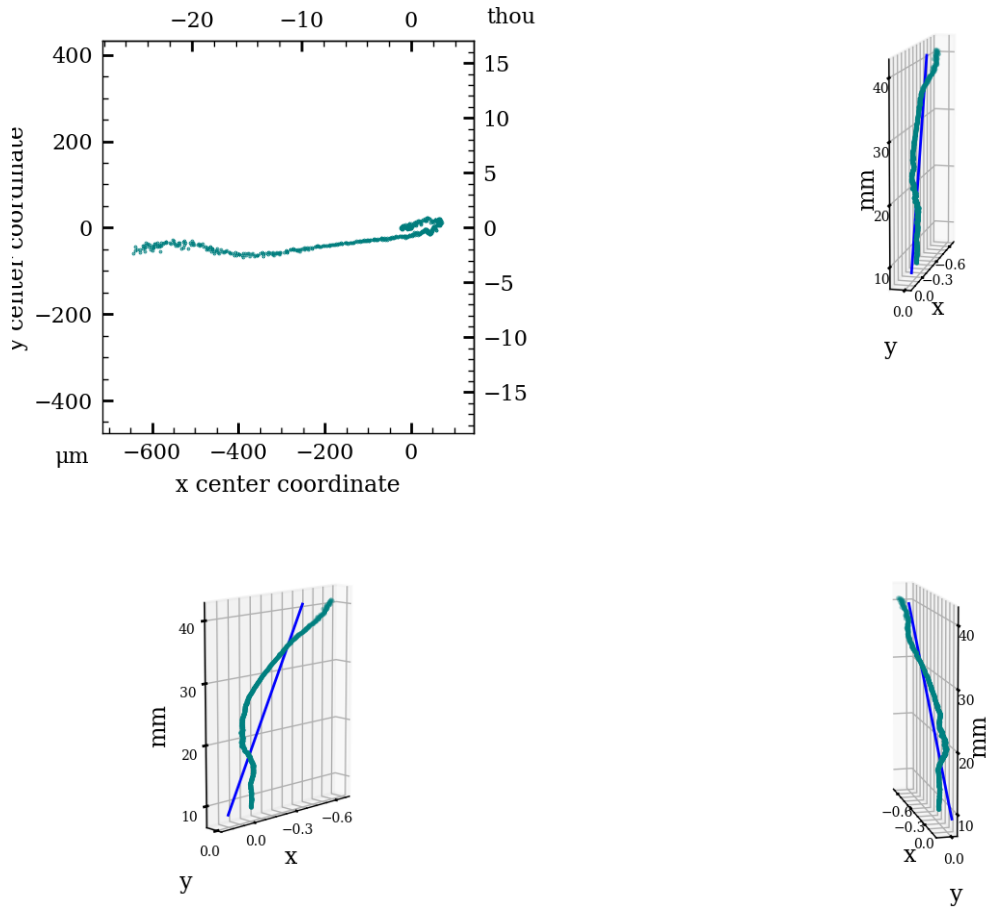## Coaxiality residuals from fitted axis, exterior surface

Figure 50: Coaxiality residual plots of exterior surface, MV009.

Coaxiality plots, interior surface

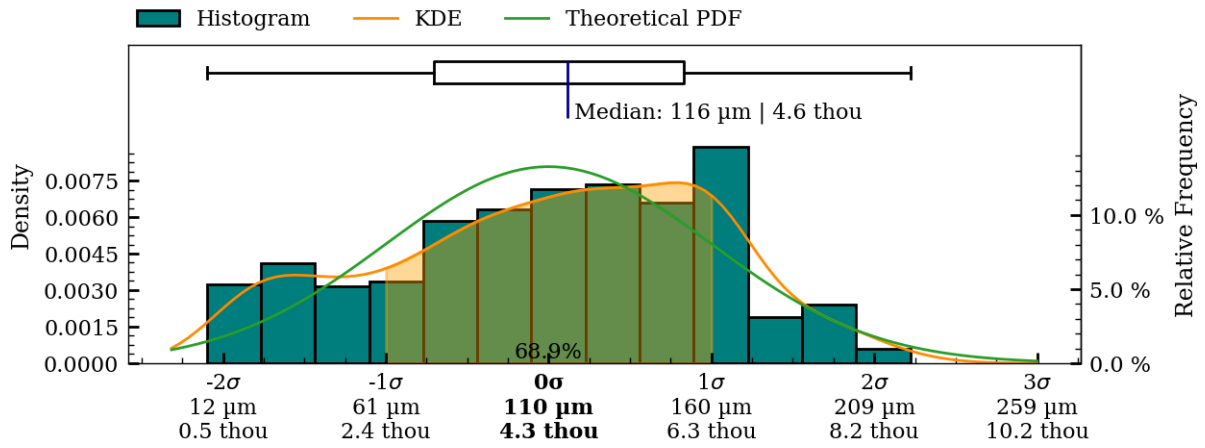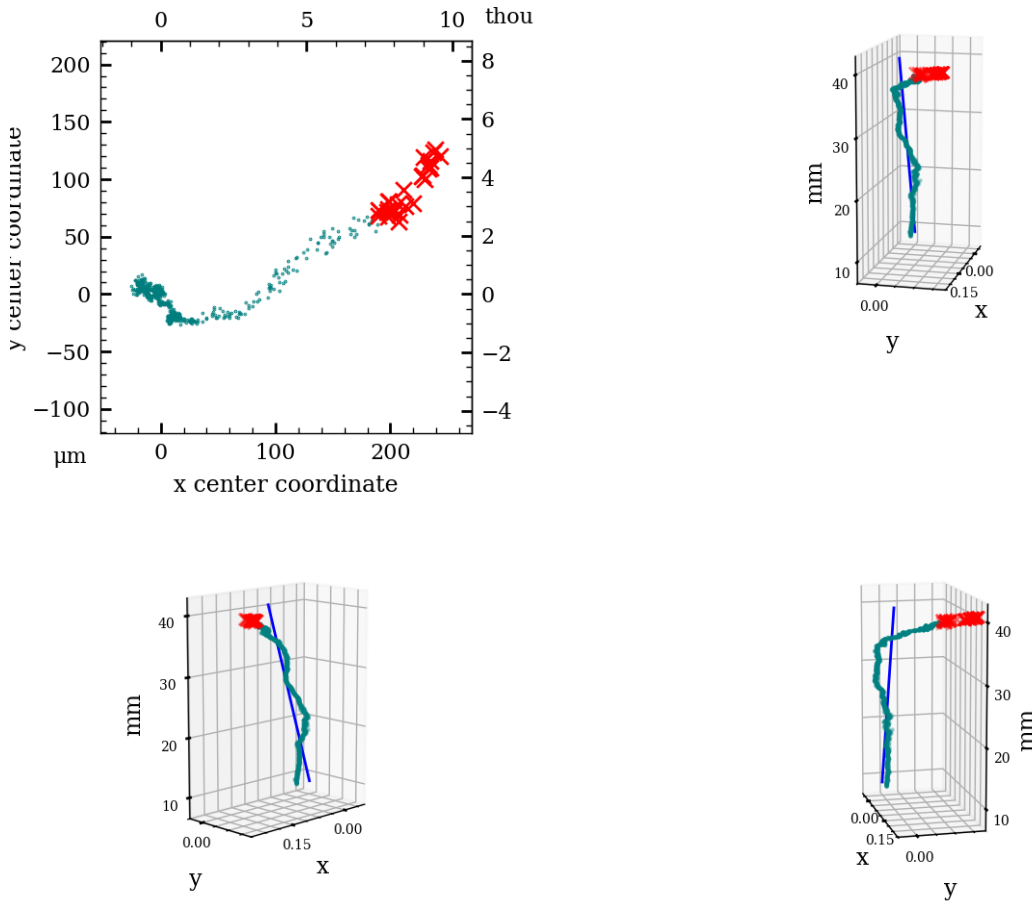## Coaxiality residuals from fitted axis, interior surface

Figure 51: Coaxiality residual plots of interior surface, MV009.

Coaxiality plots, interior separately aligned surface

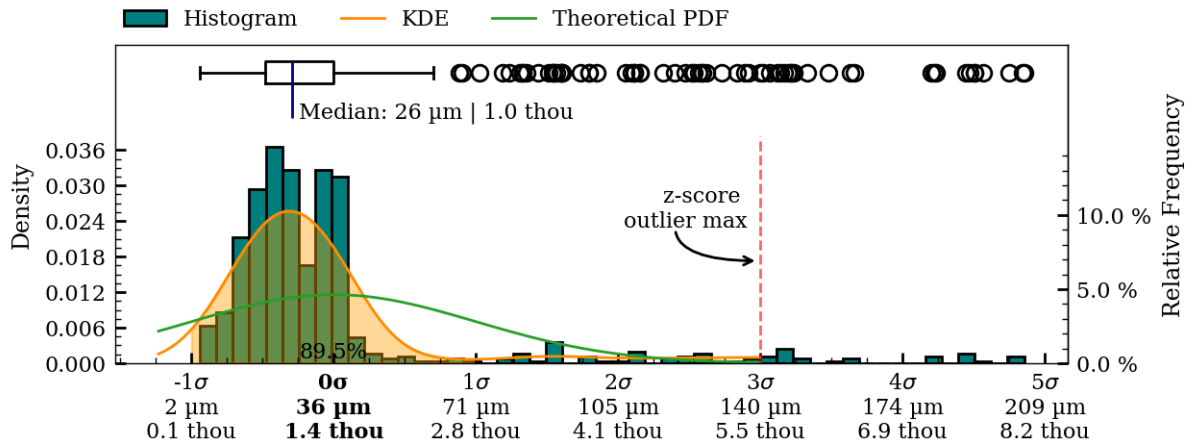## Coaxiality residuals from fitted axis, interior separately aligned surface

Figure 52: Coaxiality residual plots of interior_separate surface, MV009.

Surface Variability

To illustrate the overall surface deviations of the object, a surface variability heatmap has been created. This heatmap provides an accessible overview of the topography of the manufacturing precision and surface structure of the object.

The surface variability measurements are created by fitting a number of higher-order polynomials to the two-dimensional folded profile of the scan data. This process creates an idealized mathematical representation of actual surface curvature of object, and as such provides a continuous model representation of the actual object. It is important to note that only such a non-discretized representation is sufficient to avoid introducing inconsistently varying errors in the mapping of the final surface deviation results, that the rendered heatmaps are based on.

To produce the final surface variability map, the distance from each scanned vertex to the fitted polynomial is calculated and used as the mapping function input, for applying colours to the surface of the object.

It is important to note that this variability map does not describe deviations from the original *intended* shape of the artifact (if any), as this shape (the *intended design*, so to speak) will have been lost to time. It does however provide a very informative visualization of the texture and structure of the surface and very importantly, *does* hightlight potential manufacturing-relevant patterns in the surface texture (if present). Such patterns are, as an example, clearly evident on the interior surface of artifact PV001.
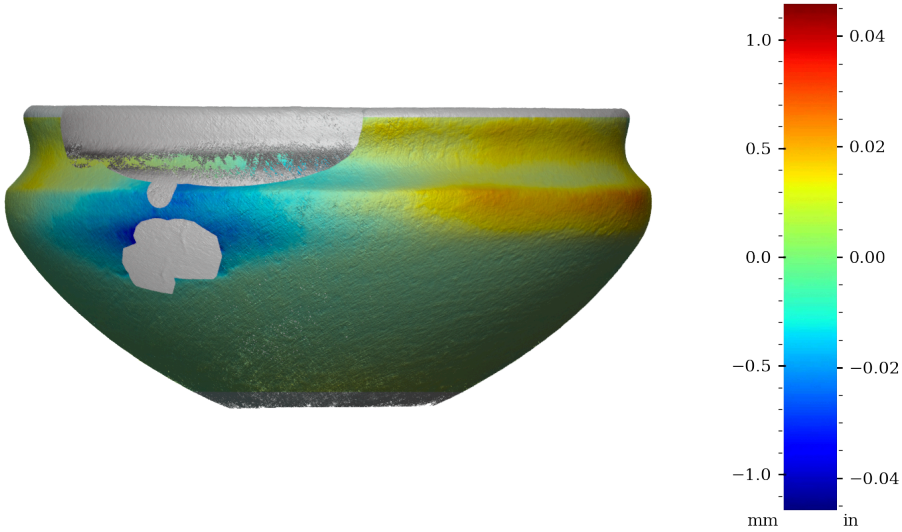
Exterior surface

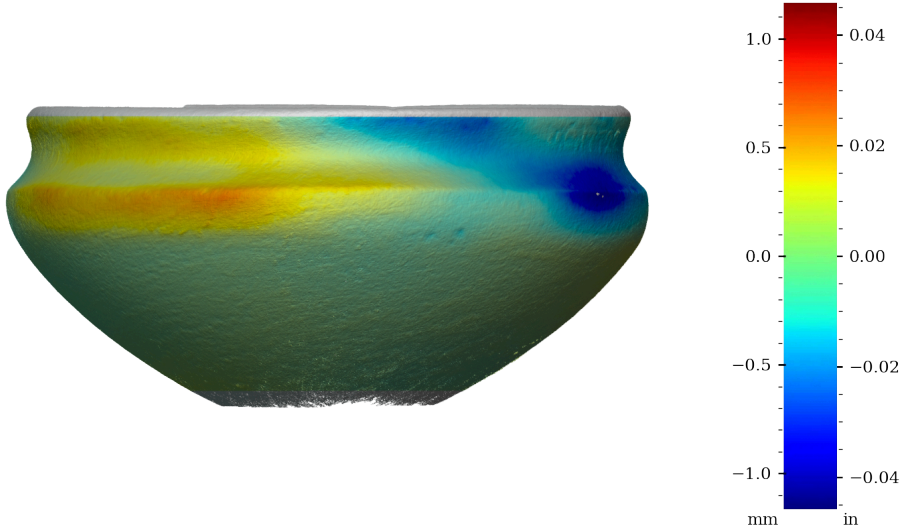Figure 53: Surface variability heatmap of MV009, front view

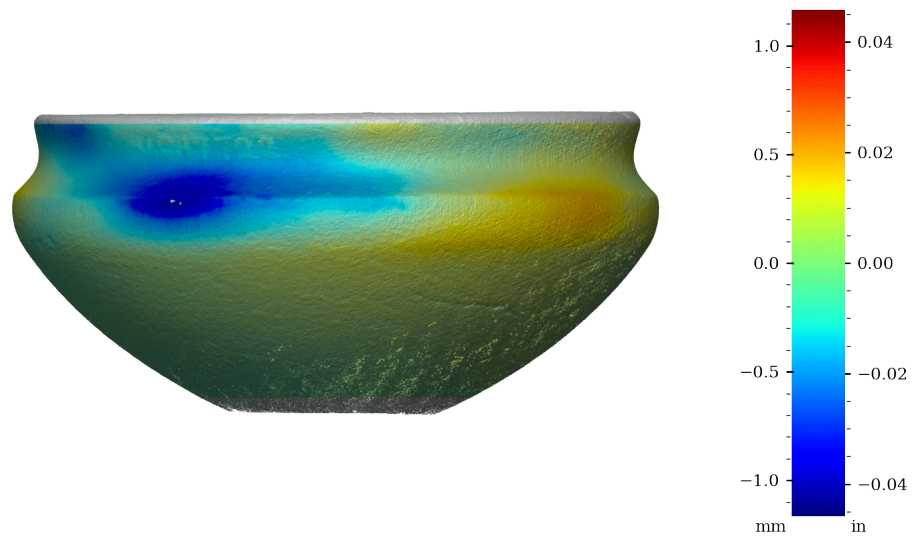Figure 54: Surface variability heatmap of MV009, rotated 90°

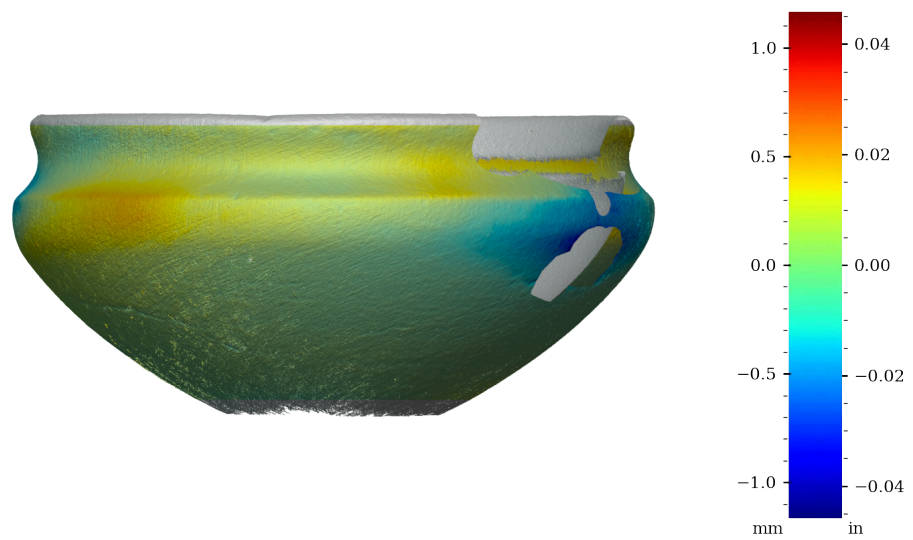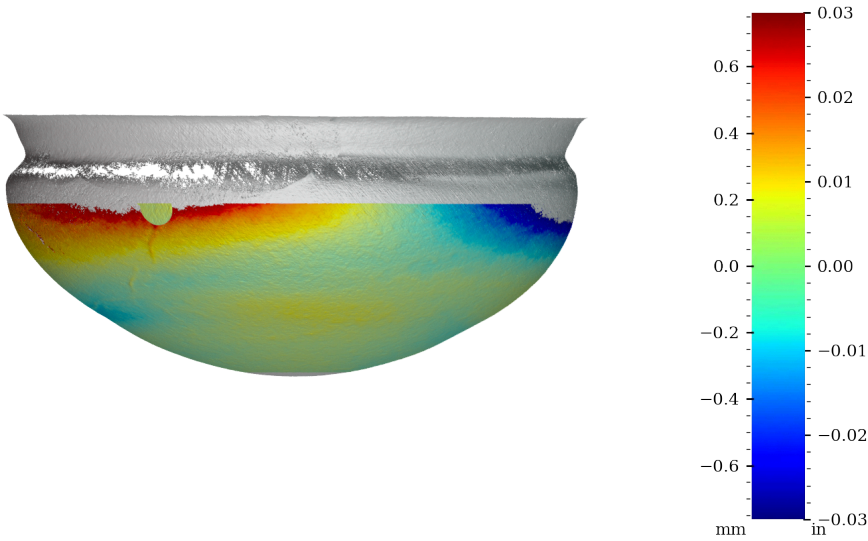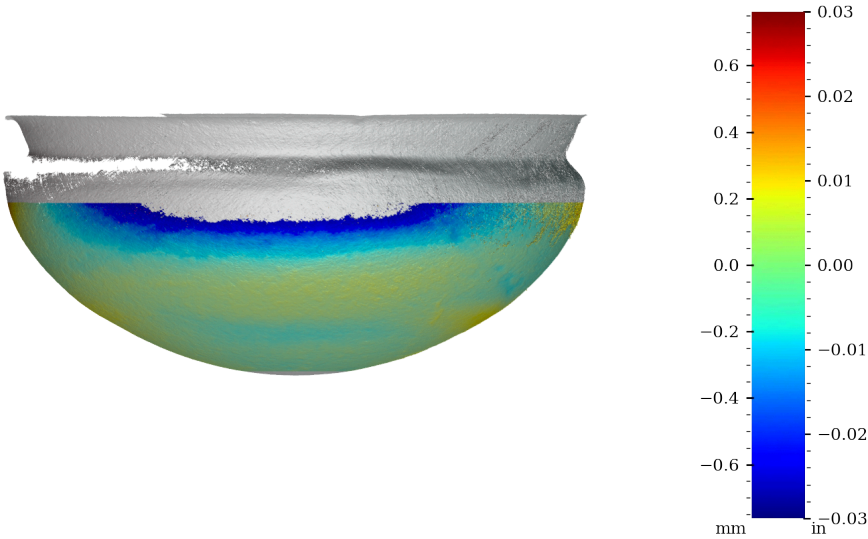Figure 55: Surface variability heatmap of MV009, rotated 180°

Figure 56: Surface variability heatmap of MV009, rotated 270°

Interior surface

Figure 57: Surface variability heatmap of MV009, front view

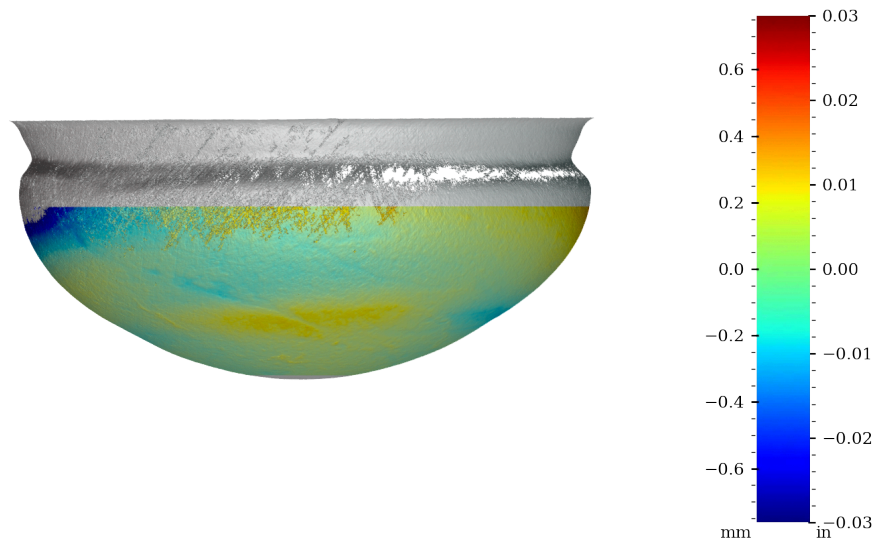Figure 58: Surface variability heatmap of MV009, rotated 90°

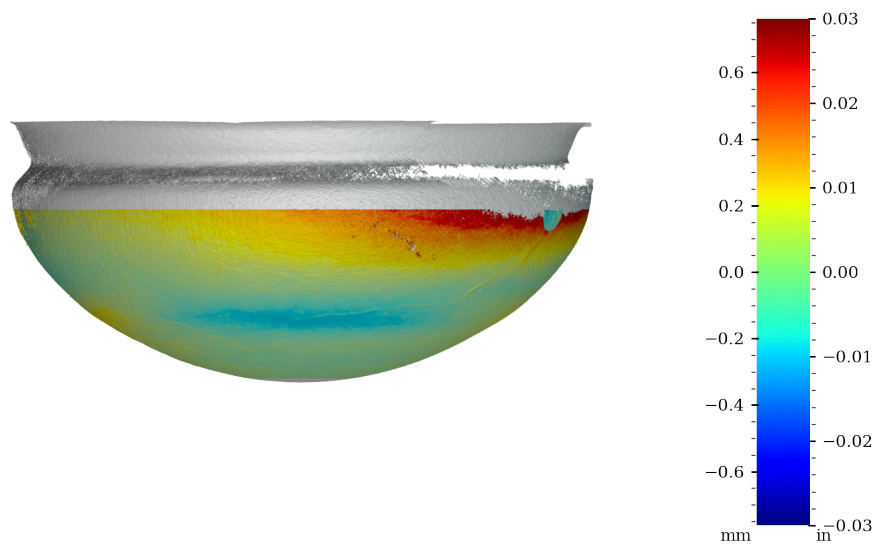Figure 59: Surface variability heatmap of MV009, rotated 180°

Figure 60: Surface variability heatmap of MV009, rotated 270°

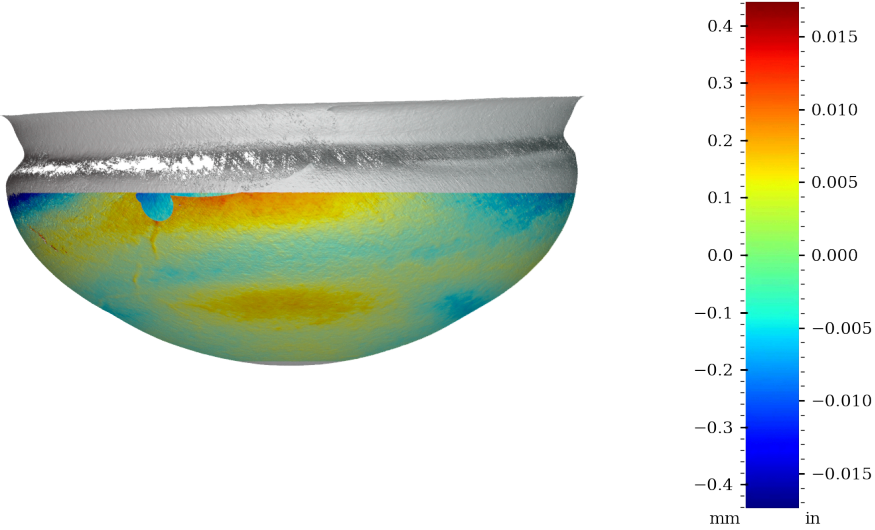## Interior surface aligned separately

Figure 61: Surface variability heatmap of MV009, front view
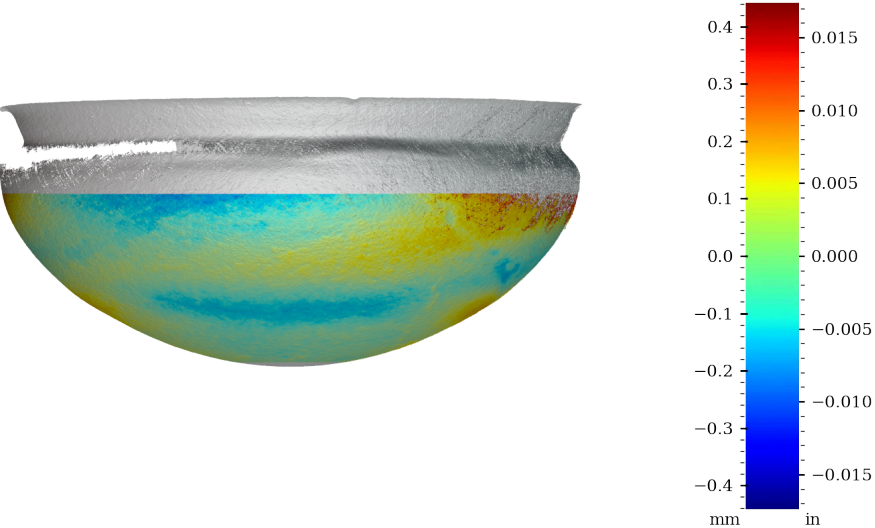

Figure 62: Surface variability heatmap of MV009, rotated 90°
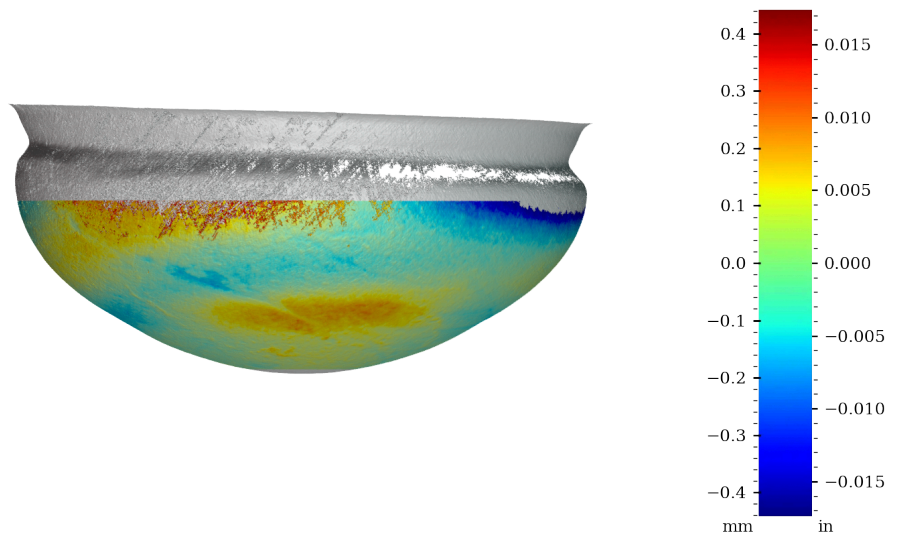
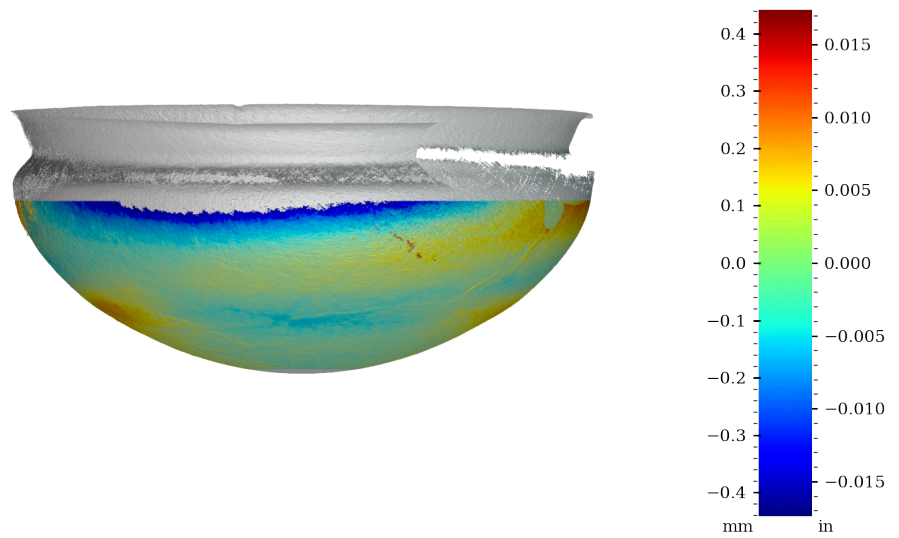Figure 63: Surface variability heatmap of MV009, rotated 180°

Figure 64: Surface variability heatmap of MV009, rotated 270°

Surface variability statistics

Area	MSD	RMSD	SD	Median AD	Range	Min	Max	Sample size
	mm²	mm	mm	mm	mm	mm	mm	
Exterior	0.0668	0.258	0.193	0.071	2.036	−1.218	0.818	3980685
Interior	0.0474	0.218	0.168	0.052	2.073	−1.023	1.049	2504454
Interior separate	0.0158	0.126	0.089	0.039	1.473	−0.723	0.751	2484789
	in²	in	in	in	in	in	in	
Exterior	0.000104	0.0102	0.0076	0.0028	0.0801	−0.0479	0.0322	3980685
Interior	0.000073	0.0086	0.0066	0.0020	0.0816	−0.0403	0.0413	2504454
Interior separate	0.000025	0.0050	0.0035	0.0016	0.0580	−0.0285	0.0295	2484789

Table 5: Surface variability statistics, MV009

Table 5 shows the statistics of the distance from the scan vertices to the best fit object model. These statistics are briefly explained below.

Histogram, KDE and Box-plot of measured surface variability - exterior surface

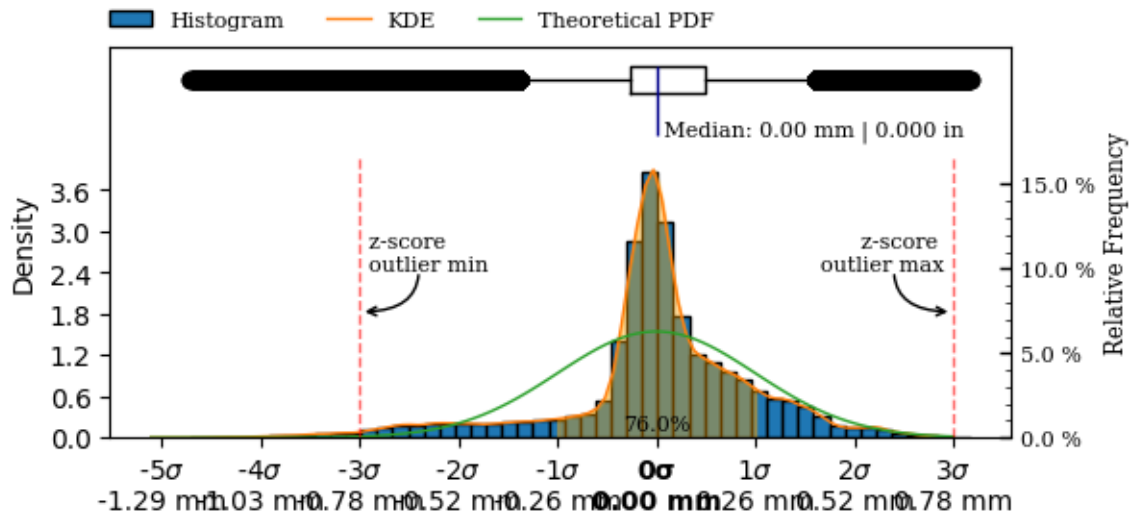Figure 65: Exterior surface variability boxplot, kds and histogram.

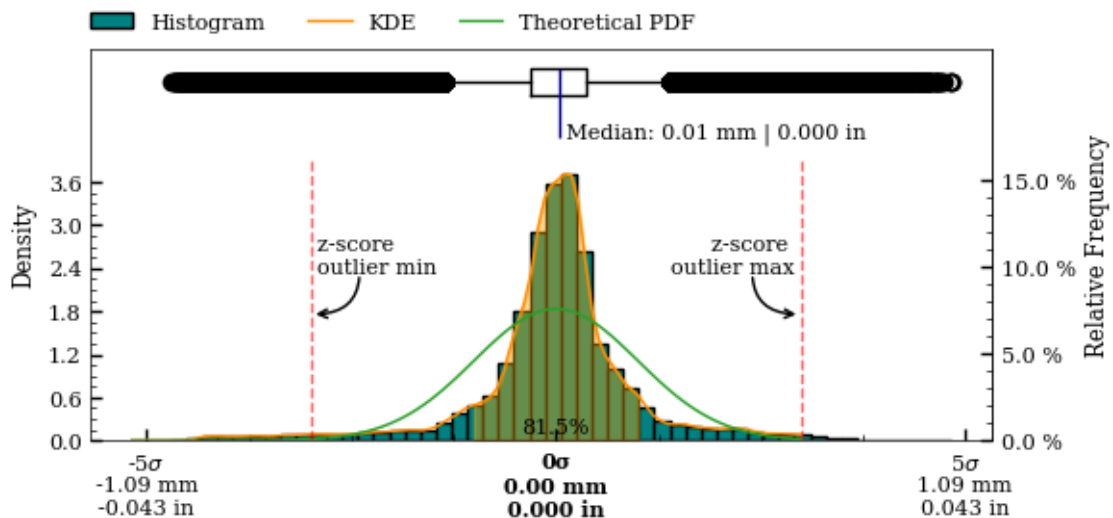## Histogram, KDE and Box-plot of measured surface variability - interior surface

Figure 66: Interior surface variability boxplot, kds and histogram.

Histogram, KDE and Box-plot of measured surface variability - interior separately aligned surface
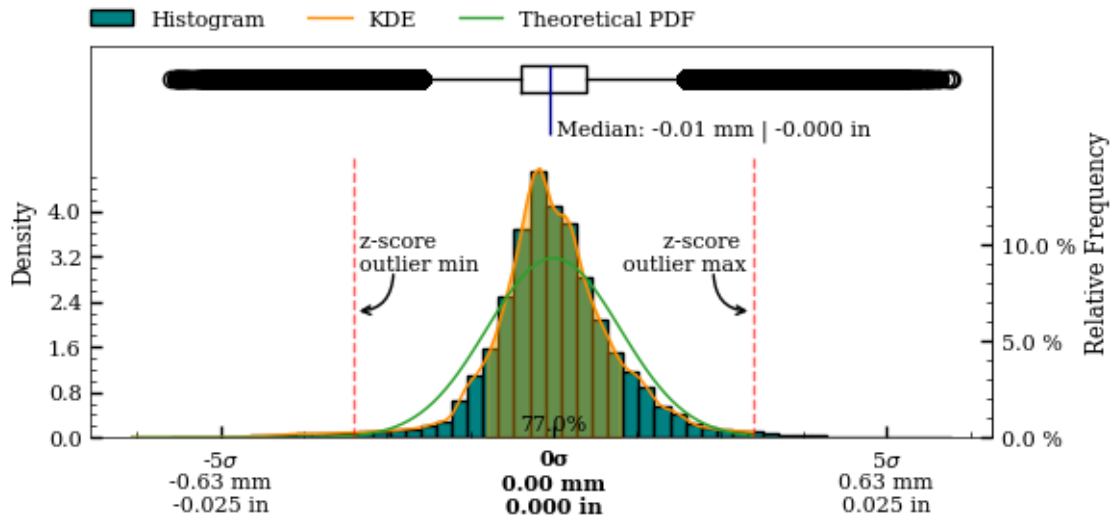

Figure 67: Interior separately aligned surface variability boxplot, kds and histogram.

Precision Score Of The Artifact

To enable valid comparison of the manufacturing precision of different artifacts, a metric that robustly quantifies the overall precision of the object is required. The considerations for such a metric will be explored in this section.

Based on these considerations, a *Precision Score* metric will be defined.

For an object to be described as having been manufactured with high precision, several qualities must be present *concurrently*, and throughout the *entire* geometry of the final object. A given object may exhibit high levels of one or more *components* of precision, but be lacking in others. For example:

- An object may present high levels of coaxiality, but lack circularity.
- An object may exhibit good circularity, but show imperfections in the surface structure.
- An object may be smoothed to perfection *without* any circularity or coaxiality.
- An object may exhibit high levels of all of the above metrics in *some* areas, but not in others.

Therefore, a precision score metric **must** account for *all* aspects of the individual, underlying precision metrics (circularity, concentricity, coaxiality and surface variability) throughout the *entire* surface area of the object.

The composite high order polynomial model, used to generate the surface variability map (described in Surface Variability, p. 52) is the best continuous mathematical representation of the object available to us (lacking any original design plans, as would normally be available in metrological analysis). This idealized model encompasses all of the above component metrics.

In the creation of the model, all scan data-points are taken into account (excluding areas with extensive damage), making it the best possible idealized representation we can achieve. When this model has been accurately created, the deviation between the model and the scanned data-points can be calculated over the non-discretized polynomials, *without* the need for an "original" CAD model (and importantly, unless such a CAD model *actually* corresponded to the original design intent, it would be an insufficient comparison basis).

Within the context of defining a valid, overall precision metric, this approach satisfies the incorporation of all of the necessary metrics:

- **Circularity**: Because the reconstructed polynomial model is revolved around the Z-plane, the idealized representation is perfectly circular, and thus incorporates the circularity component.
- **Concentricity and coaxiality**: Because the Z-axis (datum axis) is the center axis of the model, it incorporates the concentricity and coaxiality components.
- **Surface variability**: Because the model is continuous and non-discretized, it can be used accurately for all points of the scan data, and incorporates the surface variability component.

The level of precision ultimately achieved in a physical object does not share a linear relationship with its manufacturing requirements. Since continuously higher levels of final precision becomes progressively harder to achieve, an overall precision metric must take this relationship into account.

A robust statistical metric that satisfies this requirement is the *Mean Squared Deviation* (MSD or MSE). Here specifically, we can utilize the mean square of the deviations between the model ($\hat{y}$) and the data-points (y_i).

Combining all of the above considerations, we can express a well-defined *Precision Score* metric, that provides an immediately accessible way to understand the overall precision of an object, while being statistically valid. Since the Mean Squared Deviation tends towards zero as the overall precision increases, the inverse of the Mean Squared Deviation is taken to obtain a precision score metric that increases as precision increases[12]:

$$\text{Precision Score} = \frac{n}{\sum_{i=1}^{n} (y_i - \hat{y})^2}$$
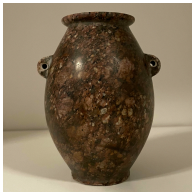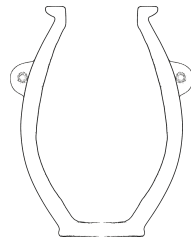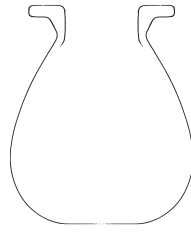
---

[12]The precision score unit is $\frac{1}{\text{mm}^2}$

The precision score of MV009 have been calculated separately for:

- Precision score, exterior surface: 15
- Precision score, separately aligned interior surface: 63
- Precision score, interior surface: 21
- Precision score, full surface: 21

The precision score of a Zeiss 1.00000 inch reference sphere have been calculated to 43,943 (RMSE = 0.00477 mm / 0.00010 in). The scan was obtained by Max Fomitchev-Zamilov using a Keyence VL −500 scanner with a rated accuracy of 10 microns. The precision analysis of the reference sphere scan indicates at the maximum possible precision score obtainable.

Table 6 shows the precision score of this artifact (MV009), compared to the two most precise, and the two least precise vessels currently analyzed.

Artifact			Material	Precision Score	Link to Report
		PV001	Red Granite	**1980** Full: 1177 Exterior: 1980 Interior separate: 798 Interior: 722	Report Publication
		PV006	Dark grey granite	**621** Full: 610 Exterior: 621 Interior separate: 479 Interior: 152	Report Publication
		MV009	Diorite	**15** Full: 21 Exterior: 15 Interior separate: 63 Interior: 21	Report Publication
		RV003	Marble breccia	**1.46** Full: 1.49 Exterior: 1.46 Interior separate: 1.53 Interior: 0.54	Report Publication
		MV010	Calcite (Egyptian Alabaster)	**1.17** Full: 1.32 Exterior: 1.17 Interior separate: 11 Interior: 0.17	Report Publication

Analysis Roadmap

While the current iteration of this work already provides valuable results, continued future additions and improvements will enhance their utility further. This section details planned iterative updates and improvements, to both the reports themselves, and to the underlying methodology and software they are created with.

Alignment Section
- Detailed exploration of different circle regression algorithms
- If handles are present on the vessel, exploring alignment of the vessels so the handle positions match each other
- Add optimization of the perpendicular surface deviation, with the best results of the coaxial alignment
- Align by minimizing circularity results (of rotated sample slice, to compensate for sample height distortions)

Measurements of Precision
- Section detailing how measurements perpendicular to the surface curvature are obtained
- Detailed surface area analysis, exploring the residual patterns throughout subsequent sample slices of the artifact surface
- Wall thickness deviation color map
- Robust outlier identification on circularity, to better handle analysis of damaged areas of the artifacts in addition to removal of interior crystalline structure points present in CT scans
- Layout updates to the charts and tables

Visibility of Outliers and Damaged Sections
- Identification and marking of damaged parts
- Visualization of outliers on the artifact surface

Exploration of Mathematical Primitives
- Analysis of selected curvatures and flat surfaces on the vessel in both the horizontal and vertical planes
  - ‣ Circles
  - ‣ Parabolas
  - ‣ Ellipsoids
  - ‣ Hyperbolas
  - ‣ Cones
- Implementation of robust regressions models suitable for this domain, based on RANSAC.

Metrics on Primary Features
- Measurements of features in the horizontal plane
- Measurements of features in the vertical plane
- Measurements of angles
- Measurements of volume

Exploration of Potential Design Ratios
- π, φ, e, 1, 2, 3, 4 etc.

Raw Dataset Attachments
- Including all measurement and sample coordinates as CSV-files embedded in the report
- Including an STL file of the aligned object alongside the report, for easier external replication and validation of the research results

Appendix A - Comparison Of Circularity Measurements (Z-plane vs. surface-perpendicular)
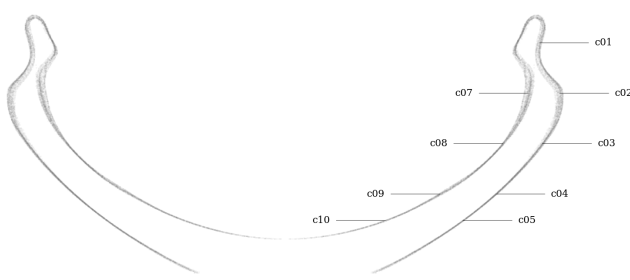

Figure 68: Circularity measurement sample locations, full mesh aligned to exterior surface
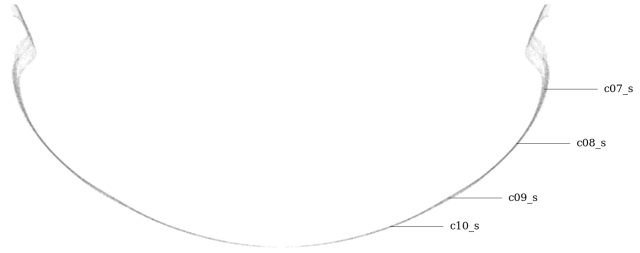

Figure 69: Circularity measurement sample location, separately aligned interior mesh

Samples perpendicular to the surface curvature

Tag	Area	Measured deviation[8]	Residuals				Sample size	Slice		
			Range	RMSD[9]	MAD[10]	SD		Height	Z coord.	Radius[11]
		mm	mm	mm	mm	mm		mm	mm	mm
c01	exterior	Ø113.245±0.700	1.175	0.310	0.110	0.158	2721	0.050	51.298	56.623
c02	exterior	Ø122.219±1.187	1.980	0.493	0.190	0.256	3572	0.050	40.124	61.110
c03	exterior	Ø114.580±0.622	0.924	0.174	0.060	0.123	2724	0.050	28.951	57.290
c04	exterior	Ø93.798±0.362	0.539	0.058	0.026	0.034	1899	0.050	17.777	46.899
c05	exterior	Ø79.189±0.246	0.384	0.038	0.013	0.025	1441	0.050	11.921	39.595
c07	interior	Ø108.298±0.990	1.909	0.477	0.204	0.289	4299	0.050	40.124	54.149
c07_s	interior sep.	Ø108.483±0.661	1.320	0.302	0.110	0.156	4069	0.050	40.124	54.242
c08	interior	Ø96.988±0.205	0.384	0.094	0.038	0.046	2221	0.050	28.951	48.494
c08_s	interior sep.	Ø97.142±0.160	0.310	0.064	0.028	0.035	2196	0.050	28.951	48.571
c09	interior	Ø69.021±0.269	0.499	0.124	0.049	0.066	969	0.050	17.777	34.510
c09_s	interior sep.	Ø69.145±0.272	0.467	0.133	0.041	0.057	1007	0.050	17.777	34.573
c10	interior	Ø44.703±0.154	0.242	0.045	0.016	0.023	391	0.050	11.921	22.352
c10_s	interior sep.	Ø45.002±0.150	0.242	0.046	0.017	0.026	425	0.050	11.921	22.501

Table 7: Detailed circularity measurements at selected samples in z-plane, vessel MV009.

Samples in the Z-plane

Tag	Area	Measured deviation[8]	Residuals				Sample size	Slice		
			Range	RMSD[9]	MAD[10]	SD		Height	Z coord.	Radius[11]
		mm	mm	mm	mm	mm		mm	mm	mm
c01	exterior	Ø113.358±0.769	1.208	0.327	0.133	0.181	2827	0.050	51.298	56.679
c02	exterior	Ø122.446±1.310	2.003	0.515	0.204	0.298	3528	0.050	40.124	61.223
c03	exterior	Ø114.563±0.741	1.155	0.211	0.078	0.148	4091	0.050	28.951	57.281
c04	exterior	Ø93.787±0.427	0.741	0.087	0.037	0.050	4233	0.050	17.777	46.894
c05	exterior	Ø79.186±0.459	0.720	0.068	0.026	0.043	4104	0.050	11.921	39.593
c07	interior	Ø108.439±1.074	1.869	0.498	0.224	0.314	4504	0.050	40.124	54.220
c07_s	interior sep.	Ø108.571±0.763	1.381	0.305	0.111	0.164	4309	0.050	40.124	54.286
c08	interior	Ø96.966±0.283	0.502	0.122	0.051	0.063	3744	0.050	28.951	48.483
c08_s	interior sep.	Ø97.125±0.229	0.427	0.083	0.036	0.047	3696	0.050	28.951	48.562
c09	interior	Ø68.943±0.636	1.070	0.249	0.117	0.139	4156	0.050	17.777	34.471
c09_s	interior sep.	Ø69.034±0.698	1.074	0.272	0.093	0.131	4199	0.050	17.777	34.517
c10	interior	Ø44.640±0.573	0.821	0.151	0.057	0.093	3829	0.050	11.921	22.320
c10_s	interior sep.	Ø44.959±0.562	0.894	0.146	0.055	0.092	3875	0.050	11.921	22.480

Table 8: Detailed circularity measurements at selected samples perpendicular to vessel curvature, vessel MV009.
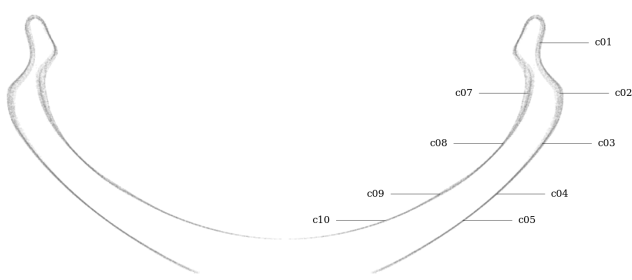
Figure 70: Circularity measurement sample locations, full mesh aligned to exterior surface
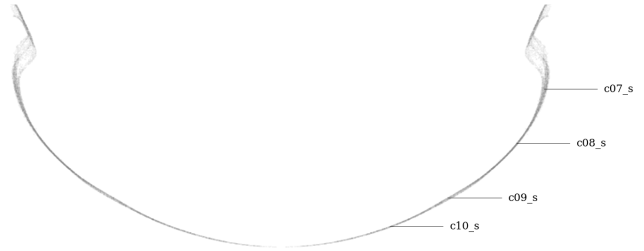
Figure 71: Circularity measurement sample location, separately aligned interior mesh

Samples perpendicular to the surface curvature

Tag	Area	Measured deviation[8]	Residuals				Sample size	Slice		
			Range	RMSD[9]	MAD[10]	SD		Height	Z coord.	Radius[11]
		in	in	in	in	in		in	in	in
c01	exterior	Ø4.4585±0.0276	0.0463	0.0122	0.0043	0.0062	2721	0.0020	2.0196	2.2292
c02	exterior	Ø4.8118±0.0467	0.0780	0.0194	0.0075	0.0101	3572	0.0020	1.5797	2.4059
c03	exterior	Ø4.5110±0.0245	0.0364	0.0068	0.0024	0.0048	2724	0.0020	1.1398	2.2555
c04	exterior	Ø3.6928±0.0143	0.0212	0.0023	0.0010	0.0013	1899	0.0020	0.6999	1.8464
c05	exterior	Ø3.1177±0.0097	0.0151	0.0015	0.0005	0.0010	1441	0.0020	0.4693	1.5588
c07	interior	Ø4.2637±0.0390	0.0752	0.0188	0.0080	0.0114	4299	0.0020	1.5797	2.1319
c07_s	interior sep.	Ø4.2710±0.0260	0.0520	0.0119	0.0043	0.0061	4069	0.0020	1.5797	2.1355
c08	interior	Ø3.8184±0.0081	0.0151	0.0037	0.0015	0.0018	2221	0.0020	1.1398	1.9092
c08_s	interior sep.	Ø3.8245±0.0063	0.0122	0.0025	0.0011	0.0014	2196	0.0020	1.1398	1.9123
c09	interior	Ø2.7174±0.0106	0.0196	0.0049	0.0019	0.0026	969	0.0020	0.6999	1.3587
c09_s	interior sep.	Ø2.7223±0.0107	0.0184	0.0052	0.0016	0.0022	1007	0.0020	0.6999	1.3611
c10	interior	Ø1.7600±0.0061	0.0095	0.0018	0.0006	0.0009	391	0.0020	0.4693	0.8800
c10_s	interior sep.	Ø1.7717±0.0059	0.0095	0.0018	0.0007	0.0010	425	0.0020	0.4693	0.8859

Table 9: Detailed circularity measurements at selected samples in z-plane, vessel MV009.

Samples in the Z-plane

Tag	Area	Measured deviation[8]	Residuals				Sample size	Slice		
			Range	RMSD[9]	MAD[10]	SD		Height	Z coord.	Radius[11]
		in	in	in	in	in		in	in	in
c01	exterior	Ø4.4629±0.0303	0.0475	0.0129	0.0052	0.0071	2827	0.0020	2.0196	2.2315
c02	exterior	Ø4.8207±0.0516	0.0789	0.0203	0.0080	0.0117	3528	0.0020	1.5797	2.4104
c03	exterior	Ø4.5103±0.0292	0.0455	0.0083	0.0031	0.0058	4091	0.0020	1.1398	2.2552
c04	exterior	Ø3.6924±0.0168	0.0292	0.0034	0.0014	0.0020	4233	0.0020	0.6999	1.8462
c05	exterior	Ø3.1176±0.0181	0.0283	0.0027	0.0010	0.0017	4104	0.0020	0.4693	1.5588
c07	interior	Ø4.2693±0.0423	0.0736	0.0196	0.0088	0.0123	4504	0.0020	1.5797	2.1346
c07_s	interior sep.	Ø4.2745±0.0301	0.0544	0.0120	0.0044	0.0064	4309	0.0020	1.5797	2.1372
c08	interior	Ø3.8176±0.0112	0.0198	0.0048	0.0020	0.0025	3744	0.0020	1.1398	1.9088
c08_s	interior sep.	Ø3.8238±0.0090	0.0168	0.0033	0.0014	0.0018	3696	0.0020	1.1398	1.9119
c09	interior	Ø2.7143±0.0251	0.0421	0.0098	0.0046	0.0055	4156	0.0020	0.6999	1.3571
c09_s	interior sep.	Ø2.7179±0.0275	0.0423	0.0107	0.0037	0.0052	4199	0.0020	0.6999	1.3589
c10	interior	Ø1.7575±0.0226	0.0323	0.0059	0.0022	0.0036	3829	0.0020	0.4693	0.8787
c10_s	interior sep.	Ø1.7700±0.0221	0.0352	0.0057	0.0022	0.0036	3875	0.0020	0.4693	0.8850

Table 10: Detailed circularity measurements at selected samples perpendicular to vessel curvature, vessel MV009.

Comparison of circularity on the full vessel surface

Metric

Samples perpendicular to the surface curvature

Area	Range			Standard Deviation			RMSD			Slices	Slice height
	Median	Min.	Max.	Median	Min.	Max.	Median	Min.	Max.		
	mm	mm	mm	mm	mm	mm	mm	mm	mm		mm
Exterior	1.055	0.241	1.989	0.131	0.021	0.259	0.184	0.034	0.498	1042	0.050
Interior	0.454	0.146	1.999	0.057	0.018	0.296	0.108	0.034	0.497	637	0.050
Interior separate	0.424	0.107	1.403	0.040	0.014	0.158	0.077	0.027	0.310	637	0.050

Table 11: Detailed circularity measurements at selected samples in z-plane, vessel MV009.

Samples in the z-plane

Area	Range			Standard Deviation			RMSD			Slices	Slice height
	Median	Min.	Max.	Median	Min.	Max.	Median	Min.	Max.		
	mm	mm	mm	mm	mm	mm	mm	mm	mm		mm
Exterior	1.135	0.488	2.213	0.155	0.037	0.429	0.219	0.059	0.635	1040	0.050
Interior	0.931	0.391	2.049	0.111	0.046	0.320	0.197	0.075	0.507	639	0.050
Interior separate	0.840	0.395	1.454	0.082	0.045	0.171	0.147	0.068	0.316	639	0.050

Table 12: Detailed circularity measurements at selected samples perpendicular to vessel curvature, vessel MV009.

Imperial

Samples perpendicular to the surface curvature

Area	Range			Standard Deviation			RMSD			Slices	Slice height
	Median	Min.	Max.	Median	Min.	Max.	Median	Min.	Max.		
	in	in	in	in	in	in	in	in	in		in
Exterior	1.055	0.241	1.989	0.131	0.021	0.259	0.184	0.034	0.498	1042	0.050
Interior	0.454	0.146	1.999	0.057	0.018	0.296	0.108	0.034	0.497	637	0.050
Interior separate	0.424	0.107	1.403	0.040	0.014	0.158	0.077	0.027	0.310	637	0.050

Table 13: Detailed circularity measurements at selected samples in z-plane, vessel MV009.

Samples in the z-plane

Area	Range			Standard Deviation			RMSD			Slices	Slice height
	Median	Min.	Max.	Median	Min.	Max.	Median	Min.	Max.		
	in	in	in	in	in	in	in	in	in		in
Exterior	1.135	0.488	2.213	0.155	0.037	0.429	0.219	0.059	0.635	1040	0.050
Interior	0.931	0.391	2.049	0.111	0.046	0.320	0.197	0.075	0.507	639	0.050
Interior separate	0.840	0.395	1.454	0.082	0.045	0.171	0.147	0.068	0.316	639	0.050

Table 14: Detailed circularity measurements at selected samples perpendicular to vessel curvature, vessel MV009.

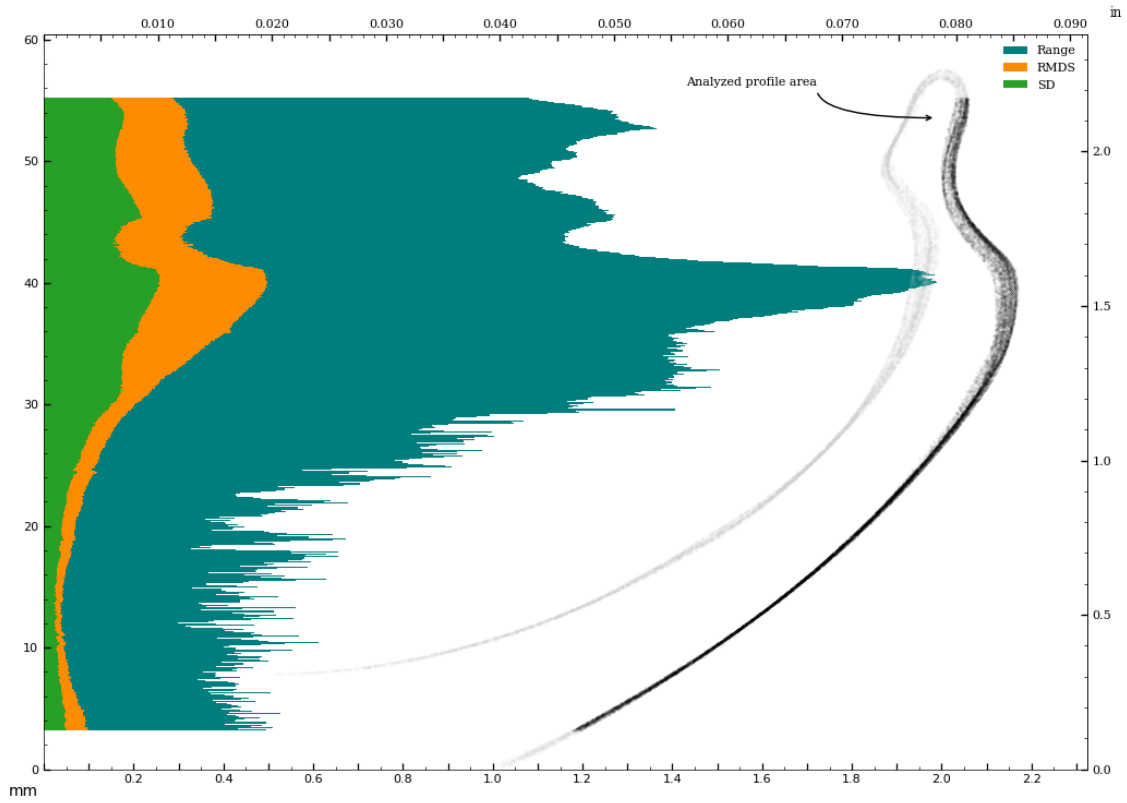## Circularity analysis of exterior surface - perpendicular to surface curvature

Figure 72: Circularity of exterior surface - perpendicular to surface curvature.

Circularity analysis of exterior surface - in z-plane

Figure 73: Circularity of exterior surface - in z-plane.

Circularity analysis of exterior surface, perpendicular to surface curvature, Standard Deviation and Root Mean Squared Deviation

Figure 74: Vessel circularity of exterior surface, perpendicular to surface curvature, standard deviation and median absolute deviation.

Circularity analysis of exterior surface, in z-plane, Standard Deviation and Root Mean Squared Deviation

Figure 75: Vessel circularity of exterior surface, in z-plane, standard deviation and median absolute deviation.

Circularity analysis of interior surface - perpendicular to surface curvature

Figure 76: Circularity of interior surface - perpendicular to surface curvature.
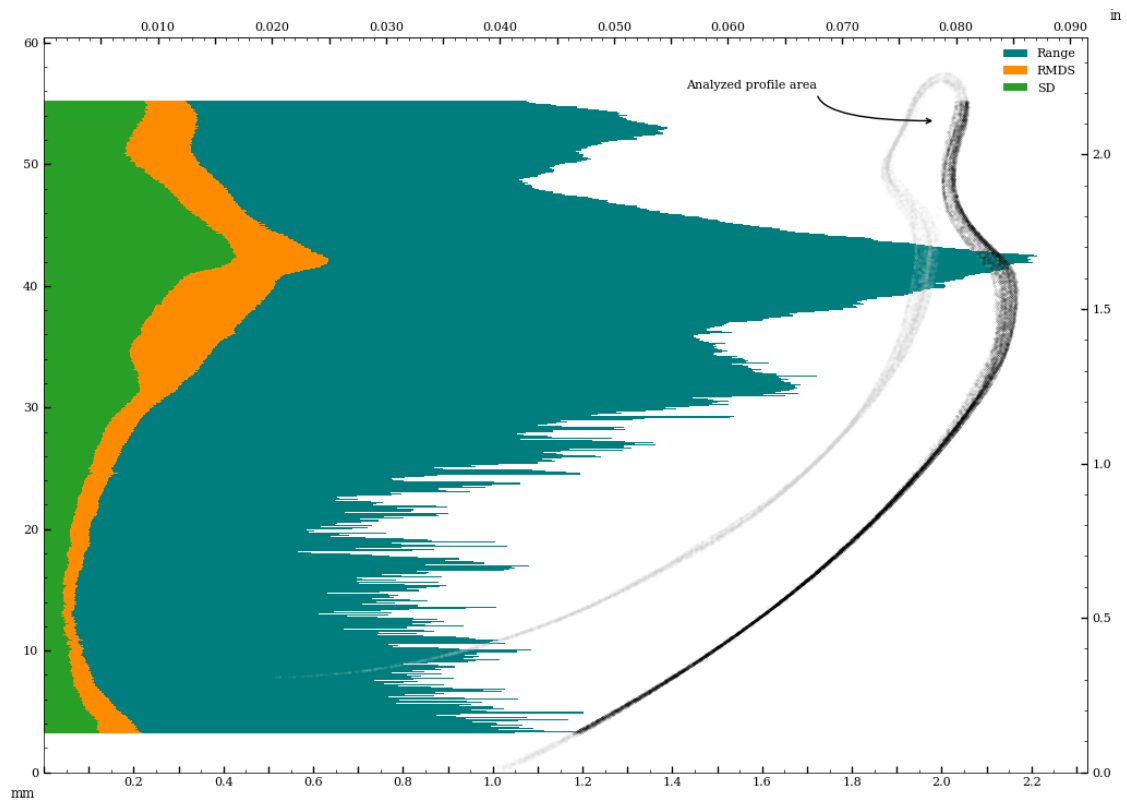
Circularity analysis of interior surface - in z-plane

Figure 77: Circularity of interior surface - in z-plane.

Circularity analysis of interior surface, perpendicular to surface curvature, Standard Deviation and Root Mean Squared Deviation
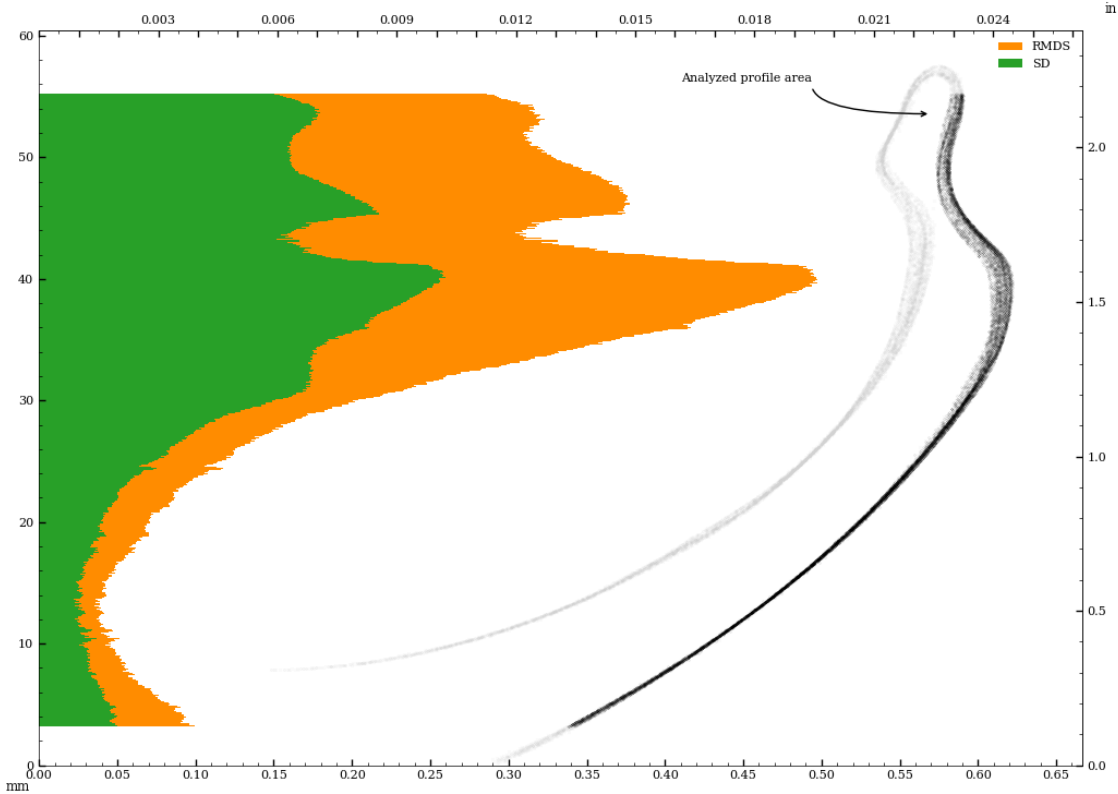

Figure 78: Vessel circularity of interior surface, perpendicular to surface curvature, standard deviation and median absolute deviation.

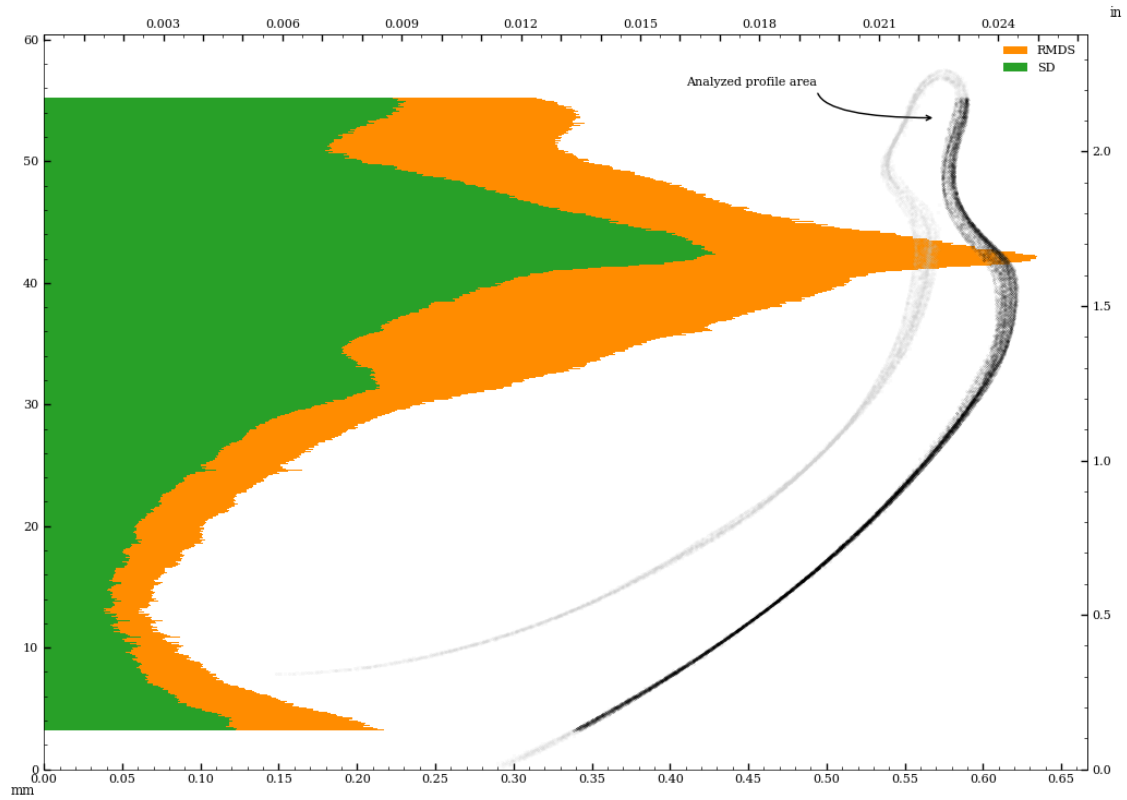## Circularity analysis of interior surface, in z-plane, Standard Deviation and Root Mean Squared Deviation

Figure 79: Vessel circularity of interior surface, in z-plane, standard deviation and median absolute deviation.

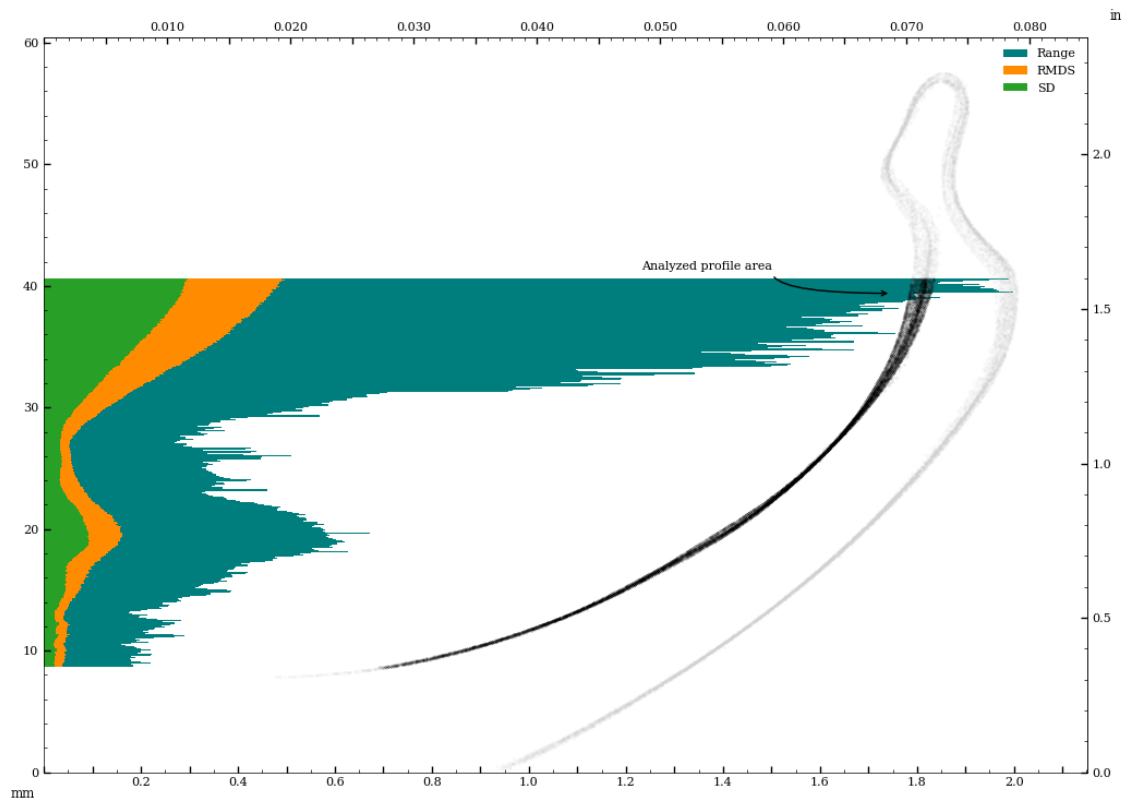## Circularity analysis of interior separately aligned surface - perpendicular to surface curvature

Figure 80: Circularity of interior_separate surface - perpendicular to surface curvature.
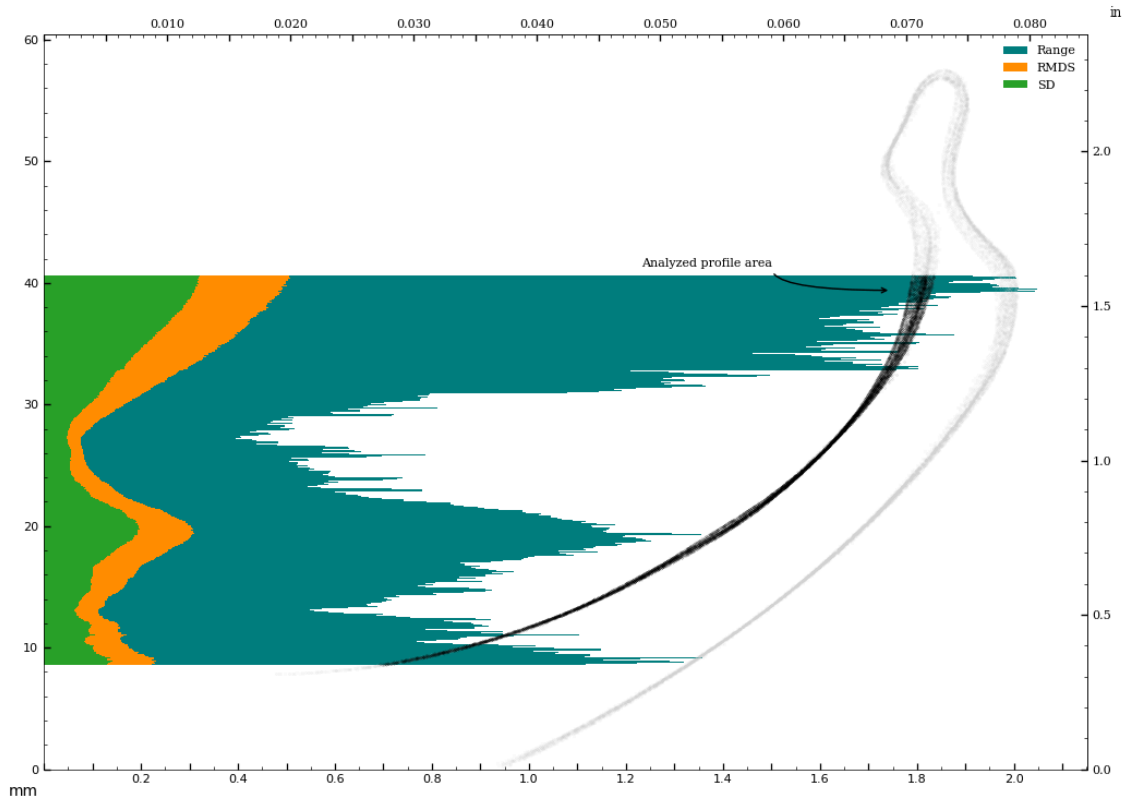
Circularity analysis of interior separately aligned surface - in z-plane
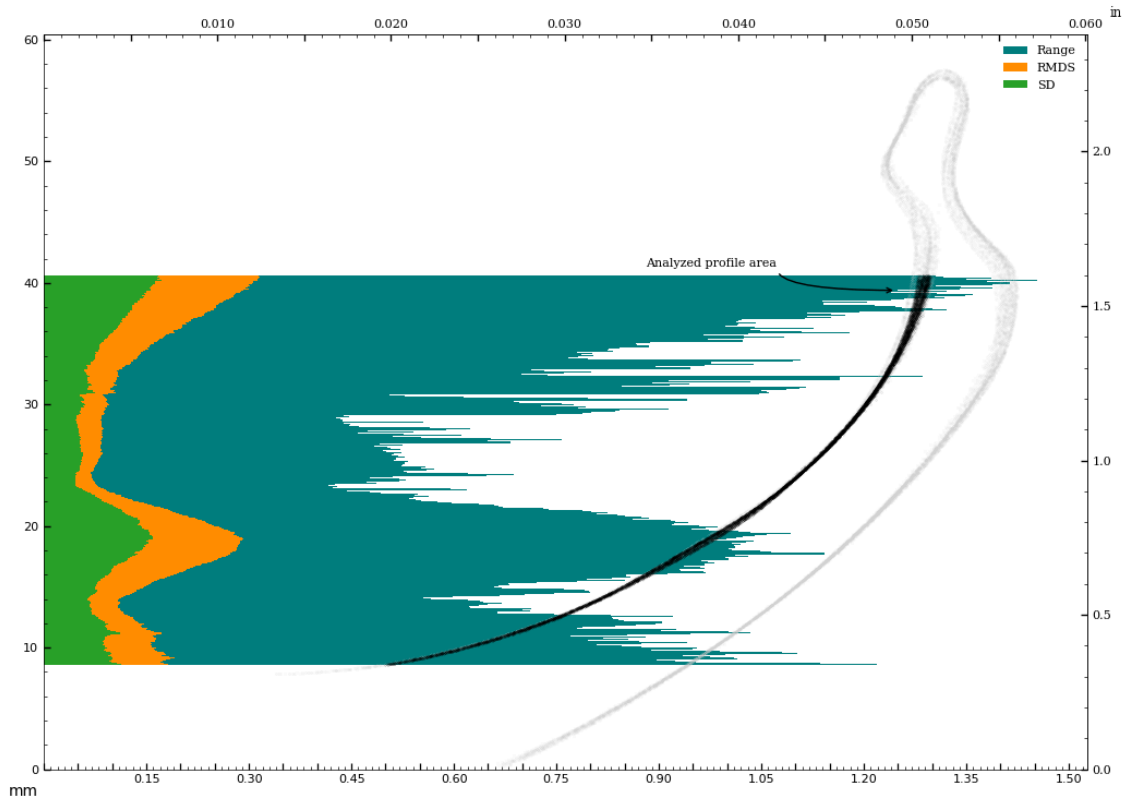
Figure 81: Circularity of interior_separate surface - in z-plane.

Circularity analysis of interior separately aligned surface, perpendicular to surface curvature, Standard Deviation and Root Mean Squared Deviation

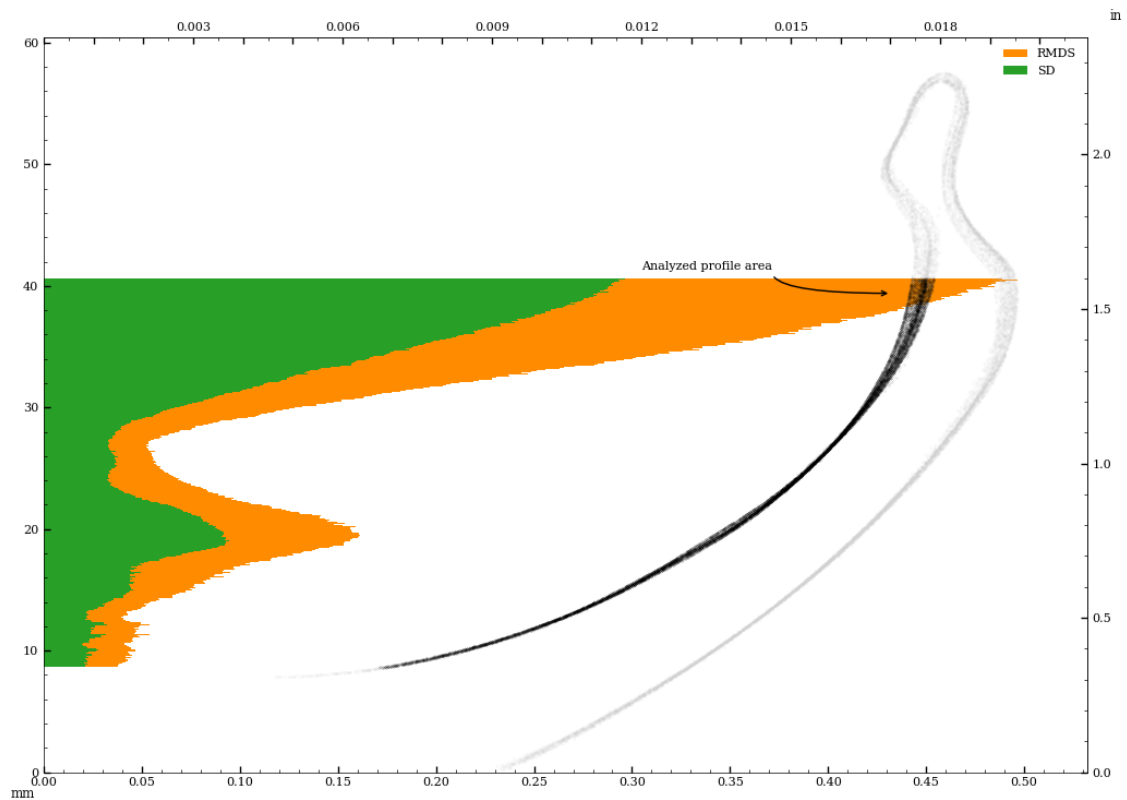Figure 82: Vessel circularity of interior_separate surface, perpendicular to surface curvature, standard deviation and median absolute deviation.

Circularity analysis of interior separately aligned surface, in z-plane, Standard Deviation and Root Mean Squared Deviation
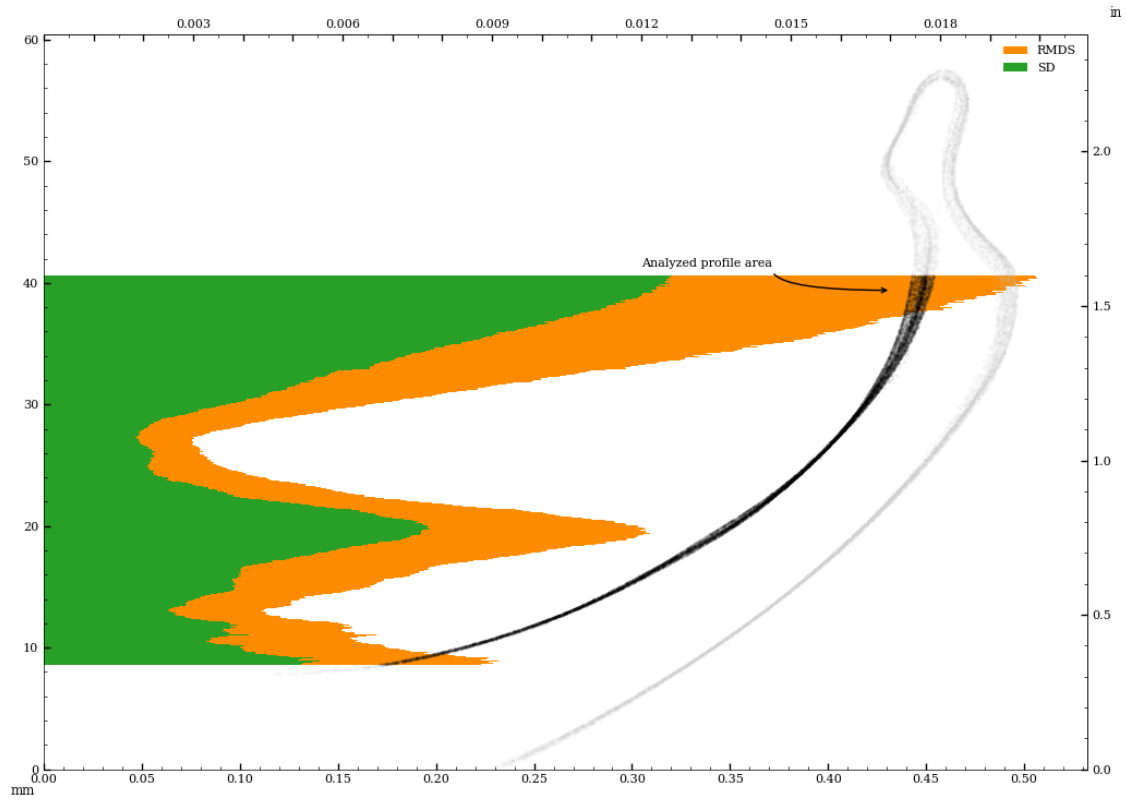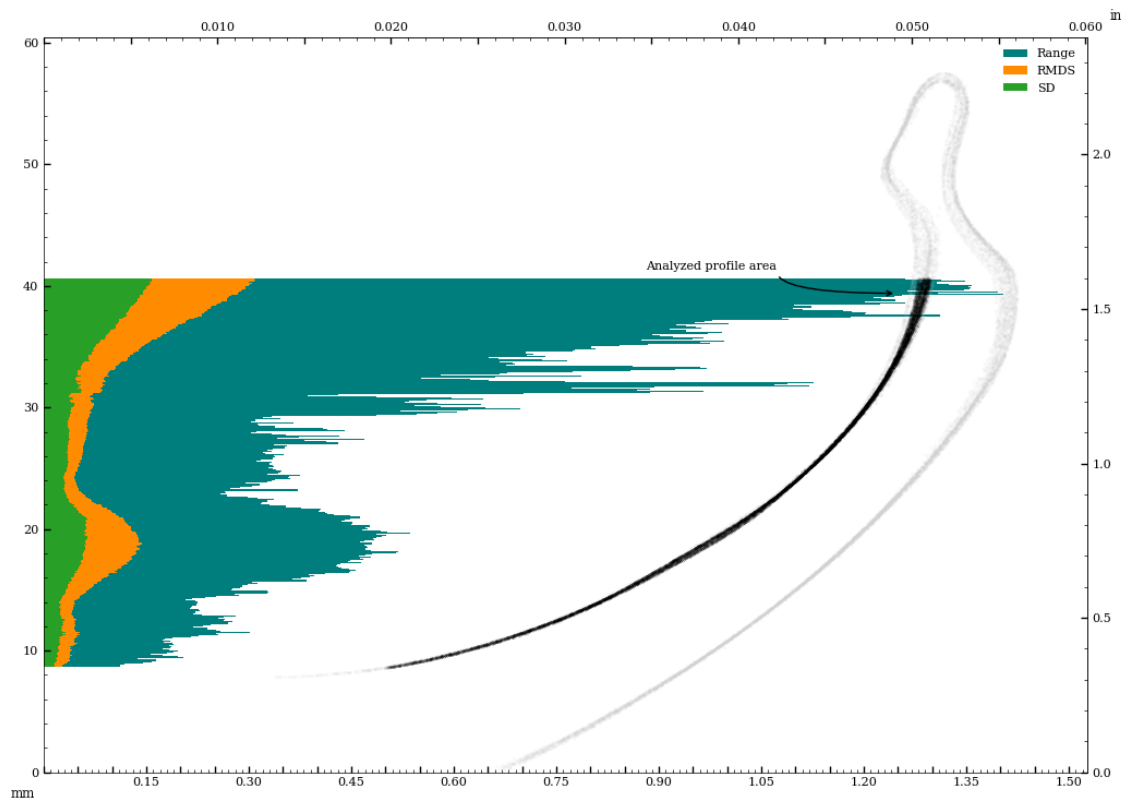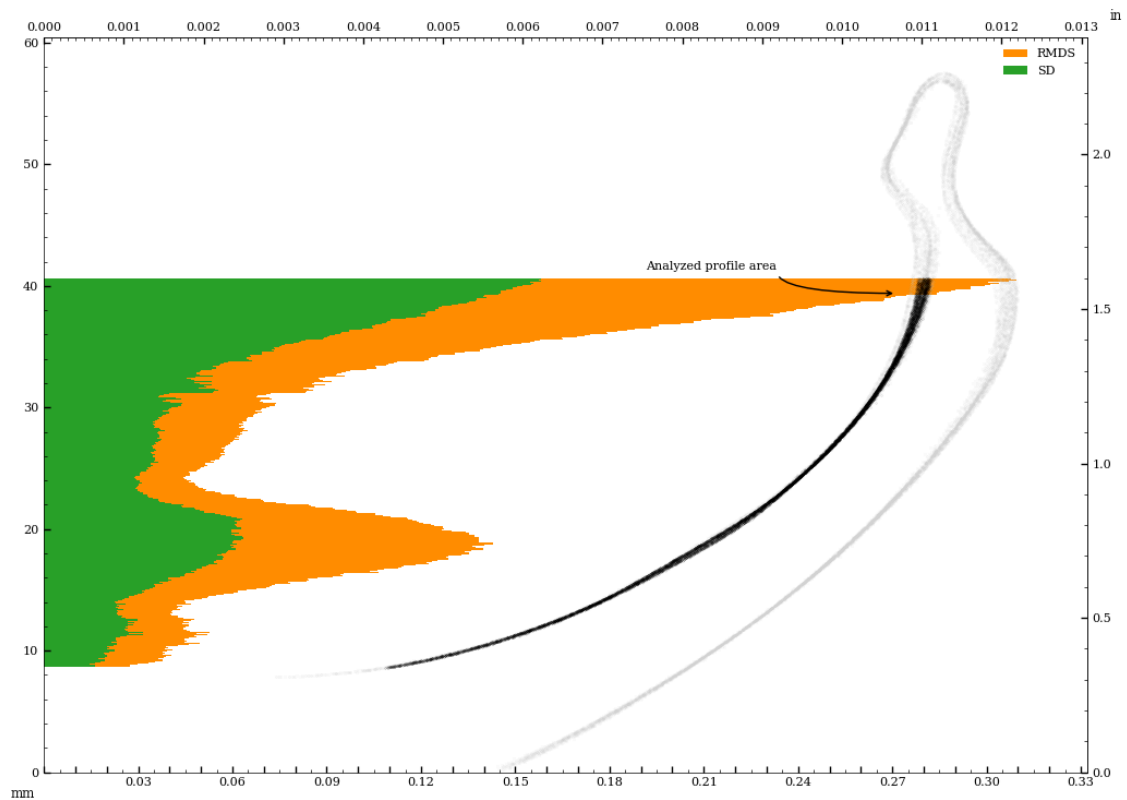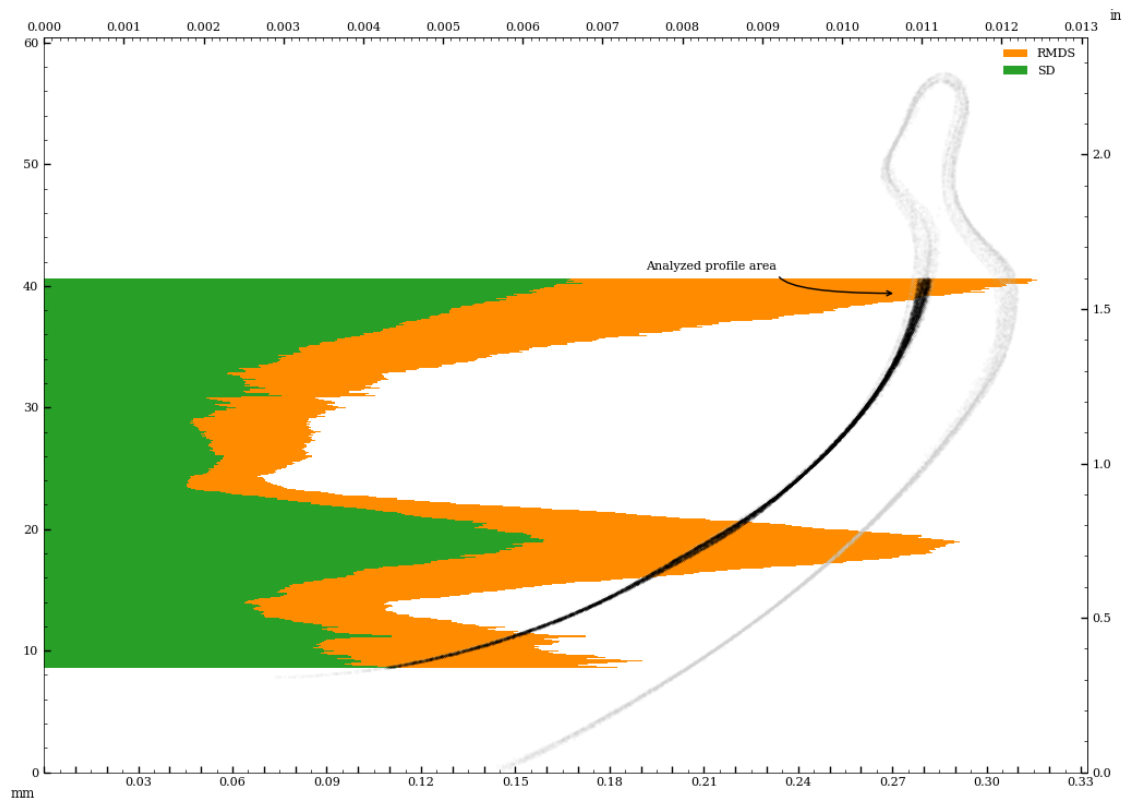

Figure 83: Vessel circularity of interior_separate surface, in z-plane, standard deviation and median absolute deviation.

Appendix B - Comparison Of Concentricity Measurements (Z-plane vs. surface-perpendicular)

Figure 84: Circularity measurement sample locations, full mesh aligned to exterior surface

Figure 85: Circularity measurement sample location, separately aligned interior mesh

Concentricity measurements perpendicular to surface curvature

Tag	Reference	Deviation	Sample size	Circle fit residuals analysis for sample listed in Tag column						Center (x,y)
				Range full	Range inliers	RMSD full	RMDS inliers	SD full	SD inliers	
		mm		mm	mm	mm	mm	mm	mm	μm
c01	z-axis	0.445	2827	2.088	2.088	0.664	0.664	0.366	0.366	−200, −397
c02	z-axis	0.192	3528	2.190	2.190	0.561	0.561	0.312	0.312	40, −188
c03	z-axis	0.219	4091	1.631	1.508	0.368	0.352	0.211	0.196	12, 218
c04	z-axis	0.094	4233	0.757	0.629	0.158	0.157	0.074	0.073	10, 93
c05	z-axis	0.027	4104	0.727	0.388	0.072	0.066	0.044	0.038	−24, −12
c07	z-axis	0.644	4504	1.994	1.994	0.529	0.529	0.323	0.323	−642, −48
c07_s	z-axis	0.252	4309	1.587	1.587	0.370	0.370	0.198	0.198	232, 99
c08	z-axis	0.145	3744	0.612	0.594	0.160	0.161	0.076	0.075	−138, −46
c08_s	z-axis	0.035	3696	0.454	0.454	0.093	0.093	0.053	0.053	12, −33
c09	z-axis	0.114	4156	1.194	1.194	0.272	0.272	0.162	0.162	96, 61
c09_s	z-axis	0.068	4199	1.126	1.126	0.269	0.269	0.123	0.123	−55, 40
c10	z-axis	0.020	3829	0.851	0.818	0.149	0.147	0.085	0.083	−10, 18
c10_s	z-axis	0.049	3875	0.925	0.870	0.152	0.150	0.093	0.091	−22, 43
c02	c07	0.696								681, −140
c03	c08	0.304								149, 265
c04	c09	0.092								−86, 32
c05	c10	0.033								−14, −29

Concentricity measurements in z-plane

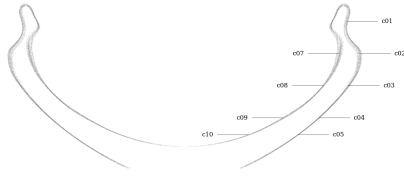| Tag	Reference	Deviation	Sample size	Circle fit residuals analysis for sample listed in Tag column						Center (x,y)
				Range full	Range inliers	RMSD full	RMDS inliers	SD full	SD inliers	
		mm		mm	mm	mm	mm	mm	mm	μm
c01	z-axis	0.445	2827	2.088	2.088	0.664	0.664	0.366	0.366	−200, −397
c02	z-axis	0.192	3528	2.190	2.190	0.561	0.561	0.312	0.312	40, −188
c03	z-axis	0.219	4091	1.631	1.508	0.368	0.352	0.211	0.196	12, 218
c04	z-axis	0.094	4233	0.757	0.629	0.158	0.157	0.074	0.073	10, 93
c05	z-axis	0.027	4104	0.727	0.388	0.072	0.066	0.044	0.038	−24, −12
c07	z-axis	0.644	4504	1.994	1.994	0.529	0.529	0.323	0.323	−642, −48
c07_s	z-axis	0.252	4309	1.587	1.587	0.370	0.370	0.198	0.198	232, 99
c08	z-axis	0.145	3744	0.612	0.594	0.160	0.161	0.076	0.075	−138, −46
c08_s	z-axis	0.035	3696	0.454	0.454	0.093	0.093	0.053	0.053	12, −33
c09	z-axis	0.114	4156	1.194	1.194	0.272	0.272	0.162	0.162	96, 61
c09_s	z-axis	0.068	4199	1.126	1.126	0.269	0.269	0.123	0.123	−55, 40
c10	z-axis	0.020	3829	0.851	0.818	0.149	0.147	0.085	0.083	−10, 18
c10_s	z-axis	0.049	3875	0.925	0.870	0.152	0.150	0.093	0.091	−22, 43
c02	c07	0.696								681, −140
c03	c08	0.304								149, 265
c04	c09	0.092								−86, 32
c05	c10	0.033								−14, −29

Figure 86: Circularity measurement sample locations,
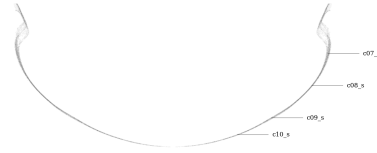full mesh aligned to exterior surface

Figure 87: Circularity measurement sample location,
separately aligned interior mesh

Concentricity measurements perpendicular to surface curvature

Tag	Reference	Deviation	Sample size	Circle fit residuals analysis for sample listed in Tag column						Center (x,y)
				Range full	Range inliers	RMSD full	RMDS inliers	SD full	SD inliers	
		in		in	in	in	in	in	in	thou
c01	z-axis	0.0175	2827	0.0822	0.0822	0.0261	0.0261	0.0144	0.0144	−7.9, −15.6
c02	z-axis	0.0076	3528	0.0862	0.0862	0.0221	0.0221	0.0123	0.0123	1.6, −7.4
c03	z-axis	0.0086	4091	0.0642	0.0594	0.0145	0.0139	0.0083	0.0077	0.5, 8.6
c04	z-axis	0.0037	4233	0.0298	0.0248	0.0062	0.0062	0.0029	0.0029	0.4, 3.7
c05	z-axis	0.0010	4104	0.0286	0.0153	0.0028	0.0026	0.0018	0.0015	−0.9, −0.5
c07	z-axis	0.0253	4504	0.0785	0.0785	0.0208	0.0208	0.0127	0.0127	−25.3, −1.9
c07_s	z-axis	0.0099	4309	0.0625	0.0625	0.0146	0.0146	0.0078	0.0078	9.1, 3.9
c08	z-axis	0.0057	3744	0.0241	0.0234	0.0063	0.0063	0.0030	0.0030	−5.4, −1.8
c08_s	z-axis	0.0014	3696	0.0179	0.0179	0.0037	0.0037	0.0021	0.0021	0.5, −1.3
c09	z-axis	0.0045	4156	0.0470	0.0470	0.0107	0.0107	0.0064	0.0064	3.8, 2.4
c09_s	z-axis	0.0027	4199	0.0443	0.0443	0.0106	0.0106	0.0048	0.0048	−2.2, 1.6
c10	z-axis	0.0008	3829	0.0335	0.0322	0.0059	0.0058	0.0033	0.0033	−0.4, 0.7
c10_s	z-axis	0.0019	3875	0.0364	0.0343	0.0060	0.0059	0.0037	0.0036	−0.9, 1.7
c02	c07	0.0274								26.8, −5.5
c03	c08	0.0120								5.9, 10.4
c04	c09	0.0036								−3.4, 1.3
c05	c10	0.0013								−0.6, −1.2

Concentricity measurements in z-plane

Tag	Reference	Deviation	Sample size	Circle fit residuals analysis for sample listed in Tag column						Center (x,y)
				Range full	Range inliers	RMSD full	RMDS inliers	SD full	SD inliers	
		in		in	in	in	in	in	in	thou
c01	z-axis	0.0175	2827	0.0822	0.0822	0.0261	0.0261	0.0144	0.0144	−7.9, −15.6
c02	z-axis	0.0076	3528	0.0862	0.0862	0.0221	0.0221	0.0123	0.0123	1.6, −7.4
c03	z-axis	0.0086	4091	0.0642	0.0594	0.0145	0.0139	0.0083	0.0077	0.5, 8.6
c04	z-axis	0.0037	4233	0.0298	0.0248	0.0062	0.0062	0.0029	0.0029	0.4, 3.7
c05	z-axis	0.0010	4104	0.0286	0.0153	0.0028	0.0026	0.0018	0.0015	−0.9, −0.5
c07	z-axis	0.0253	4504	0.0785	0.0785	0.0208	0.0208	0.0127	0.0127	−25.3, −1.9
c07_s	z-axis	0.0099	4309	0.0625	0.0625	0.0146	0.0146	0.0078	0.0078	9.1, 3.9
c08	z-axis	0.0057	3744	0.0241	0.0234	0.0063	0.0063	0.0030	0.0030	−5.4, −1.8
c08_s	z-axis	0.0014	3696	0.0179	0.0179	0.0037	0.0037	0.0021	0.0021	0.5, −1.3
c09	z-axis	0.0045	4156	0.0470	0.0470	0.0107	0.0107	0.0064	0.0064	3.8, 2.4
c09_s	z-axis	0.0027	4199	0.0443	0.0443	0.0106	0.0106	0.0048	0.0048	−2.2, 1.6
c10	z-axis	0.0008	3829	0.0335	0.0322	0.0059	0.0058	0.0033	0.0033	−0.4, 0.7
c10_s	z-axis	0.0019	3875	0.0364	0.0343	0.0060	0.0059	0.0037	0.0036	−0.9, 1.7
c02	c07	0.0274								26.8, −5.5
c03	c08	0.0120								5.9, 10.4
c04	c09	0.0036								−3.4, 1.3
c05	c10	0.0013								−0.6, −1.2